ACTA PROTOZOOLOGICA

NENCKI INSTITUTE OF EXPERIMENTAL BIOLOGY
WARSAW, POLAND

1997

VOLUME 36 NUMBER 3

ISSN 0065-1583

Polish Academy of Sciences
Nencki Institute of Experimental Biology
and
Polish Society of Cell Biology

ACTA PROTOZOOLOGICA

International Journal on Protistology

ACTA PROTOZOOLOGICA appears quarterly.

The price (including Air Mail postage) of subscription to ACTA PROTOZOOLOGICA at 1998 is: US $ 180.- by institutions and US $ 120.- by individual subscribers. Limited number of back volumes at reduced rate are available. TERMS OF PAYMENT: Cheque, money oder or payment to be made to the Nencki Institute of Experimental Biology. Account Number: 11101053-3522-2700-1-34 at Państwowy Bank Kredytowy XIII Oddz. Warszawa, Poland. WITH NOTE: ACTA PROTOZOOLOGICA! For matters regarding ACTA PROTOZOOLOGICA, contact Managing Editor, Nencki Institute of Experimental Biology, ul. Pasteura 3, 02-093 Warszawa, Poland; Fax: 48-22 225342; E-mail: jurek@ameba.nencki.gov.pl (for more information see web page **http://www.nencki.gov.pl/public.htm**).

Front cover: *Raphidiophrys pallida*. *In*: J.J.Lee, S.H.Hunter and E.C.Bovee, Editors - An illustrated guide to the protozoa Society of Protozoologists 1985

This publication is supported by the State Committee for Scientific Research
Printed at the MARBIS, ul. Kombatantów 60, 05-070 Sulejówek, Poland

Acta Protozoologica (1997) 36: 157 - 169

ACTA
PROTOZOOLOGICA

Review Article

The Taxonomic Consequences of Morphological and Genetic Variability in *Euglena agilis* Carter (*Euglenophyta*): Species or Clones in *Euglena*? *

Bożena ZAKRYŚ

Department of Plant Systematics and Geography, Warsaw University, Poland

Summary. Natural populations of *Euglena agilis* Carter (= *E. pisciformis* Klebs) are collections of genetic clones representing different reproductive and life strategies; the genetic variability bears no relationship to the morphology of the cells. Therefore, on the basis of investigations described herein 14 intraspecific taxa and four other species (i.e., *E. bichloris* Schiller, *E. bipyrenoidata* Prošk.-Lavr., *E. nana* Johnson and *E. van-goori* Deflandre) with similar morphologies are proposed as synonyms of *E. agilis* Carter. As in *E. agilis* a high degree of DNA polymorphism occurs between clones of other species, e.g., *E. gracilis* Klebs or *E. viridis* Ehrenb. However, interspecific genetic variability is so much greater than intraspecific variability that the boundaries between hitherto accepted species should be maintained only if they were delineated on the basis of morphological characters that are reflected in the genotype. In the case of so-called critical species, i.e., species which are very similar morphologically (*E. stellata* and *E. viridis*), molecular data have shown that the previous authors' choices of diagnostic morphological characters were incorrect. For example, the clones representing these two species are more similar to each other genetically than to any other pair of clones representing another species. In the light of the research presented here it is now essential to conduct a taxonomic revision of the genus *Euglena* on the basis of diagnostic morphological characters, primarily chloroplasts, that are reflected in molecular data.

Key words: *Euglena, Euglena agilis,* molecular genetics, morphology, phylogeny, RAPD, RFLP, taxonomy.

INTRODUCTION

Euglena agilis Carter (= *E. pisciformis* Klebs) is a common unicellular flagellate classified in the division *Euglenophyta,* family *Euglenaceae,* which includes green, myxotrophic representatives (i.e., they may also take up dissolved organic substances). The decided majority of euglenins live in fresh water rich in organic and humic substances. Their main habitats are small, astatic freshwater bodies (puddles, ponds, ditches, manure, littoral areas of lakes, and slowly flowing rivers) in larger bodies of water they are rare.

Euglenins may play an important role in aquatic ecosystems as purifying agents of sewage and contaminated waters. Largely because of the difficulty of identifying particular taxa, the authors of many papers, especially those concerning plankton, seston and microbenthos often limit themselves to determining only the family or genus. Identification of lower taxa is complicated by the often-unrecognized morphological variability on the interpopulation and population levels, and even within the same

* I dedicate this paper to the memory of my teacher and friend Professor Andrzej Batko

Address for correspondence: Bożena Zakryś, Department of Plant Systematics and Geography, Warsaw University, Al. Ujazdowskie 4, 00-478 Warszawa, Poland; E-mail: zakrys@bot.astrouw.edu.pl

clone (Pringsheim 1956, Zakryś and Kucharski 1996, Zakryś et al. 1996).

Since interspecific change has not yet been the subject of a comprehensive analysis, taxonomists continue to describe many new forms and varieties, and often even new species. As a result, at least a few, sometimes many, intraspecific taxa have been described for most species. In the entire genus *Euglena* there are numerous morphologically similar species (so-called critical species: e.g., *E. stellata, E. myxocylindracea, E. pseudoviridis, E. viridis,* all in the same group), which are nearly impossible to distinguish from each other. Because of the difficulty in distinguishing them, these critical species are inadequately investigated, even though they may be common and cosmopolitan.

Moreover, most of the accumulated information concerns only some laboratory strains of *Euglena* - especially one species - *E. gracilis* Klebs, an excellent experimental material that has been used for years in physiological analysis (Miller and Staehelin 1973, Acuna and Bovee 1979, Kiss et al. 1986, Barsanti et al. 1993, Uribe et al. 1994, Petersenmahrt et al. 1995), in cytological analysis (Ueda 1957, Buetow 1968, Palisano and Walne 1976, Triemer 1980, Leedale 1982, Hayashi-Ishimaru et al. 1993, Bonaly and Brochiero 1994, Foltinova et al. 1994), in biochemical analysis (Spare et al. 1978, Aviram and Weissmann 1978, Briand et al. 1993, Watanabe et al. 1993, Saidha and Schiff 1994), and in genetic analysis (Schnare et al. 1990; Hallik et al. 1993; Cui et al. 1994; Koo and Spremulli 1994a, b; Lin et al. 1994; Orsat et al. 1994; Saint-Guily et al. 1994; Stange-Thomann et al. 1994; Stevenson and Hallick 1994; Greenwood et al. 1996; Thompson et al. 1997).

Phylogenetic considerations of *Euglena* cell structure

The structure of the flagellated *Euglena* cell is different from cells of higher plants in several important ways that may reflect its origins: (1) the presence of three phospholipid membranes surrounding the chloroplasts of euglenins (Gibbs 1978, Palisano et al. 1980, Dubertret and Lefort-Tran 1982); (2) the presence of an apical complex composed of a canal, reservoir, stigma, photoreceptor and two flagella (Walne and Arnott 1967, Walne 1971, Kivic and Vesk 1972, Hilenski et al. 1976, Wolken 1977, Piccini and Mammi 1978, Diehn 1979, Pagni et al. 1981, Bouck 1982, Melkonian et al. 1982, Robenek and Melkonian 1983, Bertaux et al. 1989, Barsanti et al. 1997); (3) the mitotic division of the nucleus with retention of the nuclear envelope and the lack of a karyokinetic spindle, whose function is ensured by the endosome - a structure that is not present in other plants (Leedale 1958a-c, 1959 a, b, 1968; Saito 1961; O'Donnell 1965; Adams 1973; Moyne et al. 1975; Pickett-Heaps and Weik 1977; Magnaval et al. 1980; Ueda and Hayashiishimaru 1996); (4) lack of a cell wall and the presence of a periplast (pellicle) - an elastic structure surrounding the cell (Leedale 1964, Schwelitz et al. 1970, Silverman and Hikida 1976, Miller and Miller 1978, Dawson et al. 1988). In many species trichocysts occur under the periplast.

The structural peculiarities of euglenin cells are due to their presumed formation as the result of symbiosis between a unicellular chlorophyte with an animal organism (Gibbs 1978), an hypothesis supported by numerous similarities in the morphological structure of euglenins and currently living zooflagellates (Bovee 1972, Kivic and Walne 1984, Walne and Kivic 1990, Kuźnicki and Walne 1993), as well as by results of molecular analyses. Nuclear DNA and ribosomal RNA show a close relationship between *Euglena* and *Trypanosoma*, and the chloroplast DNA shows a relatedness to chlorophytes (Bremer et al. 1987, Sourdis and Krimbas 1987, Woese et al. 1990, Hendriks et al. 1991, Sogin 1991, Gogarten 1995, Henze et al. 1995, McFadden and Gilson 1995, Keeling and Doolittle 1996, Lockhart et al. 1996).

Identification of taxa in the genus *Euglena*

The identification of *Euglena* taxa is based primarily on morphological characters at the level of optical microscopy, since only on this commonly used level has variation been sufficiently well analyzed. The morphological investigations conducted so far, however, have not led to the establishment of uniform, reliable criteria in distinguishing intrageneric taxa of *Euglena*. The opinions among scientists on this matter are divided - for example, the diverse viewpoints of the authors of four basic monographs of this genus: Gojdics (1953), Huber-Pestalozzi (1955), Pringsheim (1956) and Popova (1966). The number of currently known intrageneric taxa (species, varieties and forms, henceforth referred to as taxa) varies from 64 (Pringsheim 1956) to 148 (Huber-Pestalozzi 1955). The discrepancies in number are due not only to differences in the scope of the data but also to different treatment of a species in *Euglena*. The choice of morphological characters that distinguish particular taxa is made by the author, guided by his or her knowledge of the whole group. For example Pringsheim (1956) presented a list of 200 taxa but accepted only 64 of them, the majority (52) as monotypic species, and only four as polytypic species. It is clear that

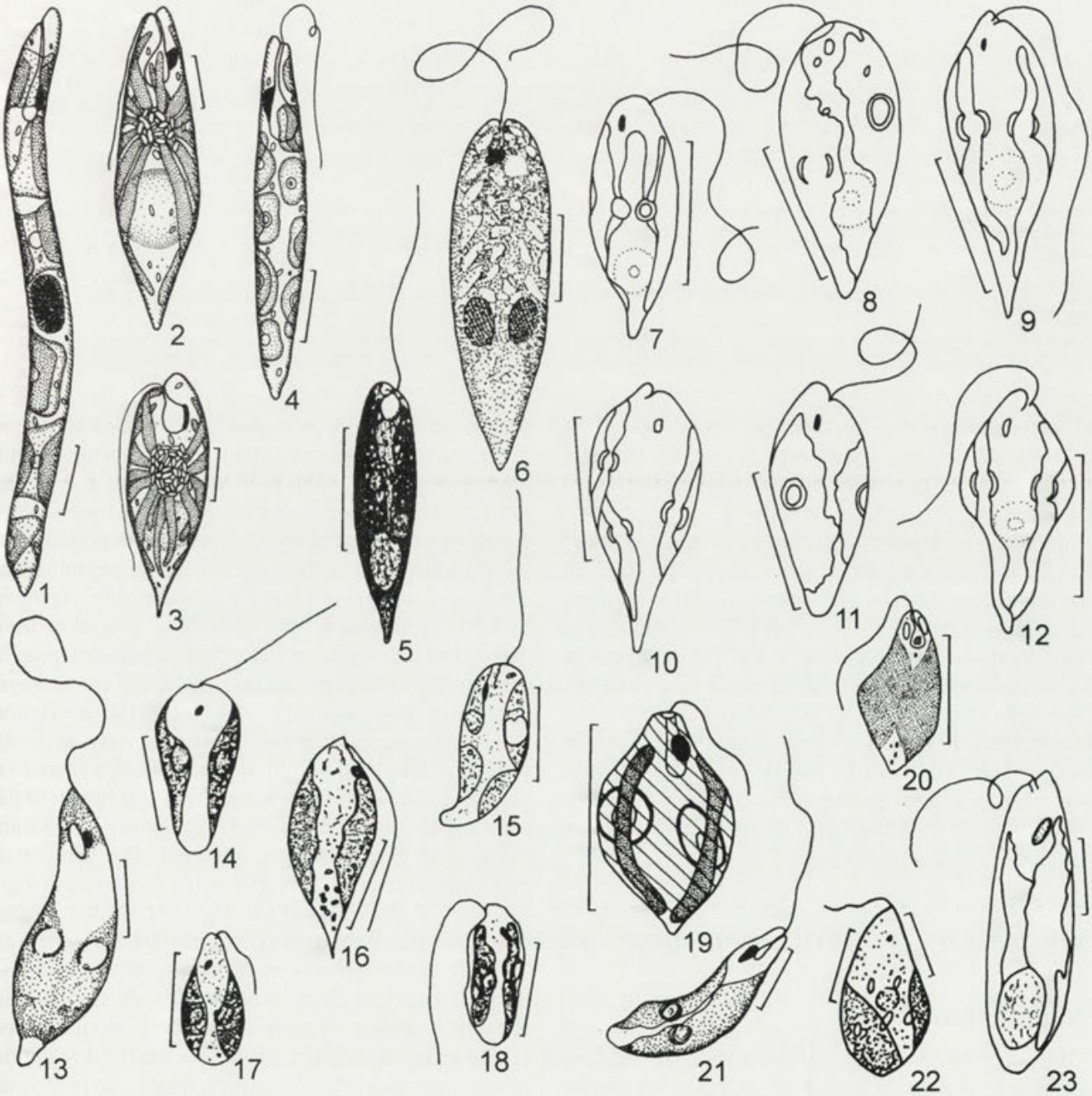

Figs. 1-23. 1 - *Euglena mutabilis* Schmitz. 2 - *E. viridis* Ehrenb. 3 - *E. stellata* Mainx. 4 - *E. gracilis* Klebs. 5-12 - *E. pisciformis* Klebs (5 - var. *typica* Klebs, after Klebs 1883; 6 - var. *granulosa* Playfair, after Playfair 1923; 7 - var. *mucronata* Pringsh., after Pringsheim 1956; 8 - var. *lata* Pringsh., after Pringsheim 1956; 9 - var. *procera* Pringsh., after Pringsheim 1956; 10 - var. *striata* Pringsh., after Pringsheim 1956; 11 - var. *obtusa* Pringsh., after Pringsheim 1956; 12 - var. *fallax* Pringsh., after Pringsheim 1956). 13-18 - *E. agilis* Carter (13 - iconotype, after Carter 1853, 14- var. *varians* Schiller, after Schiller 1956; 15 - f. *coeruleoviridis* Schiller, after Schiller 1956; 16 - var. *apyrenoidea* Schiller, after Schiller 1956; 17 - var. *circumsulcata* Schiller, after Schiller 1956; 18 - var. *praeexcisa* Schiller, after Schiller 1956). 19 - *E. pisciformis* var. *piriformis* Szabados, after Szabados 1936. 20 - *E. nana* Johnson, after Johnson 1944. 21 - *E. bipyrenoidata* Prošk.-Lavr., from Popova 1966. 22 - *E. bichloris* Schiller, from Huber-Pestalozzi 1955. 23 - *E. van-goori* Defl., after Van Goor 1925. Bars-10µm

Table 1. Number of monotypic and polytypic species of *Euglena* in the world flora

Source of data	Total number of taxa	Number of species	Number of varieties and forms	Number of monotypic species	Number of polytypic species	Ratio of monotypic to polytypic species
Gojdics (1953)	183	155	28	127	16	8 : 1
Huber-Pestalozzi (1955)	148	101	47	82	19	4 : 1
Pringsheim (1956)	64	56	8	52	4	13 : 1
Popova (1966)	78	52	26	37	15	2.5 : 1

he favoured the idea of a monotypic species, since the ratio of monotypic to polytypic species is 1:13. The ratio for Gojdics (1953) is 1:8, for Huber-Pestalozzi (1956) 1:4 and for Popova (1966) 1:2.5 (Table 1).

In order to obtain the total number of taxa (i.e., more than the 183 indicated above), other taxa should be added that are not included by Gojdics (1953) but cited elsewhere: Skvortzov 1946, 1967; Fott 1953, 1956; Johnson 1956; Perman 1956; Skuja 1956; Ettl 1960; Skvortzov and Noda 1968; Bold and MacEntee 1973; Philipose 1982; Kato 1983; Starmach 1983; Tell and Conforti 1986; Zakryś 1986, 1994; Zakryś and Walne 1994. Thus, the total number of currently known taxa of the genus *Euglena* is over 250. For comparison it should be mentioned that the Polish flora currently contains 84 taxa, or about 30% of the world flora.

INTRASPECIFIC VARIATION OF *E. AGILIS*

Diagnostic characters

The problem of intraspecific variation in *Euglena agilis* Carter (=*E. pisciformis* Klebs) has been of interest to scientists for a long time (Hansgirg 1892, Playfair 1923, Szabados 1936, Pringsheim 1956, Schiller 1956, Zakryś 1988, Zakryś and Kucharski 1996, Zakryś et al. 1996) even though this species is characterized by a very simple structure: small metabolic cells (15-45 x 6-12 μm) with two lobate, often parietal chloroplasts, each having a single pyrenoid; a few monomorphic paramylon grains are scattered in the cytoplasm.

The observed variation which occurs in natural populations of this species has not yet been the subject of a detailed analysis, a situation that has led to the description of 14 varieties and forms and four new species with a morphology very similar to *E. agilis* (Figs. 5-23). The distinguishing criteria are not sharp, because they concern small differences in cell size and shape and in chloroplast morphology that may be the result of the physiological state of the cell in division or the reaction of the organism to habitat conditions. The authors of new taxa have considered the following characters as differentiating in comparison to the type species - e.g. *E. agilis* var. *agilis* Carter and at the same time sufficient for the description of new species and intraspecific taxa: (1) body metaboly (high plasticity of the cells, ability to change shape) - a character difficult to describe, depending on the size of the cells and the number of paramylon grains giving a certain stiffness to cells lacking a cell wall. The amount of accumulated storage material depends on the physiological state of the cell and that, in turn, on the habitat conditions (Kiss et al. 1986, Conforti 1991, Conforti et al. 1995). Together with strong metaboly, other taxonomic characters such as shape, symmetry or cell size are also difficult to define. Therefore, metaboly should not be considered as diagnostic, as it has been in the description of some new taxa (var. *striata* Pringsheim, var. *piriformis* Szbados); (2) shape and dimensions of the cells - these characters were most frequently the reason for distinguishing new varieties (var. *minor* Hansgirg, var. *piriformis* Szabados, var. *mucronata* Pringsheim, var. *obtusa* Pringsheim, var. *procera* Pringsheim, var. *varians* Schiller, var. *praeexcisa* Schiller, var. *circumsulcata* Schiller). The shape of *Euglena* cells may be described only during their movement (swimming) and even this possess difficulties in interpretation due to their metaboly. It also depends to some extent on the size of the cells, and

that, in turn, on the stage of the cell cycle. For example, the shape of small cells just after division gradually changes from fusiform to cylindrical, as the cells increase to twice the size just before division. However, the length of the *Euglena* cell does not increase in proportion to its width. The precise measurement of small, swimming cells is extremely difficult, especially when using the micrometric glass method. Therefore, large discrepancies occur in the literature on the subject of cellular dimensions; (3) pyrenoids - their presence or absence in chloroplasts has become the basis for distinguishing not only a new variety (var. *apyrenoidea* Schiller) but also four new species (*E. bipyrenoidata* Prošk.-Lav., *E. van-goori* Deflandre, *E. nana* Johnson and *E. bichloris* Schiller). In all *Euglena* taxa investigated so far under the light microscope, pyrenoids are located in the chloroplast - inside, not on its surface (de Haller 1959; Leedale et al. 1965; Mignot 1965, 1966; Buetow 1968; Leedale 1968; Ploaie 1971; Ophir and Ben-Shaul 1974; Ehara et al. 1975; Dragos et al. 1979; Péterfi et al. 1979; Palisano et al. 1980; Zakryś and Walne in press). In the cytoplasm immediately adjacent to the pyrenoids, storage material (paramylon) is accumulated, whose dense clusters form large protruding caps on both sides of the chloroplast. In the light microscope, paramylon caps are prominent and indicate the presence of pyrenoids. Under unfavourable habitat conditions paramylon is used up, the caps diminish in size and become invisible; (4) the number, shape and location of chloroplasts in the cell - the presence of three chloroplasts instead of two in a certain number of individuals in the population, their shift from a central location towards the posterior or the anterior, the shape of the chloroplast margin (deeper or shallower indentations), and even their colour were major criteria for describing new taxa: var. *fallax* Pringsheim, var. *striata* Pringsheim, var. *lata* Pringsheim, var. *granulosa* Playfair, f. *coeruleoviridis* Schiller. As is generally known, however, the number of cell organelles may increase before cell division and the location of the large nucleus which occupies much of the cell width is also linked to the physiology of cell division. In euglenins it shifts forward just before cell division occurs and returns to its previous position just after division (Leedale 1958a, 1959a, 1968; Saitô 1961; Pickett-Heaps 1977; Zakryś 1980, 1983, 1988). Thus, the location of the chloroplasts changes only with respect to the nucleus; their location in the cytoplasm (distance from the cell surface) does not change, however, nor does their position with respect to other cell organelles. The location of chloroplasts in the cell is one of the conditions of effective photosynthesis and seems to be a character with little variation. Therefore, many authors have considered it as the major criterion of an intrageneric classification of *Euglena* (Lemmermann 1913, Chu 1946, Gojdics 1953, Pringsheim 1956, Zakryś 1986).

Among the above authors Pringsheim was the first to carry out a systematic analysis of morphology on intraspecific variation in *E. agilis*. In 1956 he published the results of laboratory observations. His comments indicate that he cloned the strain isolated in 1927 by Mainx and obtained a number of clones with morphological differences (as he himself admits, not endogeneously uniform) which he described as new variations. Since he did not then have the possibility of testing his observations against molecular data, as we can today, the diagnostic characters that he used as a basis for describing new taxa were more problematic.

Now, forty years later new molecular techniques and computer programmes have created novel research opportunities. It has become possible to determine the extent of variability at the level of genotype and phenotype, to compare them, to select morphologically differentiating traits and to draw taxonomic conclusions. The research presented here is thus a continuation of Pringsheim's work, but using the more recently available combination of morphological and molecular methods, as outlined below.

Morphological variability

More recent analyses of morphological variation in *E. agilis* have encompassed microscopic observations of 100 clones isolated from 10 populations collected in Poland and grown under identical physico-chemical conditions (Zakryś et al. 1996). Precise biometric analyses were also performed using computer image analysis. Five cellular parameters were measured - length, width, „circularity", cross section and circumference. For each of these, 10 statistical parameters were calculated (Zakryś et al. 1996).

Microscopic observations have shown that in all populations a certain constant morphological variation was maintained. The cells of all clones always had two parietal, lobate chloroplasts, each containing one pyrenoid; however, the number of plastids increased sporadically to three just before cell division, but only in 1-2% of the dividing cells. Small, difficult-to-evaluate differences of chloroplast size, the shape of the margin and the shift (anterior or posterior in the cell), observed in about 40% of the cells, were distinctly related to the physiology of cell division, occurring about every two days (Zakryś et al. 1996).

Detailed biometric analysis, however, did not indicate significant differences in the shape and size of the cells,

even though microscopic observations might suggest that some clones had cells larger than others or of a different shape. The visual effect depended on the number of swimming cells, their physiological state, the age of the culture, habitat conditions and most importantly, the time of the observation. After a period of darkness (i.e., of intensified cell division) on fresh media and in not overly dense cultures small, fusiform, actively swimming cells predominated. In older cultures, where the rate of division was lower, cells were less active, often crawling, larger and more cylindrical, even strongly rounded because they were filled with a large amount of storage material (Zakryś et al. 1996).

The only morphological characteristic that distinguished the clones of *E. agilis* was the ability to form slime both on liquid and solid media by dividing cells. With respect to this one trait, the presence of two groups of clones was apparent, henceforth referred to as „unslimy" and „slimy". In the „unslimy" group the cells did not form slime. On agar they formed matte, elevated colonies which did not spread, and the rate of cell division was very fast, especially after they were transferred to a new medium. In the „slimy" group the dividing cells formed different amounts of slime (difficult to estimate quantitatively) whose volume increased as the culture aged and the conditions deteriorated. On agar they formed shiny, spreading colonies. Their rate of cell division was much slower in comparison to „unslimy" ones (even immediately after being transferred to fresh medium) depending on the amount of slime formed, i.e., the more slime, the fewer daughter cells (Zakryś et al. 1996).

Only in aging cultures, as nutrients were exhausted did gradual changes take place, leading ultimately to degradation of the cells. First the storage material was used up, paramylon grains disappeared, the cells became less stiff and the pyrenoids became invisible. In the cytoplasm hematochrome accumulated, chloroplasts changed location and finally decomposed into smaller fragments and disappeared. The rate of cell division slowed, irregularities in karyo- and cytokinesis increased, and unusually large cells with many nuclei appeared (Asaul 1967; Zakryś 1980, 1983, 1988).

The large plasticity of euglenin cells as a reaction to environmental changes has been known for a long time (Léfévre 1931, Conrad 1943, Fasulo et al. 1982). Not only a lack but also an excess of organic compounds causes morphological changes, phenomena that have been shown in experiments with *E. acus*, *E. gracilis* and *E. spirogyra*. These changes are manifested by a considerable increase in cell size and the accumulation in the cytoplasm of a large number of paramylon grains, which affect metaboly, cell shape and the ornamentation of the periplast (Kiss et al. 1986, Conforti 1991, Conforti et al. 1995, Conforti in press).

Similar phenomena occur in nature. In astatic water bodies in which euglenins live, the changes of physicochemical conditions occur very fast and are reflected in cellular morphology, factors that may help to explain the continuing proliferation of descriptions of so many new intraspecific taxa of euglenins, in general, not only for *E. agilis*.

Genetic variability

Comparison of the results of morphological investigations with molecular data obtained by RAPD (randomly amplified polymorphic DNA) and RFLP (restriction fragment length polymorphism) indicated that: (1) in natural populations of *E. agilis* a high degree of genetic polymorphism is maintained between the clones, which is the result of intense microevolutionary processes on the intraspecific level. Not a single pair of clones has been found with an identical genetic pattern (Zakryś and Kucharski 1996, Zakryś et al. 1996). A similar phenomenon of genetic variability was noted in natural populations of many organisms (in all kingdoms), including freshwater zooplankton (Wood 1973, Backus and Mukai 1987, Hugnes 1989, Browne and Hoopes 1990, Mort 1991, Okamura et al. 1993), parasitic protozoans (Tibayrenc et al. 1990, 1991) or fungi (Muthomeenakshi et al. 1994, Zimard et al. 1994). These organisms have a clonal model of reproduction in the life cycle and form populations in the asexual reproduction mode. However, most of these organisms have also maintained the ability to reproduce sexually, with a lesser or greater frequency, thus permitting recombination and genetic segregation. In *Euglena* so far sexual reproduction has not been observed and it is a good model of an asexual organism. Unfortunately, there are not enough empirical data on genetic polymorphism in other uniparental organisms, to compare with *Euglena*. The only known case is the large genetic variability in the fungal genus *Trichoderma* (Muthomeenakshi et al. 1994, Zimard et al. 1994). Fungi are not good models of asexual organisms, however, due to the rather poorly understood sexual and parasexual processes occurring in individual taxonomic groups; (2) the genetic variability of clones of *E. agilis* does not have its counterpart in the morphology of cells, with the exception of the trait of producing slime during division stages. No correlation was found between the size or shape of cells and the genetic characteristics of clones (Zakryś et al. 1996). Biometric analysis also did not

justify the taxonomic separation of groups of „slimy" and „unslimy" clones. However, the analyses of the results of RAPD (for 10 primers) and of RFLP (for 17 restriction enzymes) did confirm not only the existence of the „slimy" and „unslimy" clones but also their separation was reflected in the molecular data; i. e.,genotype. All calculation methods for both phenetic and phylogenetic analyses indicated genetic distinctness of the „slimy" and „unslimy" clones (Zakryś et al. 1996). Comparison of both of the accepted phenetic trees based on RAPD and RFLP results (each counted for 9 primary trees - Figs. 24, 25) shows that they are not identical. Rather, the differences in the trees concern small transpositions in the „slimy" and „unslimy" groups that maintain the same general structure, and may be explained in two ways: i - a high degree of genetic polymorphism between the clones and, ii - a difference in the number of bands (characters) obtained by each of the methods (for RFLP - 198 characters, for RAPD - 270). Moreover, among the 17 restriction enzymes used there were some which differentiated the clones poorly and some which differentiated them very well (Zakryś and Kucharski 1996). Similar results were obtained by phylogenetic analysis (Figs. 26, 27). The results of both phenetic and phylogenetic analyses suggest the occurrence of two main evolutionary trends in *E. agilis*. The first is a maximum increase in the rate of cell division and a concomitant cessation of slime capsule formation during division; the second is the protection of division stages by the formation of thick slime sheaths at the expense of the rate of cell division. Such evolutionary tendencies may be the result of two different life strategies that may be imposed by a highly variable environment. Euglenins live mainly in small astatic water bodies such as puddles, ponds, draining ditches, and sewer canals, in which changes in physicochemical conditions may occur from hour to hour, often until they become fully dry and then are rehydrated during the next rain. Some clones thus multiply very rapidly, giving up the protection of their survival stages (cysts). Among the enormous number of cells only relatively few have a chance to survive the period of drought. If the akinetes are not formed quickly enough, the whole population will die. For the second group of clones there is a different strategy. Most of its energy is expended on the protection of its division stages. The dividing cells form thick slime sheaths protecting them from rapid changes of the environment and from drought, a phenomenon very clearly seen in cultures. On fresh media immediately after transfer, the rate of cell division increases slightly, and there is distinctly less slime. A small deterioration of living conditions is, however, sufficient to cause an increase in the amount of slime, and the rate of cell division decreases. However, there is never even a brief interruption in the formation of protective slime (Zakryś et al. 1996); (3) no correlation has been found between the sample site in Poland, the type of water body (pond, lake, puddle) and the genetic or morphological variability of the clones.

Thus, natural populations of *E. agilis* are a collection of genetically different clones which represent different reproductive strategies. There is no justification, therefore for distinguishing 18 taxa on the basis of small morphological differences, which are not reflected in the genotype. The only differentiating diagnostic character is the chloroplast - two lobate chloroplasts, each having a pyrenoid. The remaining characters, including the body metaboly, shape and size of the cells, the number and distribution of paramylon grains and small differences in chloroplast morphology are the result of intraspecific variability, the physiological state of the cell, or adaptation and are not due to genetic differences (Zakryś in press).

Thus, the lack of tenable morphological diagnostic characters (i.e., reflected in the genotype) which could be used to create more than one taxon has led to the following taxonomic proposal (Zakryś, in press): the acceptance of only one taxon at the rank of species with the name *Euglena agilis* Carter (1856) and the treatment as synonyms of *E. agilis* Carter, all of the other names of taxa published after 1856: *E. pisciformis* Klebs (1883), *E. pisciformis* var. *minor* Hansgirg (1892), *E. pisciformis* var. *granulata* Playfair (1923), *E. pisciformis* var. *piriformis* Szabados (1936), *E. pisciformis* var. *fallax* Pringsh. (1956), *E. pisciformis* var. *lata* Pringsh. (1956), *E. pisciformis* var. *mucronata* Pringsh. (1956), *E. pisciformis* var. *obtusa* Pringsh. (1956), *E. pisciformis* var. *procera* Pringsh. (1956), *E. agilis* var. *apyrenoidea* Schiller (1956), *E. agilis* f. *coeruleoviridis* Schiller (1956), *E. agilis* var. *circumsulcata* Schiller (1956), *E. agilis* var. *praeexcisa* Schiller (1956), *E. agilis* var. *varians* Schiller(1956), *E. bichloris* Schiller (1956), *E. bipyrenoidata* Prošk.-Lavr. (1937), *E. nana* Johnson (1944), *E. van-goori* Deflandre (1925) (Figs.1-23).

SPECIES OR CLONES IN *EUGLENA* ?

The results of the investigations presented above led to the posing of an important question: Does the large genetic variability between clones blur the boundaries between species accepted so far and described on the basis of morphological characters? Can we thus speak of *Euglena* species or only of clones?

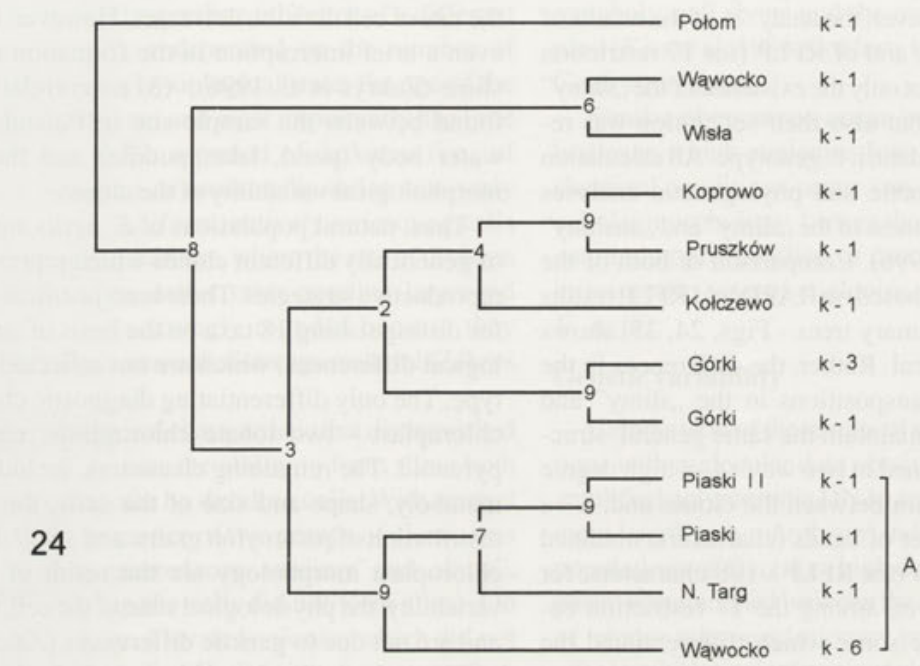

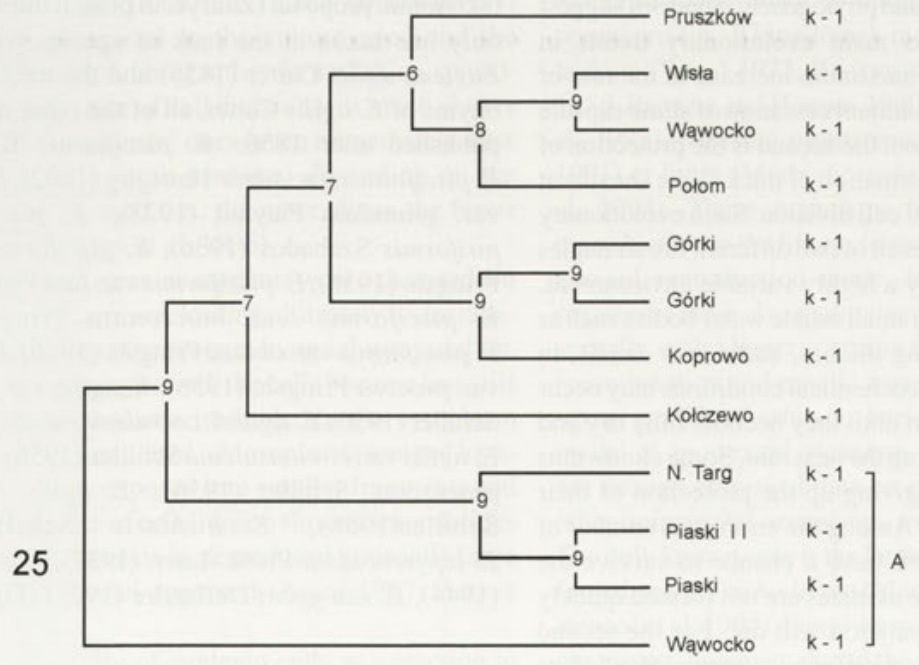

Fig. 24. Phenetic consensus tree resulting from nine primary trees obtained for RFLP data; these clones of *E. pisciformis* were named according to the localities or sites from which they were collected in Poland (Zakryś et al. 1996); A: unslimy clones

Fig. 25. Phenetic consensus tree resulting from nine primary trees obtained for RAPD data; these clones of *E. pisciformis* were named according to the localities or sites from which they were collected in Poland (Zakryś et al. 1996); A: unslimy clones

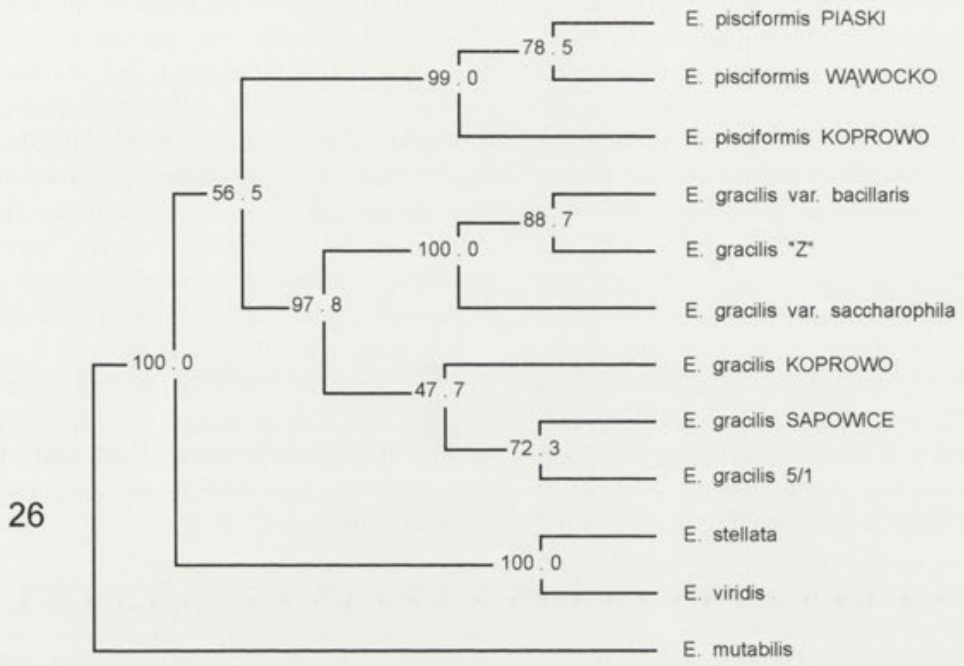

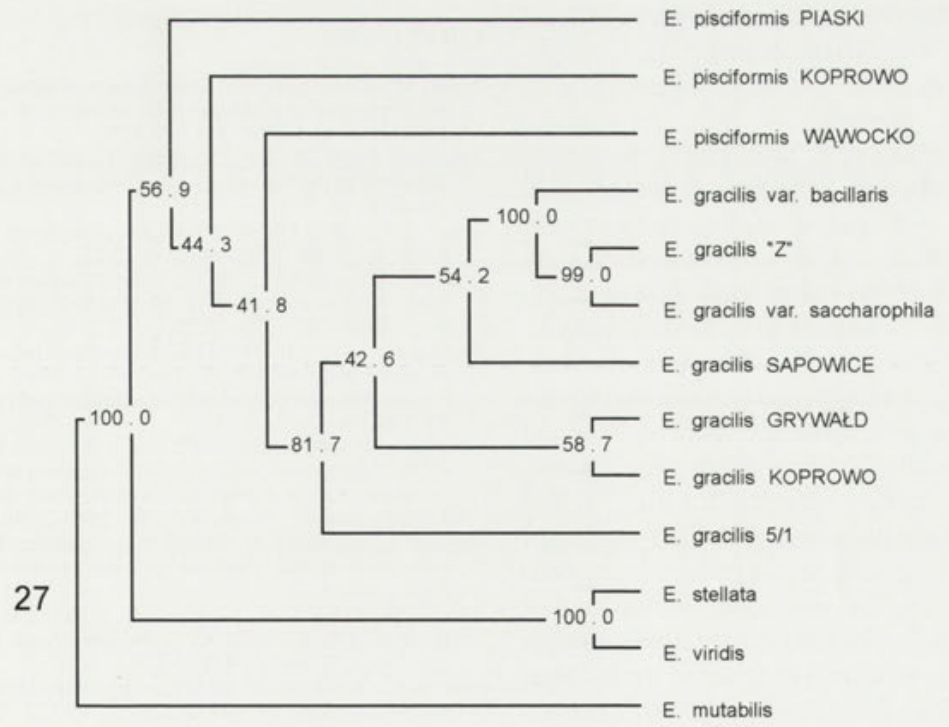

Fig. 26. Unrooted phylogenetic consensus tree of a hundred trees obtained by bootstrap resampling (for RFLP data); the clones of *E. pisciformis* (Piaski, Wąwocko, Koprowo) and *E. gracilis* (Koprowo, Sapowice) were named according to the localities or sites from which they were collected in Poland (Zakryś et al. 1996); the other clones were obtained from the Sammlung von Algenkulturen at Göttingen (Zakryś et al. in press)

Fig. 27. Unrooted phylogenetic consensus tree of a hundred trees obtained by bootstrap resampling (for RAPD data); the clones of *E. pisciformis* (Piaski, Wąwocko, Koprowo) and *E. gracilis* (Koprowo, Sapowice, Grywałd) were named according to the localities or sites from which they were collected in Poland (Zakryś et al. 1996); the other clones were obtained from the Sammlung von Algenkulturen at Göttingen (Zakryś et al. in press)

Most of the abundant literature concerning the idea of species in biology deals with biparental species. In uniparental (asexual) species genetically different clones represent distinct sequences of generations and evolve independently (Simpson 1961; Mayr 1963, 1969, 1984; Sokal and Crovello 1970). The clones are joined into groups (species) by a link of morphological and genetic similarities and isomorphic ecological niches. Although the biotic and abiotic parameters of astatic water bodies where euglenins live have not yet been analyzed, it can be assumed that similar clones, especially with regard to molecular characters, live in similar habitats and occupy similar ecological niches. Moreover, if they form a monophyletic group, they may unquestionably be considered a species. Whereas in sexually reproducing organisms, species are defined genetically by participation in breeding, in uniparental organisms the increasingly accepted major criteria for delineating species are monophyletism, ecological niches, morphological and genetic similarities.

Although our understanding of phylogenetic relationships within *Euglena* based on molecular evidence is still rudimentary, some recently obtained molecular data (Zakryś and Kucharski 1996, Zakryś et al. in press) should facilitate an answer to the question posed at the outset - species or clones in *Euglena* ? Namely, clones representing five species of *Euglena: E. agilis, E. gracilis, E. mutabilis, E. stellata* and *E. viridis* have been compared morphologically and genetically (Figs. 1-4, 12). With the exception of the pair *E. stellata* and *E. viridis* (which are very similar) all the other species clearly differed from each other. My research has shown that: (1) some discontinuities in morphological variation are reflected in the phylogenetic tree based on molecular data. The most important trait with diagnostic value also for this group of species is the chloroplast - the shape, number and stable location in the cell; (2) interspecific genetic variability was so much greater than intraspecific variability that the clones representing the same species were grouped together, and in dendrograms formed groups corresponding to particular species. The only exception was the pair *E. stellata* and *E. viridis*. They were more similar to each other genetically than were any other pair of clones, even those representing the same species (Figs. 26, 27).

The examples described above strongly suggest that one may speak of *Euglena* species distinguished only on the basis of such morphological characters as are justified by the genotype. In the case of the pair of critical species, *E. stellata* and *E. viridis,* the historical choice of diagnostic morphological characters was incorrect, as was shown more recently by the molecular data (Zakryś et al. in press). In the light of the large morphological variation observed in euglenins, many morphological characters are differently viewed by scientists and, in contrast to molecular characters, are not objective traits. Molecular (genetic) similarities are thus proving more valuable than morphological criteria in phylogenetic reconstruction, even though they do not yet allow a complete verification of the morphological diagnostic characters currently used in *Euglena* classification, because it is sometimes difficult to distinguish a genetic from an epigenetic component.

In summary this direction of research, i.e., the combination of morphological and molecular analyses, is the only effective way to obtain a clear and useful classification of the genus *Euglena*, (and ultimately of other euglenins) which should be the practical result of the work of a taxonomist.

Acknowledgments. The author is very grateful to Professor Dr A. Batko (recently deceased) and to Dr K. Spalik for their significant contributions and valuable comments and discussion during the preparation of this work, and to Professor Dr. Patricia L. Walne (Department of Botany, University of Tennessee, Knoxville, USA) for her helpfulness, interest, assistance with the organization of the manuscript, and correction and revision of the English text.

REFERENCES

Acuna M., Bovee E. (1979) Some effects of adenosine triphosphate on swimming and photophobic response of *Euglena gracilis. Univ. Kans. Sci. Bull.* **51:** 669-678

Adams K. J. (1973) Characterisation of a cell division commitment threshold in the cell cycle of *Euglena gracilis. Brit. phycol. J.* **8:** 204-209

Asaul Z. I. (1967) On morphological changes in *Euglena gracilis* Klebs in culture. *Ukr. Bot. J.* **4:** 22-27

Aviram J., Weissmann C. (1978) Spectrophotometric and fluorometric study of the denaturation of *Euglena* cytochrome C-552. *Biochemistry* **17:** 2020-2025

Backus B., Mukai H. (1987) Chromosomal heteromorphism in a Japanese population of *Pectinatella gelatinosa* and karyotypic comparison with some other phylactolaemate bryozoans. *Genetica* **73:** 189-196

Barsanti L., Passarelli V., Lenzi P., Walne P. L., Dunlap J. R., Gualtieri P. (1993) Effects of hydroxylamine digitonin and triton X-100 on photoreceptor (paraflagellar swelling) and photoreception of *Euglena gracilis. Vision. Res.* **33:** 2043-2050

Barsanti L., Passarelli V., Walne P. L., Gualtieri P. (1997) *In vivo* photocycle of the *Euglena gracilis* photoreceptor. *Biophys. J.* **72:** 545-553

Bertaux O., Valencia R., Magnaval R. (1989) The nucleus. In: The Biology of *Euglena* (Ed. D. E. Buetow). Acad. Press, New York, San Diego, California, **4:** 210-220

Bold H. C., MacEntee F. J. (1973) Phycological notes. II. *Euglena myxocylindracea* sp. nov. *J. Phycol.* **9:** 152-156

Bonaly J., Brochiero E. (1994) Cell-surface changes in cadmium-resistant *Euglena*: Studies using lectin-binding techniques and flow cytometry. *Bull. Environ. Contam. Toxicol.* **52:** 54-60

Bouck G. (1982) Flagella and the cell surface. In: The Biology of *Euglena* (Ed. D. E. Buetow). Acad. Press, New York, London, **3:** 29-51

Bovee, E. C. (1972) The Trypanosomatidae: possibly descendant from euglenoids? *J. Protozool. Suppl.* **18:** 14

Bremer K., Humphries C. J., Mishler B. D., Churchill S. P. (1987) On cladistic relationships in green plants. *Taxon* **36:** 33 9-349

Briand S., Julistiono H., Beaune P., Flinois J. P., de-Waziers I., Leroux J. P. (1993) Presence of proteins recognized by mammalian cytochrome P-450 antibodies in *Euglena gracilis*. *Biochim. Biophys. Acta* **1203:** 199-204

Browne R. A., Hoppes C. W. (1990) Genotype diversity and selection in asexual shrimp (*Artemia*). *Evolution* **44:** 1035-1051

Buetow D.E. (1968): Morphology and ultrastructure of *Euglena*. In: The Biology of *Euglena* (Ed. D. E. Buetow). Acad. Press, New York, London, **1:** 110-181

Carter H. (1856) Notes on the Freshwater Infusoria of the Island of Bombay. 1. Organization. *Ann. Mag. Nat. Hist.* **2:** 18(103) 115-132; (105) 221-248

Chu S. P. (1946) Contributions to our knowledge of the genus *Euglena*. *Sinensia* **17:** 75-134

Conforti V. (1991) Taxonomic study of the *Euglenophyta* of a highly polluted river of Argentina. *Nova. Hedwigia* **53:** 73-98

Conforti V.(0000) Morphological changes of *Euglenophyta* in response to organic enrichment. *Hydrobiologia* (in press).

Conforti V., Alberghina J., Urda E. G. (1995) Structural changes and dynamics of the phytoplankton along a highly polluted lowland river of Argentina. *J. Aquatic Ecosystem Health* **4:** 59-75

Conrad W. (1943) Remarques sur le genre *Phacus* Duj., 1841. *Bull. Mus. Roy. Hist. Nat. Belg.* **19:** 1-16

Cui J.Y., Mukai K., Seaki K., Matsubara H (1994) Molecular cloning and nucleotide sequences of cDNAs encoding subunits I, II and IX of *Euglena gracilis* mitochondrial complex III. *J. Biochem Tokyo*. **115:** 98-107

Dawson N. S., Dunlap J. R., Walne P. L. (1988) Structure and elemental composition of pellicular warts of *Euglena spirogyra (Euglenophyceae). Br. phycol. J.* **23:** 61-69

Deflandre G. (1925) Algues d'eau douce du Vénézuéla. *Rev. Algol.* **3:** 212-241

de Haller D. E. (1959) Structure submicroscopique d'*Euglena viridis*. *Arch. Sci., Genéve* **12:** 309-340

Diehn B. (1979) The interactions of photic and chemical stimulus/response systems in *Euglena gracilis*. *Acta Protozool.* **18:** 7-16

Dragos N., Péterfi L. S., Craciun C. (1979) Fine structure of *Euglena*. II. *Euglena stellata* Mainx and *Euglena viridis* Ehrenberg. *Nova Hedwigia* **31:** 223-246

Dubertret G., Lefort-Tran M (1982) Chloroplast molecular structure with particular reference to thylakoids and envelopes. In: The Biology of *Euglena* (Ed. D. E. Buetow). Acad. Press, New York, London, **3:** 253-307

Ehara T., Shihira-Ishikawa I., Osafune T., Hase E., Ohkuro I. (1975) Some structural characteristics of chloroplast degeneration in cells of *Euglena gracilis* „Z" during their heterotrophic growth in darkness. *J. Electr. Micr.* **24:** 253-261

Ettl H. (1960) Die Algenflora des Schönhengstes und Seiner Umgebung. I. *Nova Hedwigia* **2:** 509-544

Fasulo M. P., Bassi M., Domini A. (1982) Cytotoxic effects of hexavalent chromium in *Euglena gracilis*. I. First observations. *Protoplasma* **110:** 39-47

Foltinova P., Lahitova N., Ebringer L. (1994) Antimutagenicity in *Euglena gracilis*. *Mutat. Res.* **323:** 167-171

Fott B. (1953) New species of flagellates. *Preslia* **25:** 143-156

Fott B. (1956) *Euglena physeter* species nova. *Preslia* **28:** 415-417

Gogarten J. P. (1995) The early evolution of cellular life. *Tree* **10:** 147-151

Gojdics M. (1953): The Genus *Euglena*. The University of Wisconsin Press, Madison

Gibbs S. P. (1978) The chloroplasts of *Euglena* may have evolved from symbiotic green algae. *Can. J. Bot.* **56:** 2883-2889

Greenwood S. J., Schnare M. N., Gray M. W. (1996) Molecular characterization of U3 small nucleolar RNA from the early diverging protist, *Euglena gracilis*. *Current Genetics* **30:** 338-346

Hallick R. B., Hong L., Drager R. G., Favreau M. R., Monfort A., Orsat B., Spielmann A., Stutz E. (1993) Complete sequence of *Euglana gracilis* chloroplast DNA. *Nucleic Acids Research* **21:** 3537-3544

Hansgirg A. (1892) Prodromus der Algenflora Theil II. Die blaugrünen Algen (*Myxophyceen, Cyanophyceen*) nebst Nachträgen zum ersten Theile und einer systematischen Bearbeitung der in Böhmen vertreiten saprophytischen Bacterien und Euglenen enthält. *Arch. Naturw. Durchforsch Böhmen* **8:** 1-266

Hayashi-Isimaru Y., Ueda K., Nonaka M. (1993) Detection of DNA in the nucleoids of chloroplasts and mitochondria in *Euglena gracilis* by immunoelectron microscopy. *J. Cell. Sci.* **105:** 1159-1164

Hendriks L., De Baere Y., Van De Peer J., Neefs A., Goris A., De Wachter R. (1991) The evolutionary position of the Rhodophyte *Porphyra umbilicalis* and the Basidiomycete *Leucosporidium scottii* among other eucaryotes as deduced from complete sequences of small ribosomal subunit RNA. *J. Mol. Evol.* **32:** 167-177

Henze K., Badr A., Wettern M., Cerff R., Martin W. (1995) A nuclear gene of eubacterial origin in *Euglena gracilis* reflects cryptic endosymbioses during protist evolution. *Proc. Natl. Acad. Sci U.S.A.* **92:** 9122-9126

Hilenski L. L., Walne P. L., Snyder F. (1976) Aliphatic chains of esterified lipids in isolated eyespots of *Euglena gracilis* var. *bacillaris*. *Plant Physiol* **57:** 645-646

Huber-Pestalozzi P. (1955) Das Phytoplankton des Süsswassers, 4. Teil: Euglenophyceen. Die Binnengewässer, Stuttgart **16:** 1-606

Hugnes R. N. (1989) A Functional Biology of Clonal Animals. Chapman and Hall London,

Johnson L. P. (1944) *Euglenae* of Iowa. *Trans. Amer. Microsc. Soc.* **63:** 97-135

Johnson L. (1956) Observations on *Euglena fracta* sp. nova., with special reference to the locomotor apparatus. *Trans. Amer. Microsc. Soc.* **75:** 271-280

Kato S. (1983) A new species of *Euglena (Euglenophyceae)* from Japan. *J. Jap. Bot* **58:** 237-239

Keeling P. J., Doolittle W. F. (1996) Alpha-tubulin from early-diverging eucaryotic lineages and evolution of the tubulin family. *Mol. Biol. Evol.* **13:** 1297-1305

Kiss J., Vasconcelos A., Triemer R. (1986) Paramylon synthesis and chloroplast structure associated with nutrient levels in *Euglena (Euglenophyceae). J. Phycol.* **22:** 327-333

Kivic P. A., Vesk M. (1972) Structure and function of the euglenoid eyespot. *J. Exp. Bot.* **23:** 1070-1075

Kivic P. A., Walne P. L. (1984) An evaluation of a possible phylogenetic relationship between the Euglenophyta and Kinetoplastida. *Origins of Life* **13:** 269-288

Klebs G. (1883) Über die Organization einiger Flagellatengruppen und ihre Beziehungen zu anderen Infusorien. *Unters. Bot. Inst. Tübingen*. **1:** 233-362

Koo J. S., Spremulli L. L. (1994a) Analysis of the translational initiation region on the *Euglena gracilis* chloroplast ribulose-bisphosphate carboxylase/oxygenase (rbcL) messenger RNA. *J. Biol. Chem.* **269:** 7494-7500

Koo J. S., Spremulli L. L. (1994b) Effect of the secondary structure in the *Euglena gracilis* chloroplast ribulose-bisphosphate carboxylase/oxygenase messenger RNA on translational initiation. *J. Biol. Chem.* **269:** 7501-7508

Kuźnicki L., Walne P. L. (1993) Protistan evolution and phylogeny: current controversies. *Acta Protozool.* **32:** 135-140

Leedale G. F. (1958a) Nuclear structure and mitosis in the Euglenineae. *Arch. Microbiol.* **32:** 32-64

Leedale G. F. (1958b) Mitosis and chromosome numbers in the Euglenineae (Flagellata). *Nature* **181:** 502-503

Leedale G. F. (1958c) Nuclear divisions in the Euglenineae: a new form of mitosis. *Bull.Brit. Phycol. Soc.* **1/6:** 28-29

Leedale G. F. (1959a) The time-scale of mitosis in the Eugleninae. *Arch. Microbiol.* **32:** 352-360

Leedale G .F. (1959b) Amitosis in three species of *Euglena*. *Cytologia* (Tokyo), **24:** 213-219

Leedale G. F. (1964) Pellicle structure in *Euglena*. *Br. Phycol. Bull.* **2:** 291-306

Leedale G. F. (1968) The nucleus in *Euglena*. In: The Biology of *Euglena* (Ed. D. E. Buetow). Acad. Press, New York, London, **1:** 185-242

Leedale G. F. (1982) Ultrastructure. In: The Biology of *Euglena* (Ed. D. E. Buetow). Acad. Press, New York, London, **4:** 1-25

Leedale G. F., Meeuse B. J. D., Pringsheim E. G. (1965) Structure and physiology of *Euglena spirogyra*. I. and II. *Arch Microbiol*. **50:** 68-102

Léfévre M. (1931) De la valeur des caractéres specifiques chez quelques Eugleniens. *Rec. Trav. Cryptog. dediés a L. Manguin:* 343-354

Lemmermann E. (1913) Eugleninae. In: Die Süßwasserflora Deutschlands, Österreichs und der Schweiz (Ed. G. Fisher). Jena, 115-174

Lin Q., Ma L., Burkhart W., Spremulli L. L. (1994) Isolation and characterization of cDNA clones for chloroplast translational initiation factor-3 from *Euglena gracilis*. *J. Biol.Chem.* **269:** 9436-9444

Lockhart P. J., Steel M. A., Larkum A. W. (1996) Gene duplication and the evolution of photosynthetic reaction center proteins. *FEBS Lett*. **385:** 193-196

Magnaval R., Valencia R., Paoletti J. (1980) Subunit organization of *Euglena gracilis* chromatin. *Biochem. Biophys. Res. Commun.* **92:** 1415-1421

Mayr E. (1963) Animal Species and Evolution. Cambridge, Harvard University Press, 1-797

Mayr E. (1969) Principles of Systematic Zoology. New York, McGraw-Hill, 1-428

Mayr E. (1984) Species concepts and their application. In: Conceptual Issues in Evolutionary Biology (Ed. E. Sober). The MIT Press, Cambridge, Massachusetts, London, England, 531- 540

McFadden G., Gilson P. (1995) Something borrowed, something green: lateral transfer of chloroplasts by secondary endosymbiosis. *Tree* **10:** 12-17

Melkonian M., Robenek H., Rassat J. (1982) Flagellar membrane specializations and their relationship to mastigonemes and microtubules in *Euglena gracilis*. *J. Cell. Sci*. **55:** 115-135

Mignot J. P. (1965) Ultrastructure des Eugléniens I. Étude de la cuticule chez différentes espéces. *Protistologica* **1:** 5-15

Mignot J. P. (1966) Structure et ultrastructure de quelques Euglénomonadines. *Protistologica* **2:** 51-117

Miller K. R., Staehelin L. A. (1973) Direct identification of photosynthetic enzymes on membrane surfaces revealed by deep etching. *J. Cell Biol.* **59:** 226

Miller K. R. Miller G. J. (1978) Organization of the cell membrane in *Euglena. Protoplasma* **95:** 11-24

Mort M. A. (1991) Bridging the gap between ecology and genetics: the case of freshwater zooplankton. *Trends Ecol. Evol.* **6:** 41-45

Moyne G., Bertaux O., Puvion E. (1975) The nucleus of *Euglena*. I. An ultracytochemical study of the nucleic acids and nucleoproteins of synchronized *Euglena gracilis* Z. *J. Ultrastruct. Res.* **52:** 362-376

Muthomeenakshi S., Mills P. R., Brown A. E., Seaby D. A. (1994) Intraspecific molecular variation among *Trichoderma harzianum* isolates colonizing mushroom compost in the British Isles. *Microbiology* **4:** 769-777

O'Donnell E. H. J. (1965) Nucleolus and chromosomes in *Euglena gracilis*. *Cytologia* **30:** 118-154

Okamura B., Jones C. S., Noble L. R. (1993) Randomly amplified polymorphic DNA analysis of clonal population structure and geographic variation in a freshwater bryozoan. *Proc.R.Soc.Lond.* **253:** 147-154

Ophir I., Ben-Shaul Y. (1974) Structural organization of developing chloroplasts in *Euglena. Protoplasma* **80:** 109-127

Orsat B., Spielmann A., Marc-Martin S., Lemberger T., Stutz E. (1994) Analysis of the 22 kbp long psbD-psbC gene cluster of *Euglena gracilis* chloroplast DNA: evidence for overlapping transcription units undergoing differential processing. *Biochim. Biophys. Acta* **1218:** 75-81

Pagni P. G. S., Walne P. L., Pagni R. M. (1981) On the occurrence of a-carotene in isolated stigmata of *Euglena gracilis* var. *bacillaris*. *Phycologia* **20:** 431-434

Palisano J. R., Walne P. L. (1976) Light and electron microscopy of two permanently bleached cell lines of *Euglena gracilis* (Euglenophyceae). *Nova Hedwigia* **27:** 455-482

Palisano J. R., Walne P. L., Brown D. (1980) Ultrastructure and physical characteristics of proplastids and chloroplasts isolated by zonal centrifugation from *Euglena gracilis* var. *bacillaris*. *Eur. J. Cell Biol.* **21:** 305-312

Perman J. (1956) Noví zástupci rodu *Euglena* Ehrenb. ze slizu vláknitých zelených řas (*Chaetophorineae*). *Preslia* **29:** 28-33

Péterfi L. S., Dragos N., Craciun C. (1979) Fine structure of *Euglena*. I. *Euglena tristella* Chu. *Nova Hedwigia* **31:** 197-221

Petersenmahrt S. K., Ekelund N. G. A., Widell S. (1995) Effects of UV-B radiation and nitrogen starvation on enzyme activities in isolated plasma membranes of *Euglena gracilis*. *Physiol. Plant.* **95:** 515-522

Philipose M. T. (1982) Contributions to our knowledge of Indian algae-III. Euglenineae. Part I. The genus *Euglena* Ehrenberg. *Proc. Indian Acad. Sci. (Plant Sci.).* **91:** 551-599

Piccinni E. Mammi M. (1978) Motor apparatus of *Euglena gracilis:* ultrastructure of the basal portion of the flagellum and the paraflagellar body. *Boll. Zool.* **45:** 405-414

Pickett-Heaps J. D., Weik K. (1977) Cell division in *Euglena* and *Phacus*. I. Mitosis. In: Mechanisms of Control of Cell Division (Eds. L. Rost and E. M. Gifford). Dowden, Hutchinson and Ross, Stroudsburg, Pennsylvania, 308-336

Playfair G. J. (1923) Notes on freshwater algae. *Proc. Linn. Soc. N. S. Wales* **48:** 206-228

Ploaie P. G. (1971) The fine structure of chloroplasts and pyrenoids of *Euglena gracilis* strain „Z". *Rev. Roum. Biol. Bot.* **16:** 179-183

Popova T. G. (1966) Euglenovyje vodorosli. Vyp. 1 Part.1. Flora sporovych rastenij SSSR. Izd. Nauka, Moskva-Leningrad, **8:** 1-411

Pringsheim E. G. (1956) Contributions towards a monograph of the genus *Euglena*. *Nova Acta Leopoldina* **18:** 1-168

Proshkina-Lavrenko A. I. (1937) Novye vidy *Euglenaceae* iz solenovodnych vodojemow SSSR. *Bot. Mater. Otd. Spor. Rast. Bot. Inst. AN SSSR*, **4:** 8-9 (in Russian)

Robenek H., Melkonian M (1983) Structural specialization of the paraflagellar body membrane of *Euglena. Protoplasma* **117:** 154-157

Saidha T., Schiff J. A. (1994) Purification and properties of a phenol sulphotransferase from *Euglena* using L-tyrosine as substrate. *Biochem. J.* **1:** 45-50

Saint-Guily A., Schantz M. L., Schantz R. (1994) Structure and expression of a cDNA encoding a histone H2A from *Euglena gracilis*. *Plant. Mol. Biol.* **24:** 941- 948

Saitô M. (1961) Studies in the mitosis of *Euglena*. I. On the chromosome cycle of *Euglena viridis* Ehrbg. *J. Protozool.* **8:** 300-307

Schiller J. (1956) Untersuchungen an den planktischen Protophyten des Neusiedler Sees 1950-1954. III Teil, Euglenen. *Sitz.-Ber. Österr. Akad. Wiss*, **1:** 547-583

Schnare M. N., Cook J. R., Gray M. W. (1990) Fourteen internal transcribed spacers in the circular ribosomal DNA of *Euglena gracilis*. *J. Mol. Biol.* **215:** 85-91

Schwelitz F., Evans W. R., Mollenhauer H. H. (1970) The fine structure of the pellicle of *Euglena gracilis* as revealed by freeze-etching. *Protoplasma* **69:** 341-349

Skuja H. (1956) Taxonomische und biologische Studien über das Phytoplankton schwedischer Binnengewässer. *Nova Acta Reg. Soc. Sci. Upsal.* **16:** 1-404

Skvortzov B. V. (1946) Species novae et minus cognitae Algarum, Flagellatarum et Phycomicetarum Asiae, Africae, Americae et Japoniae nec non Ceylon anno 1931-45 descripto et illustrato per tab. 1-18. *Proceedings* **2:** 14-30

Skvortzov B. V. (1967) New and interesting species of *Euglena* Ehr. from the subtropics of Brasil. *Nova Hedwigia* **14:** 379-386

Skvortzov B. V., Noda M. (1968) *Euglena* species with one or two chromatophores recorded from South America and South Africa in 1962-1966. *J. Jap. Bot.* **43:** 225- 234

Silverman H., Hikida R. S. (1976) Pellicle complex of *Euglena gracilis:* characterization by disruptive treatments. *Protoplasma* **87:** 237-252

Simpson G. G. (1961) Principles of Animal Taxonomy. New York, Columbia Univ. Press

Sogin M. L. (1991) Early evolution and the origin of eucaryotes. *Curr. Opin. Gen. Devel.* **1:** 457-463

Sokal R. R., Crovello T. J. (1970) The biological species concept: a critical evaluation. *Am.Natur.* **104:** 127-153

Sourdis J., Krimbas C. (1987) Accuracy of phylogenetic trees estimated from DNA sequence data. *Mol. Biol. Evol.* **4:** 159-166

Spare W., Lesiewicz J. L. Herson D. S. (1978) The effect of cycloheximide on *Euglena gracilis* phenylalanyl transfer RNA synthetases. *Arch. Microbiol.* **118:** 289-292

Stange-Thomann N., Thomann H. U., Lloyd A. J., Lyman H. J., Soll D. (1994) A point mutation in *Euglena gracilis* chloroplast tRNA (Glu) uncouples protein and chlorophyll biosynthesis. *Proc. Natl. Acad. Sci. U.S.A.* **91:** 7947-7951

Starmach K. (1983) Flora słodkowodna Polski. *Euglenophyta.* 3. PWN, Warszawa-Kraków

Stevenson J. K., Hallick R. B. (1994) The psaA operon pre-mRNA of the *Euglena gracilis* chloroplast is processed into photosystem I and II mRNAs that accumulate differentially depending on the conditions of cell growth. *Plant J.* **5:** 247-260

Szabados M. (1936). *Euglena* vizsgálatok. *Acta Biol. Szeged* **4:** 49-95

Tell G., Conforti V. (1986) Euglenophyta Pigmentadas de la Argentina. Bibliotheca Phycologica, J. Cramer, Berlin, Stuttgart, 1-201

Thompson M. D., Zhang Q. L., Hong L., Hallick R. B. (1997) Two new group-II twintrons in the *Euglena gracilis* chloroplast are absent in basally branching *Euglena* species. *Current Genetics* **31:** 89-95

Tibayrenc M., Kjellberg F., Ayala F. J. (1990) A clonal theory of parasitic protozoa: The population structures of *Entamoeba, Giardia, Leishmania, Naegleria, Plasmodium,Trichomonas,* and *Trypanosoma* and their medical and taxonomical consequences. *Proc. Natl. Acad. Sci.U.S.A.* **87:** 2414-2418

Tibayrenc M., Kjellberg F., Ayala F. J. (1991) The clonal theory of Parasitic Protozoa. *Bio Science* **41:** 767-774

Triemer R. E. (1980) Role of Golgi apparatus in mucilage production and cyst formation in *Euglena gracilis* (Euglenophyceae). *J. Phycol.* **16:** 46-52

Ueda K. (1957) Structure of plant cells with special reference to lower plants. III. A cytological study of *Euglena gracilis. Cytologia* **23:** 56-67

Ueda K, Hayashi-Ishimaru Y. (1996) Localization of DNA in the condensed interphase chromosomes of *Euglena. Chromosoma* **104:** 380-385

Uribe A., Chavez E., Jimenez M., Zazueta C., Moreno-Sanchez R. (1994) Characterization of Ca^{2+} transport in *Euglena gracilis* mitochondria. *Biochim. Biophis. Acta* **1186:** 107-116

Walne P. L. (1971) Comparative ultrastructure of eyespots in selected euglenoid flagellates. In: Contributions in Phycology (Eds. B. C. Parker and R. M. Brown). Allen Press, Lawrence, Kansas, 107-120

Walne P.L., Arnott H. J. (1967) The comparative ultrastructure and possible function of eyespots: *Euglena granulata* and *Chlamydomonas eugametos. Planta* **77:** 325-353

Walne P. L., Kivic P. (1990) Euglenida. In: Handbook of Protoctista (Eds. L. Margulis, J.O. Corliss, M. Melkonian and D.J. Chapman). Jones and Bartlett Publ., Boston, 270-287

Watanabe F., Tamura Y., Stupperich E., Nakano Y. (1993) Uptake of cobalamin by *Euglena* mitochondria. *J. Biochem. Tokyo* **114:** 793-799

Woese C. R., Kandler O., Wheelis M. L. (1990) Towards a natural system of organisms: proposal for the domains Archaea, Bacteria, and Eucarya. *Proc. Natl. Acad. Sci. USA*, **87:** 4576-4579

Wolken J. J. (1977) *Euglena:* The photoreceptor system for phototaxis. *J. Protozool.* **24:** 518-522

Wood T. S. (1973) Colony development in species of *Plumatella* and *Fredericella* (Ectoprocta: Phylactolaemata). In: Animal Colonies (Eds. Boardman R.S., Cheetham A. H. and Oliver W. .A.). Pennsylvania: Dowden, Hutchinson and Ross. 395-432

Zakryś B. (1980) Aberrations in development of strain „Z" of *Euglena gracilis. Bull. Acad. Sc. Polon., Ser. sci. biol.* **28:** 117-120

Zakryś, B. (1983): Aberrative divisions of *Euglena* and their phylogenetic implications. *Nova Hedwigia* **38:** 471-476

Zakryś B. (1986) Contribution to the monograph of Polish members of the genus *Euglena* Ehr. 1830. *Nova Hedwigia* **42:** 491-540

Zakryś B. (1988) The nuclear DNA level as a potential taxonomic character in *Euglena* Ehr. (*Euglenophyta*). *Arch. Hydrob. Suppl. Algol. Studies* **49:** 483-504

Zakryś B. (1994) *Euglena walnei* sp. nova (*Euglenophyta*) - a new species from Alabama (U.S.A.). *Arch.. Hydrob. Suppl. Algol. Studies* **72:** 9-11

Zakryś B. (0000) On the identity and variation of *Euglena agilis* Carter (=*E. pisciformis* Klebs). *Arch. Hydrob. Suppl. Algol. Studies* (in press)

Zakryś B., Kucharski R. (1996) Microevolutionary processes in *Euglena pisciformis* Klebs. Genetic drift or adaptation? *Arch. Hydrob. Suppl. Algol. Studies* **81:** 21-35

Zakryś B., Walne P. L. (1994) Floristic, taxonomic and phytogeographic studies of green Euglenophyta from the Southeastern United States, with emphasis on new and rare species. *Arch. Hydrob. Suppl. Algol. Studies* **72:** 71-114

Zakryś B., Walne P. L. (0000) Comparative ultrastructure of chloroplasts in the subgenus *Euglena* (*Euglenophyta*): taxonomic significance. *Cryptogamie, Algologie* (in press)

Zakryś B., Kucharski R., Moraczewski I. (1996) Genetic and morphological variability among clones of *Euglena pisciformis* Klebs based on RAPD and biometric analysis. *Arch. Hydrobiol. Suppl. Algo. Studies* **81:** 1-20

Zakryś B., Moraczewski I., Kucharski R. (0000) The species concept in *Euglena* in the light of DNA polymorphism analysis. *Arch. Hydrob. Suppl. Algol. Studies* (in press)

Zimand G., Valinsky L., Elad Y., Chet I., Manulis S. (1994) Use of the RAPD procedure for the identification of *Trichoderma* strains. *Mycol. Res.* **98:** 531-534

Received on 6th May, 1997; accepted on 4th July, 1997

Acta Protozoologica (1997) 36: 171 - 179

ACTA
PROTOZOOLOGICA

Ultrastructural Study of *Sphaeromyxa balbianii*, Thélohan 1892 (Myxozoa, Myxosporea: Bivalvulida), a Parasite of *Cepola macrophthalma*, Linnaeus 1758

María Pilar GRACIA, Pedro Andrés MAÍLLO, Josep Maria AMIGÓ and Humbert SALVADÓ

Laboratori de Protozoologia, Departament de Biologia Animal, Facultat de Biologia, Universitat de Barcelona, Barcelona, Spain

Summary. An ultrastructural study of *Sphaeromyxa balbianii* has been carried out for the first time. The parasite was found in the gall bladder of *Cepola macrophthalma* caught in the Catalan coasts (NW Mediterranean). The trophozoites of *S. balbianii* were polysporal plasmodia of big size (4-6 mm) and discoid shape. A variable number of plasmodia could be found free inside each gall bladder. The spores, proved to be one of the most defining parameters at species level. There were straight and sized 15.82 x 4.84 µm showing two polar capsules at the opposite ends. A discussion on the ultrastructure of the parasites as well as on the taxonomy of the genus *Sphaeromyxa* is provided.

Key words: *Cepola macrophthalma*, fish, gall bladder, Myxozoa, *Sphaeromyxa balbianii*, ultrastructure.

INTRODUCTION

Myxosporidia are parasites which are widely dispersed among fish (Lom and Dyková 1992). Most species have a fairly well-defined location for its host. Like all parasitic organisms, myxosporidians exert a certain pathogenic influence on their hosts, although the degree of pathogeny varies according to the parasite's biology and ecology, state of development, host's nutrition, stress level and immunological system. Parasites belonging to the genera *Myxobolus*, *Henneguya*, *Thelohanellus* and *Hoferellus* are usually considered among the most damaging. Of great importance in fish-breeding is *Myxobolus cerebralis*, which causes whirling disease of trout, and which has serious effects if it parasitises a vital organ (Markiw and Wolf 1983, Hamilton and Canning 1987). *Ceratomyxa shasta* Noble causes high mortality rates in Pacific salmon.

There are many species of histozoic and coelozoic myxosporidian parasites of sea fish, but very few intracellular ones. Histozoic myxosporidians are generally considered more pathogenic since they can cause changes such as hypertrophy and hyperplasia in the host's organs, altering the function of the parasitised organ. Studies of these organs performed with electron microscopy have provided data on their development and ultrastructure.

Address for correspondence: María Pilar Gracia, Laboratori de Protozoologia, Departament de Biologia Animal, Facultat de Biologia, Universitat de Barcelona, 08028 Barcelona, Spain; Fax: +34-3-4110887

Among studies of myxosporidian ultrastructure mention must be made of, among others, those of the ultrastructure of trophozoites, spores and sporogenesis carried out by Grassé and Lavette (1978a) and Lom and de Puytorac (1965b), on the ultrastructure and development of the polar capsule by Lom and de Puytorac (1965a), as well as those of Lom (1969) on the structure of some *Sphaeromyxa*. Other authors who have worked on the ultrastructure of myxosporidians are Cheisin et al. (1961), Uspenskaya (1966, 1969, 1971,1972), Schubert (1968), Current (1979), Desser and Paterson (1978), and Grassé and Lavette (1978b). Laird (1953) divided the genus *Sphaeromyxa* into two groups: 1) the 'balbianii' group with straight or slightly curved fusiform or ovoid spores, and with ovoid polar capsules; and 2) the 'incurvata' group with arched spores and pyriform polar capsules, although some species such as *S. pultai* (Tripathi 1953) and *S. maiyai* (Morrison and Pratt 1973) may present characteristics of both groups. In both groups, the ends of the spores may be rounded or truncated.

Sphaeromyxa balbianii is a coelozoic myxosporidian which lives in the liquid of the gall bladder, an environment free of mechanical alterations. It is wide-spread both in host species, having been found parasitising *Motella tricirrata, M. maculata, Cepola macrophthalma, Clupea pilchardus, Sychostoma floridae, S. lousienae, Tryglops murrayi,* and *Blennius pavo*, and geographically, having been found in fish from two French coasts: Mediterranean (Thélohan 1892, 1895) and Atlantic (Georgévitch 1916); from Italy (Parisi 1912); the US Atlantic coast (Davis 1917); Canada (Khan et al. 1986); and the Adriatic Sea (Lubat et al. 1989).

This work involved an ultrastructural study of *S. balbianii*, which parasitises the 'red band fish' (*Cepola macrophthalma*), a fish of no great commercial value but important given the quantities which are caught.

MATERIALS AND METHODS

The species studied, *Sphaeromyxa balbianii*, was extracted from the gall bladder of *Cepola macrophthalma,* a marine teleost caught in the western Mediterranean (Catalan coast). The prevalence of the parasite was studied for 4 months, studies being performed with optical microscope (phase-contrast), transmission electron microscope (TEM) and scanning electron microscope (SEM).

Optical microscope

The myxosporidian plasmodia were studied with a phase-contrast optical microscope. Fresh spore measurements (n=25) were obtained without phase- contrast. Extrusion of polar filaments for later measurement was induced with 5% KOH.

SEM study

Vegetative stages were prefixed with 2.5% glutaraldehyde in cacodylate buffer (0.1 M, pH 7.4, 2 h, 4°C) and postfixed with 2% OsO_4 in the same buffer (30 min). After washing with double-distilled water, the fixed plasmodia were freeze-dried (-60°C, 10^{-5} tor, 48 h), then sliced and metal coated with gold-palladium.

Spore were prefixed as for vegetative stage then placed on gold grids, postfixed with osmium vapour (12h), dried on air and metal coated with gold-palladium. Observations were made with a SEM Hitachi S 2300 at 15 kV.

Transmission electron microscope study

All developmental stages examined were prefixed with 2.5% glutaraldehyde in cacodylate buffer (0.1 M, pH 7.4, 2 h, 4°C) and postfixed with 2% OsO_4 in the same buffer (30 min), dehydrated with baths of increasing concentrations of acetone and finally embedded in Spurr resin to obtain 60 nm sections. Observations were made with a TEM Phillips EM 301 (S.C.T of Barcelona University) at 80 kV after contrasting according to Reynolds (1963).

RESULTS

During April, May, June and July, 1995, 220 specimens of *Cepola macrophthalma* were dissected. Size ranged from 18 to 55 cm; 147 (67%) were parasitised by *Sphaeromyxa balbianii*. Macroscopic examination of gall bladders allowed the parasitised vesicles to be distinguished since they were hypertrophied; this may cause pathogenic effects in the host. If the phosphatase on the surface of the plasmodium (Uspenskaya, 1966) acts on the wall of the gall bladder, it is possible that, since in some cases practically the entire vesicle is occupied by plasmodia, these might interfere with the bile secretion and, consequently, with the lipid metabolism.

Vegetative stage: varying numbers of plasmodial trophozoites (number of trophozoites ≤ 13), discoid and polysporal, were found in each vesicle, often positioned inside each other, wrapped by the biggest; fresh mean sizes: 4.27 mm length, 4.01 mm width, extremes 7 x 6 mm, 0.25 x 0.25 mm (Table 1).

SEM examination of the mature plasmodial endoplasm showed it to be very spongy with alveoli (Fig. 5); under transmission electron microscope (Fig. 4) the surface of the plasmodium showed microvillosities of variable size, and above these villosities an extracellular matrix consisting of two parts: an internal fibrillar part, and a granular, electron dense, external part (Fig. 6). At the base of

Table 1. Summary of data on some *Sphaeromyxa* species

Species Reference	Trophozoite	Spore		Polar Capsule	
		Shape	Size	Shape	Size
S. balbianii Thélohan (1895)	Up to 3-4 mm in diameter	Straight, fusiform, ends truncate	15-20 by 5-6 µm	Ovoid	7 by 4.7 µm
S. balbianii Lubat et al. (1989)	Up to 3-4 mm in diameter	Fusiform, ends truncate	15-23 by 5-9.5 µm	—	6 by 3 µm
S. balbianii Present work	Up to 6-7 mm in diameter	Fusiform, straight, ends truncate	15.82±4.65 by 4.84 ±0.79 µm	Oval	5.17±0.13 by 2.95±0.05 µm
S. ovula Noble (1938)	Up to 0.8 mm in diameter	Straight, elongate-oval, ends rounded	14 µm by 4.3 µm	Ovoid	5 by 3 µm
S. reinhardti Jameson (1929)	Very small	Straight or slightly curved, fusiform, ends truncate	21.25-23.3 by 3.75-5 µm	Ovoid	—
S. magna Zhukov (1964)	Up to 4 mm	Straight, ends truncate	23 µm by 6 µm	—	8.5 by 4 µm

Table 2. Data about the plasmodial surface of genus *Sphaeromyxa*

Plasmodial surface	Authors	Species
A single membrane	Lom and de Puytorac, 1965a Schubert, 1968 Current, 1979	*Henneguya psorospermica* *Henneguya pinnae* *Henneguya adiposa*
2 membranes	Desser and Paterson, 1978	*Myxobolus* sp.
1 membrane covered by a granular layer	Current and Janovy, 1978 Current et al., 1979	*Henneguya exilis* *Myxosoma funduli*
2 membranes covered in some cases by a granular layer	Lom and de Puytorac, 1965a Current and Janovy, 1976	*Zschokkella nova* *Henneguya exilis*
A syncytial wall bordered by 2 membranes	Desser and Paterson, 1978	*Myxobolus* sp.
1 membrane covered by strands of amorphous, sticky substance, probably mucin	Lom, 1969 Present work	*Sphaeromyxa* cf. *magna* *Sphaeromyxa balbianii*

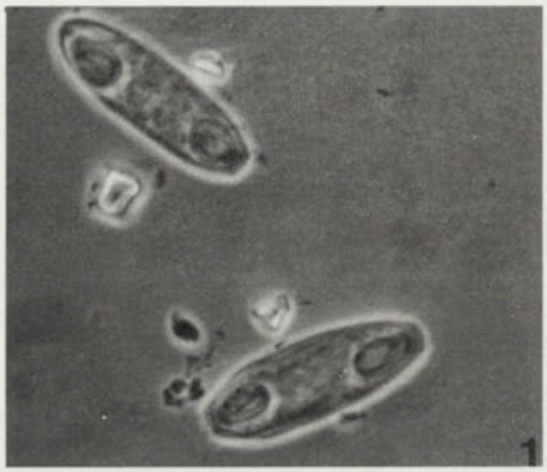

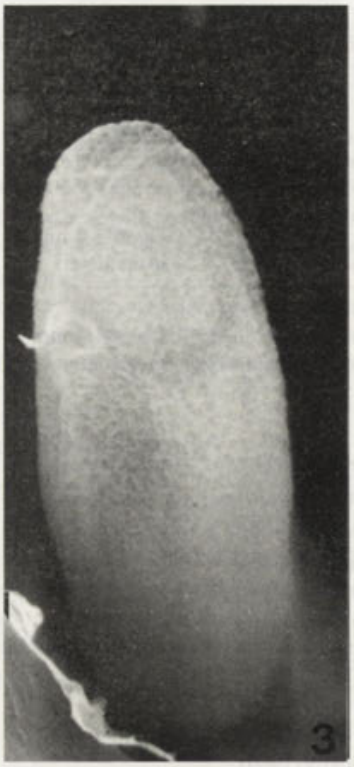

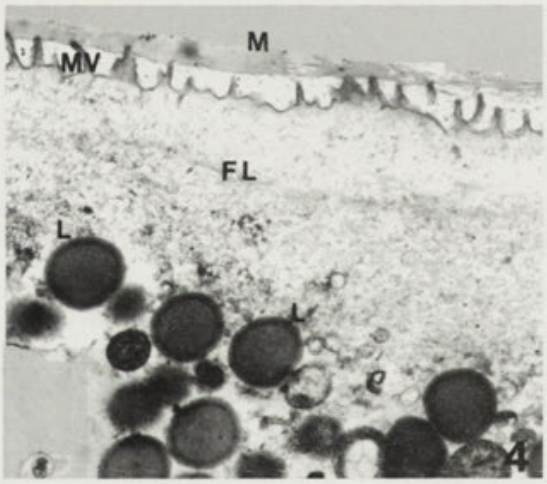

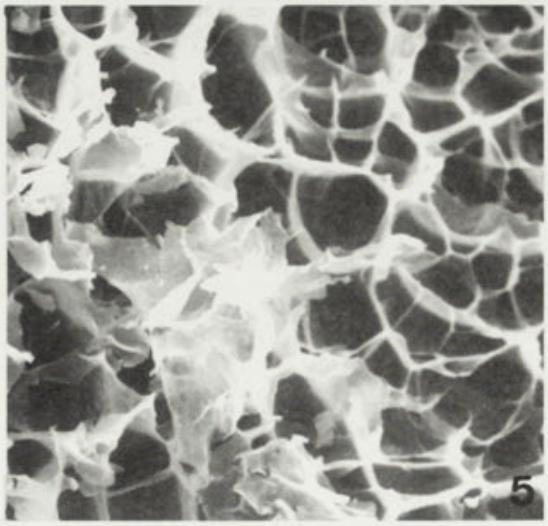

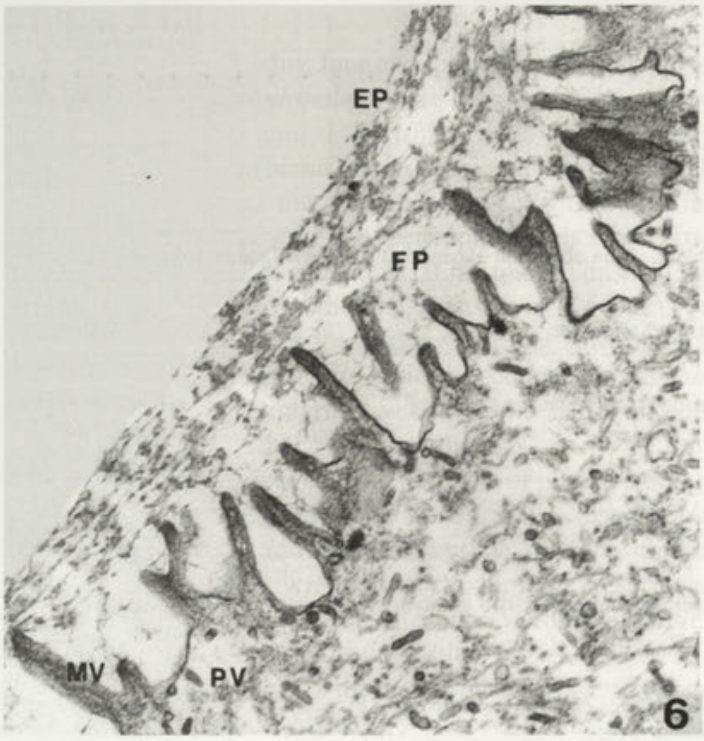

Fig. 1. Fresh spores of *Sphaeromyxa balbiani*, phase-contrast x1400. Fig. 2. Fresh spore of *S. balbianii* with both polar filaments extruded, phase-contrast x1400. Fig. 3. Immature spore within the plasmodium. Note the rounded apex, SEM x 10000. Fig. 4. Organization of the peripheral part of plasmodium. Extracellular matrix (M), microvillosities (MV), fibrillar layer (FL), lipid spherules (L), TEM x 9800. Fig. 5. Inner part of the plasmodium, SEM x 1200. Fig. 6. Detail of the plasmodium surface. Microvillosities (MV), electrodense part (EP), fibrilar part (FP), pinocytic vesicles (PV), TEM x 11000

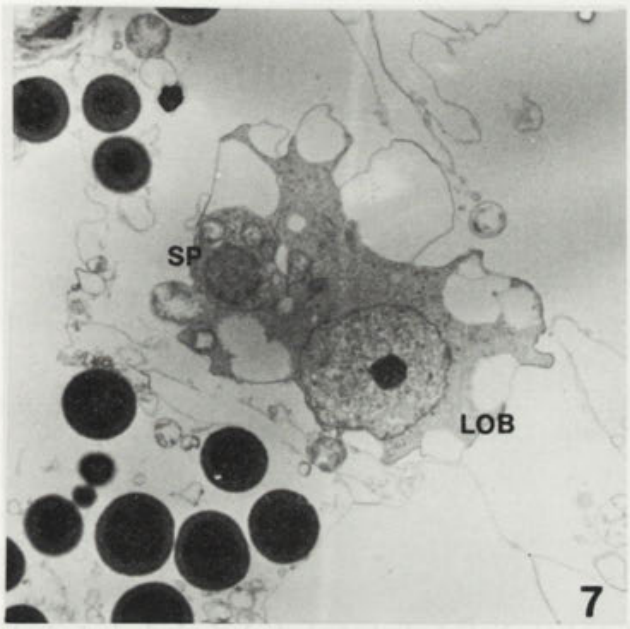

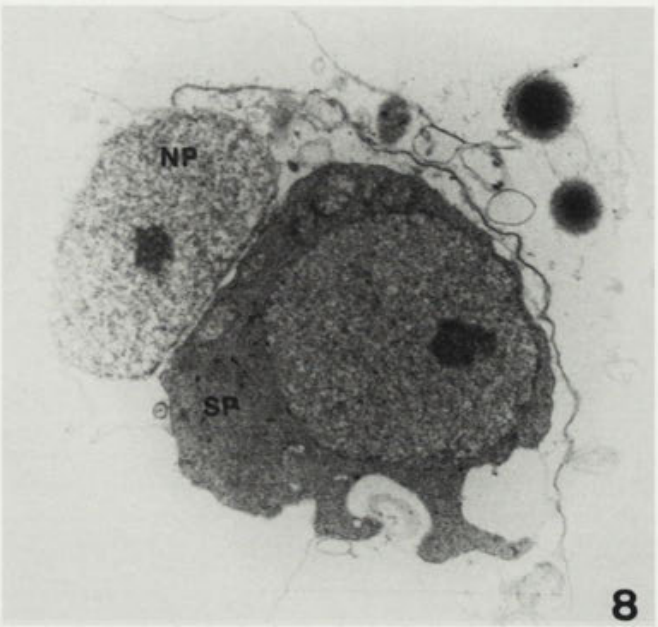

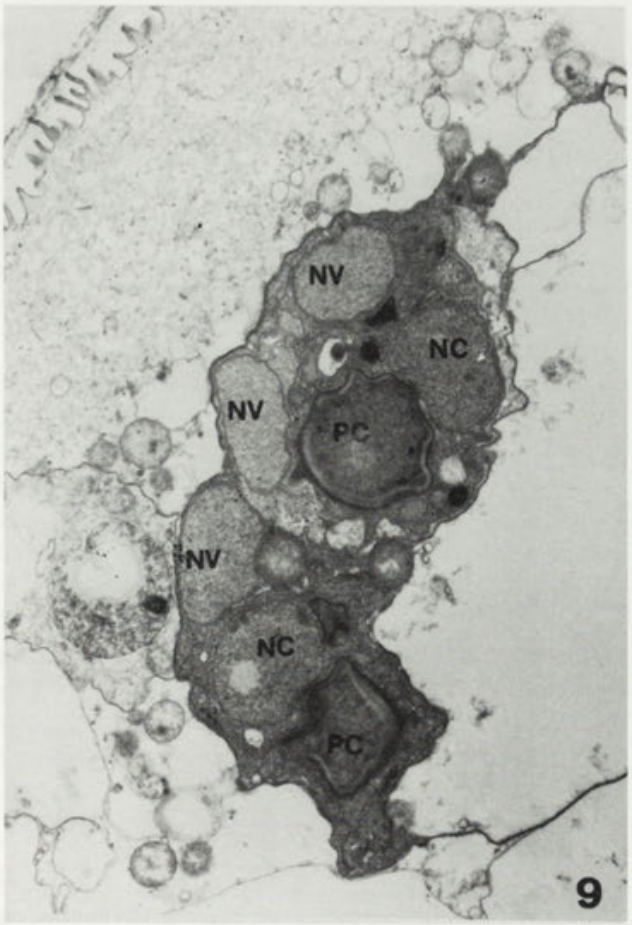

Fig.7. Lobocyte (LOB) ingesting a sporogonic cell (SP), TEM x9100. Fig. 8. Sporogonic cell (SP) with a conspicuous nucleole. Close to it the nucleous of a pericyte (NP) is evident, TEM x14700. Fig.9,10. Section of the medular part of the plasmodium with sporogenic stages. Polar capsule (PC), nucleous of the capsulogenic cell (NC), nucleous of the valves cells (NV), electrodense cap (C), manubrium (MB), valvar cell (VC), suture (S). Fig. 9. TEM x 9100, Fig. 10. TEM x 8430

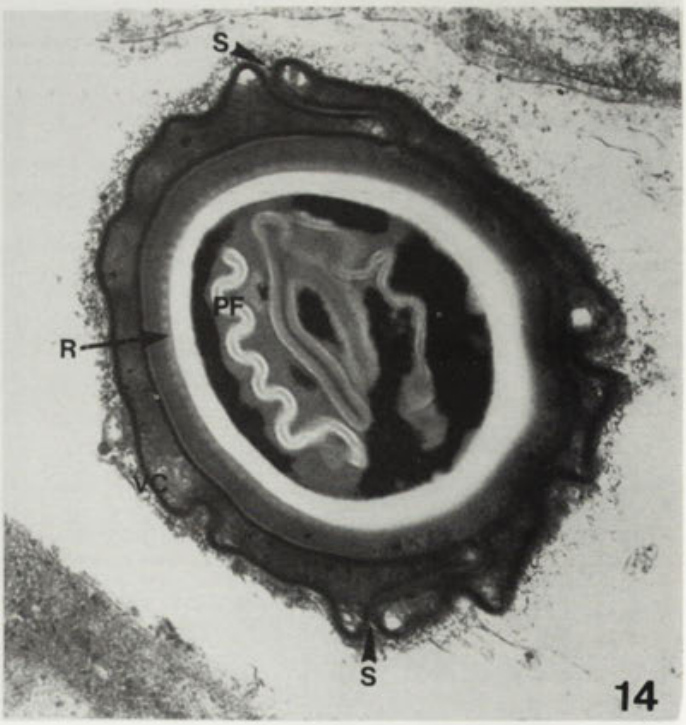

Fig. 11. Oblique section of an apical cell. Note the manubrium (MB) and the electrodense ribs (R) on the surface of the capsule, electrodense cap (C), TEM x 9100. Fig.12. Oblique section of a polar capsule. The undulated part of the polar filament is attached to a deep slit in the thick capsule wall. Note the apical cap (C), the valvar cells (VC) and the glycogen granules inside the capsule, (white arrow), TEM x 14520. Fig.13. Transverse section of a capsulogenic cell. Note the degenerated mitochondria (MI), the mielynic figures (MIE) and the polar filament (PF) with 4 longitudinal folds, TEM x 20100. Fig.14. Transverse section through on the level of the polar capsule. The polar filament (PF) makes 4 longitudinal folds in the capsule. Note the "S" shape suture (S) of the valvar cells (VC) and the longitudinal ribs (R) on the surface of the spore, TEM x 22350

the microvillosities there were endocytotic vesicles (Lom 1969, Current et al. 1979, Uspenskaya, 1982).

Plasmodial ectoplasm presents a layer of fibrils parallel to the surface (Fig. 4). Deeper in the ectoplasm there are large number of lipidic spherules, and in the endoplasm, with large alveoli, there are different types of cells: phagocytes or lobocytes, sporogonic cells, pericytes, and different stages of sporogenesis.

Sporogenesis and spores

Mature cells are situated in the center of the plasmodium. Different stages of sporogenesis (Figs. 9, 10), were observed in the reticulate endoplasm. A thorough examination showed that a number of different cell types can be observed in the plasmodium of this species: lobocytes, sporogenic cells (Fig. 7), pericytes enveloping sporogenic cells (Fig. 8). The sporogenesis is disporal since spores are formed in pairs (Fig. 9), despite that, the plasmodium is polysporic since many spores are formed within the plasmodium. The spores of *S. balbianii* are fusiform, straight, with truncated ends (Fig. 1), presenting longitudinal grooves on the valves. The truncated ends of spores indicate that the spores are already mature since the immature ones have rounded ends (Fig. 3). Fresh spores (Fig. 1) have a mean size of 15.82 ±4.65 x 4.84±0.79 µm. The spore is a pluricellular stage, and it consisted of 2 valval cells, 2 capsulogenic cells containing the polar filament, and the sporoplasm with two nuclei.

The suture line between the spore valves forms an "S" (Fig. 14). The two oval polar capsules are situated at opposite ends of the spore (equiporal spore). The extruded polar filaments are short and thick, with a mean length of 19.88±10.41 µm (Fig. 2). The polar filament is located inside the capsule, but the point of emergence of the polar filament is somewhat lateral, moreover the polar filament is a simple tube with 3-4 longitudinal creases (Figs. 12-14). The capsulogenic cell of *Sphaeromyxa balbianii* contains a cap covering the apex of the polar capsule, and a microtubular area around the polar capsule (Figs. 11, 12). Mean measurements of fresh polar capsules were 5.17±0.13 x 2.95±0.05 µm. The distance between polar capsules was 5.43±0.56 µm.

DISCUSSION

The ultrastructural data presented in this work are the first obtained on *Sphaeromyxa balbianii,* in a genus of which 31 species are known. For a long time the determination of myxosporidia was performed almost exclusively on the basis of the morphology of the spore (Schulman 1966). Currently classification follows the revision of Shulman's work made by Lom and Noble (1984), and is still based on spore morphology, although changes and improvements were introduced to make the classification less arbitrary. Consequently, for specific determination of myxosporidian parasites the morphological parameters of the spore, the characteristics of the host, and its location in the host are used.

The plasmodium of *Sphaeromyxa* is similar to that of *Myxidium, Zschokkella,* and *Chloromyxum* (Lom 1969), and like in coelozoic myxosporidians it is characterised by its discoidal shape. The size of plasmodia may vary considerably between different species of the same genus (Laird 1953, Lubat et al. 1989); in the case of *Sphaeromyxa balbianii* varied from 0.25 to 7 mm. These differences may be caused by the division of larger plasmodia, which leads us to wonder whether plasmodium size should not be an important characteristic to consider in determining the species of the genus *Sphaeromyxa*. Furthermore, the size and shape of the plasmodium is not usually an important character in the determination of the species, since in some species the plasmodium is unknown, so no comparison can be made. The arrangement of the plasmodia wrapped inside each other was also found by Morrison and Pratt (1973) in *Sphaeromyxa maiyai*, where the plasmodia may reach 1 to 2 cm.

The plasmodial microvillosities increase surface area of plasmodium, thus intensifying trophic functions, while the plasmodial fibrils, parallel to the ectoplasmic surface, provide consistency and elasticity. In the membrane, at the base of the microvillosities, there are pinocytotic vesicles with the formation of endocytosis (Lom 1969, Current et al. 1979, Uspenskaya 1982). Lom and de Puytorac (1965b) observed true pinocytotic activity. Observation of the microvillosities of the plasmodium of *S. balbianii* showed that they do not anastomose with each other as it happens in other *Sphaeromyxa* species (Uspenskaya 1982). This may be due to the different levels of phagogenicity of the various species of *Sphaeromyxa*. Data about the plasmodial surface have given rise to controversy: (see comparative data on Table 2) some authors have observed a single membrane (Lom and de Puytorac 1965a, Schubert 1968, Current 1979); others have observed 2 membranes (Desser and Paterson 1978); or 1 membrane covered by a granular layer (Current and Janovy 1978, Current et al. 1979); or 2 membranes covered in some cases by a granular layer (Lom and de Puytorac 1965a, Currrent and Janovy 1976); or even a syncytial wall bordered by 2 membranes (Desser and Paterson 1978), in the case of *S. balbianii* a single

membrane was observed, probably consisting of mucin segregated by the plasmodium in agreement with Lom (1969) observations over *Sphaeromyxa* cf. *magna*.

The definition of the morphological characteristics of the spores is essential for correct identification of the species. The spores of *Sphaeromyxa balbianii* found in *Cepola macrophthalma* show similarities with those of other species belonging to the 'balbianii' group (Table 1), such as the presence of grooves on the valves, their suture types, and their truncated ends when ripe, though unripe spores present rounded ends as was observed under SEM. Straight, fusiform spores have been described in *S. reinhardti* Jameson and in *S. ovula* Noble, but in both cases the plasmodia are smaller, 800 µm, with ends rounded in *S. ovula* and truncated in *S. reinhardti*, which differentiates these species from the one studied here.

In our case, (Table 1) sizes of *S. balbianii* trophozoites are greater than those obtained by other authors (Thélohan, 1892, Lubat et al. 1989). However, the spore seems to be smaller, but this is not easy to compare since we obtained a mean measure and previous measures were only a range. Nevertheless, the remaining characteristics of the species studied coincide completely with the original descriptions provided by Thélohan (1892, 1895): a trophozoite, folded upon itself, with forms an opaque body and occupies a variable part of the gall bladder, often constituted by numerous individuals. It is easy to observe with the naked eye inside the gall bladder, which is transparent; yellow or greenish-yellow. Ectoplasm with rounded lobes. Fusiform spores, with abruptly truncated ends of the spore. Short polar filament, conical, with a diameter that is almost the same as the width of the end of the spores.

Data presented here confirm the relatively homogeneous organisation of *Sphaeromyxa* species: as in other genera such as *Myxobolus, Henneguya, Thelohanellus, Zschokkella, Myxidium* and *Hoferellus* the pansporoblast originates from the association of 2 germinative cells, one of which, the pericyte, wraps around the other, the sporogonic cell. The essential differences among *Sphaeromyxa* species seem to lie in the morphology of the spores.

Lom (1969) suggested that the structure of the polar filament as a simple tube with longitudinal creases in the capsule is a characteristic of genus *Sphaeromyxa*, and such is also the case of *S. balbianii* as it can be observed in both longitudinal and transverse sections (Figs. 12-14). Moreover, some species such as *S.* cf. *magna* (Lom 1969) have no electron-dense hood over the capsule membrane, whereas others, e.g. *S. balbianii* and *S. sabrazesi*, (Grassé and Lavette 1978a) have this protective cap on the apical end.

Acknowledgements. This study was supported by DGICYT project PB-0807 from the Spanish Government.

REFERENCES

Cheisin E. M., Schulman S. S., Vinnichenko L. N. (1961) Structure of Myxobolus spores. *Tsitologiya* **3:** 662-667 (in Russian).

Current W. L. (1979) Henneguya adiposa Minchew (Myxosporida) in the channel catfish: ultrastructure of the plasmodium wall and sporogenesis. *J. Protozool.* **26:** 209-217

Current W. L., Janovy J. (1976) Ultrastructure of interlamellar Henneguya exilis in the channel catfish. *J. Parasitol.* **62:** 975-981

Current W. L., Janovy J. (1978) Comparative study of ultrastructure of interlamellar and intralamellar types of Henneguya exilis Kudo from channel catfish. *J. Protozool.* **25:** 56-65

Current W. L., Janovy J. Jr., Knight S. A. (1979) Myxosoma funduli Kudo (Myxosporida) in Fundulus kansae: ultrastructure of the plasmodium wall and sporogenesis. *J. Protozool.* **26:** 574-583

Davis H. S. (1917) The myxosporidia of the Beaufort region. A systematic and biologic study. *Bull. Bur. Fish.*, U.S. **35:** 201-243

Desser S. S., Paterson W. B. (1978) Ultrastructural and cytochemical observations on sporogenesis of Myxobolus sp. (Myxosporida: Myxobolidae) from the common shiner Notropis cornutus. *J. Protozool.* **25:** 314:326

Georgévitch J. (1916) Note sur les Myxosporidies recueillies à Roscoff. *Bull. Soc. Zool. France* **41:** 86-95

Grassé P. P., Lavette A. (1978a) La myxosporidie Sphaeromyxa sabrazesi et le nouvel embranchement des Myxozoaires (Myxozoa). Recherches sur l'état pluricellulaire primitif et considérations phylogénétiques. *Ann.Sci.Nat.Zool.(Paris)* **20:** 193-285

Grassé P. P., Lavette A. (1978b) Sur la reproduction des Myxosporidies et la valeur des cellules dites germinales. *C. R. Acad. Sci. Paris série D* **286:** 757-759

Hamilton A. J., Canning E. U. (1987) Studies on the proposed role of Tubifex tubifex (Müller) as a intermediate host in the life cycle of Myxosoma cerebralis (Hofer, 1903). *J. Fish Dis.* **10:** 145-151

Jameson A. P. (1929) Myxosporidia from Californian fishes. J. Parasitol. **16:** 59-68

Khan R. A., Bowering W. R., Burgeois C., Lear H., Pippy J. H. (1986) Myxosporean parasites of marine fish from the continental shelf of Newfoundland and Labrador. *Can. J. Zool.* **64:** 2218-2226

Laird M. (1953) The protozoa of New Zealand interdidal zone fishes. *Trans. Roy. Soc. N. Z.* **81:** 79-143

Lom J. (1969) Notes on the ultrastructure and sporoblast development in fish parasitizing myxosporidian of the genus Sphaeromyxa. *Z. Zellforsch.* **97:** 416-437

Lom J., Dyková I. (1992) Protozoan parasites of fishes. In: Developments in Aquaculture and Fisheries Science. Elsevier Science Publishers, Amsterdam, **26:** 159-235

Lom J., Noble E. R. (1984) Revised classification of the class Myxosporea Bütschli, 1881. *Folia Parasitologica* **31:** 193-205

Lom J., Puytorac P.-de (1965a) Studies on the myxosporidian ultrastructure and polar capsule development. *Protistologica* **1:** 53-65

Lom J., Puytorac P.-de (1965b) Observations sur l'ultrastructure des trophozoites de Myxosporidies. *C. R. Acad. Sci.Paris série D* **260:** 2588-2590

Lubat V., Radujkovic B., Marques A., Bouix G. (1989) Parasites des poissons marins du Montenegro: Myxosporidies. *Acta Adriat.* **30:** 31-50

Markiw M. E., Wolf K. (1983) Myxosoma cerebralis (Myxozoa: Myxosporea) etiologic agent of salmonid whirling disease requires tubificid worms (Annelida: Oligochaeta) in its life cycle. *J. Protozool.* **30:** 561-564

Morrison N. D., Pratt I. (1973) Sphaeromyxa maiyai sp. n. (Protozoa: Myxosporidea), coelozoic parasite of the Pacific tomcod, Microgadus proximus. *J. Protozool.* **20:** 214-217

Noble E. R. (1938) Two new Myxosporidia from Tide Pool fishes of California. *J. Parasit.* **24:** 441-444

Parisi B. (1912) Primo contributo alla distributione geografica dei missosporidi in Italia. *Atti soc. ital. sc. nat.* **50:** 283-290

Reynolds E. S. (1963) The use of lead citrate at high pH as an electron opaque stain in electron microscopy. *J.Cell Biol.* **17:** 208-212

Schubert G. (1968) Electronenmikroskopische Untersuchungen zur Sporenentwicklung von *Henneguya pinnae* Schubert (Sporozoa, Myxosporidia, Myxobolidae). *Z. Parasitenk.* **30:** 57-77

Schulman S. S. (1966) Myxosporidia of the fauna of the USRR. Nauka, Moscow-Leningrad (in Russian)

Thélohan P. (1892) Myxosporidies de la vésicule biliaire des poissons. Espéces nouvelles. *C. R. Acad Sci.Paris série D* **115:** 1091-1094

Thélohan P. (1895) Recherches sur les Myxosporidies. *Bull. Sci. Fr. Belg.* **26:** 100-394

Tripathi Y. R. (1953) Studies on parasites of Indian fishes. 1. Protozoa Myxosporidia together with a check list of parasitic protozoa described from Indian fishes. *Rec. Indian Mus.* **50:** 63-88

Uspenskaya A. V. (1966) On the mode of nutrition of vegetative stages of *Myxidium lieberkühni* (Bütschli). *Acta Protozool.* **4:** 81-89 (in Russian)

Uspenskaya A. V. (1969) Ultrastructure of some stages of development of *Myxidium gasterostei* Noble, 1943. *Acta Protozool.* **7:** 71-77 (in Russian)

Uspenskaya A. V. (1971) Ultrastructure of some species of Myxosporidia. *Materialy I. sjezda VOPR Baku* **1:** 93 (in Russian)

Uspenskaya A. V. (1972) Ultrastructure of polar apparatus of the myxosporidian *Sphaeromyxa cottidarum*. *Tsitologiya* **14:** 779-782 [in Russian]

Uspenskaya A. V. (1982) New data on the life cycle and biology of Myxosporidia. *Arch. Protistenkd.* **126:** 309-338

Zhukov E. V. (1964) Parasites of Chukotka fishes. III. Protozoa of marine and freshwater fishes. General conclusions. *Parasitol. Sb. Inst. Zool. Akad. Nauk SSSR* **22:** 224-253 (in Russian)

Received on 22nd November, 1996; accepted on 2nd June, 1997

Acta Protozoologica (1997) 36: 181 - 185

ACTA
PROTOZOOLOGICA

Digestion and Fermentation of the Microcrystalline Cellulose by the Rumen Ciliate Protozoon *Eudiplodinium maggii*

Tadeusz MICHAŁOWSKI

Department of Vertebrate Physiology, Zoological Institute, University of Warsaw, Warszawa, and The Kielanowski Institute of Animal Physiology and Nutrition, Polish Academy of Sciences, Jabłonna, Poland

Summary. The rumen ciliate protozoon *Eudiplodinium maggii* was grown *in vitro* in a medium containing microcrystalline cellulose. A positive correlation was found between the number of protozoa and the cellulose content of the culture medium ($r = 0.998$; $P < 0.01$). The ciliates readily engulfed and digested cellulose particles intracellularly, while the supernatant fraction of broken protozoa hydrolyzed microcrystalline cellulose to reducing sugars. Polyacrylamide gel electrophoresis (PAGE) combined with CMC-ase zymogram revealed β-endoglucanase activity in protozoal proteins precipitated from the supernatant fraction of bacteria-free broken protozoa. *Eudiplodinium maggii*, free of external bacteria, incubated with microcrystalline cellulose produced volatile fatty acids in the presence of chloramphenicol. The production rate was 19.1 and 6.3 pM VFA/protozoon/h for ciliates incubated with and without cellulose respectively. Acetate followed by butyrate were the main acids produced by *Eudiplodinium maggii* from microcrystalline cellulose.

Key words: β-endoglucanase activity, *Eudiplodinium maggii*, microcrystalline cellulose, rumen ciliate.

INTRODUCTION

Cellulose, the main polysaccharide of the plant cell wall exists in two forms i.e. amorphous and crystalline. These two forms differ from each other in susceptibility to enzymatic degradation. It is well known that numerous bacteria and fungi are able to break down amorphous cellulose but only a few of them can digest its microcrystalline form (Wood 1992).

Eudiplodinium maggii, one of the most common species of rumen ciliates (Dogiel 1927) is able to digest and ferment cellulose prepared from perennial rye grass, and swollen by treatment with phosphoric acid (Coleman et al. 1976, Coleman 1978). In addition supplementing the culture medium with microcrystalline cellulose raises the population density of this protozoon (Michałowski et al. 1991). One possible explanation for these findings could be the ability of *Eudiplodinium maggii* to use energy from crystalline cellulose for growth. The experiments presented in this paper were carried out in order to examine this hypothesis.

Address for correspondence: Tadeusz Michałowski, Department of Vertebrate Physiology, Zoological Institute, University of Warsaw, ul. Żwirki i Wigury 93, 02-089 Warszawa, Poland

MATERIALS AND METHODS

Ciliates

The ciliates originated from the rumen of a cow fed a hay-concentrate diet. One *Eudiplodinium maggii* population was initiated by picking the individuals with typical features of this ciliate species and inoculating them to the small volume (1 ml) of culture salt solution (see below). About 50 cells of protozoa were transferred to each culture

vessel. The ciliates were fed every day with a food consisting of powdered hay (60 %), barley flour (20 %) and wheat gluten (20 %) at the ratio of 1 mg/ 1 ml of culture/day. A volume of fresh salt solution equal to the culture volume was also added every day to give a final volume of 40 ml for each culture. The protozoa were subsequently cultivated by the method routinely used in the laboratory (Michałowski et al. 1986). Ciliates were transferred to the continuous culture system (Michałowski 1979) when populations reached a density of about 1000 cells/ml. Protozoa in the continuous cultures were given food consisting of powdered hay (60 %), microcrystalline cellulose (Sigmacell 20, No: S 3504; 25 %) and wheat gluten (15 %). The food was given at a ratio of 2 mg/1 ml culture/day, while the volume of each culture was about 1000 ml. The protozoa from these cultures were used for each experiment presented here.

Culture salt solution

The "*caudatum*" type salt solution (Coleman et al. 1972) was used as the liquid part of the culture medium for long-term cultivation of ciliates. However, sodium acetate in this solution was replaced by an equal amount of sodium bicarbonate when the production of volatile fatty acids (VFA) was measured.

Preparation the protozoa free of bacteria

The ciliates were separated from external bacteria and food debris by six fold sedimentation followed by 24 h incubation of protozoa with chloramphenicol (50µg/ml). Finally the ciliates were washed two times with cold "*caudatum*" salt solution, resuspended in a small volume of cold deionized water and disrupted or stored at -20° C.

Supernatant fraction of broken protozoa and protozoal proteins

The ciliates, free of bacteria, were homogenized in a glass homogenizer equipped with a teflon pestle and centrifuged for 10 min. at 12000 x g and 4° C. The supernatant fraction was collected and used for determination of the cellulolytic activity or for preparation of protozoal proteins. The proteins were precipitated from the supernatant fraction with ammonium sulphate at 80 % saturation. The proteins were centrifuged down at 20000 x g during 20 min, dissolved in cold deionized water (4° C) and dialyzed overnight against deionized water at 4° C. Finally the dialyzed proteins were lyophilized and stored at -20° C.

Long-term cultivation

Cultures of protozoa were initiated and cultivated as described previously (Michałowski et al. 1986). The food consisted of powdered hay (0.6 mg/1 ml/day), wheat gluten (0.15 mg/1 ml/day) and microcrystalline cellulose (Sigmacell 20) in three different doses i.e. 0.05, 0.125 and 0.25 mg/ml/day . The ciliates were cultured for 32 days with three cultures being run simultaneously on each kind of food. The control cultures were fed with hay and wheat gluten only. Samples for protozoa and bacteria counts were taken every 4 days and were fixed with 4 % formaldehyde solution.

Intake and digestion of cellulose by protozoa

Ciliates were separated from food debris by sedimentation and starved for 24 h. Microcrystalline cellulose (0.25 mg/ml) was then given to the protozoa and the suspension was incubated for 24 h at 38°C. Samples for determination of ciliates containing cellulose particles in the endoplasmic sacs were taken just before feeding and at 2, 6, 12 and 24 h post-feed. They were fixed as described above.

Volatile fatty acid production by protozoa

Protozoa, free of food debris and external bacteria, were suspended in "*caudatum*" salt solution containing sodium bicarbonate instead sodium acetate, and incubated for 24 h in the presence of microcrystalline cellulose (0.4 mg/ml) and chloramphenicol (50 µg/ml). Control cultures were incubated without cellulose. VFA concentration and protozoal numbers were measured just before the start of the incubation and after incubation for 6, 12 and 24 h.

Enzyme assay

The supernatant fraction of broken protozoa, prepared as described above (2 ml) was incubated with microcrystalline cellulose (5 mg) in 0.1 M Mc Ilvaine buffer (2 ml) at pH 5.5 and 38° C (Michałowski 1995). Reducing sugars in the digests were quantified just before the incubation was started as well as after 2, 6, 8 and 12 h of incubation.

Electrophoresis

Non-denaturating polyacrylamide gel electrophoresis (PAGE) of protozoal proteins was performed in Tris/glycine buffer (1 mM) at pH 8.8. A 7 % polyacrylamide gel was used. No stacking gel was prepared. Carboxymethylcellulose (CMC) at a concentration of 0.1 % was copolymerized with the polyacrylamide in order to prepare a CMC-ase zymogram. Tris/glycine buffer (10 mM and pH 8.8) was used to prevent CMC breakdown during protein migration. Electrophoresis was performed at a constant voltage of 94 V in a mini dual unit for slab gel preparation (Sigma). The electrophoretic separation was followed by incubation of the gel in 0.1 M Mc Ilvaine buffer (pH 5.5) for 30 min at 38° C (Michałowski 1995). The CMC-ase zymogram was prepared using 2,3,5 triphenyltetrazolium chloride solution (0.2 %) in 1 N NaOH according to Gabriel and Wang (1969), while proteins were stained by the Coomassie brilliant blue.

Bacterial test

The ciliates, incubated with and without chloramphenicol (50µg/ml), were disrupted in a glass homogenizer with a teflon pestle and the presence of bacteria was examined by the roll tube cultivation method as well as by incubation of homogenized material in the liquid culture medium (Anaerobe Laboratory Manual 1973) containing strips of Whatman No. 1 paper.

Chemical and microscopic analysis

Volatile fatty acids were determined qualitatively and quantitatively by gas chromatography according to Ranft (1973). Reducing sugars were measured colorimetrically using ortho-toluidine reagent (Sigma No. 635 kit). Protein was measured using the Sigma 610-A kit. Protozoa and bacteria were counted as described earlier (Michałowski et al. 1986). Total protozoa and the individuals containing the cellulose particles in endoplasmic sacs were counted separately when cellulose intake by ciliates was measured.

Chemicals

All the chemicals used were of analytical purity and were supplied by Sigma Chemical Co. Wheat gluten was prepared according to Klein (1933) and Pace (1955).

Statistical analysis

The Student t-test was used to compare the differences between mean values according to Ruszczyc (1970).

RESULTS

Long-term cultivation of ciliates

The population density of *Eudiplodinium maggii* in long-term cultures increased when the cellulose content of the culture medium was increased (Fig. 1). A positive correlation ($r = 0.998$, $p<0.01$) was found between the number of protozoa and the cellulose content in the medium. However, the number of bacteria did not change significantly ($p>0.05$).

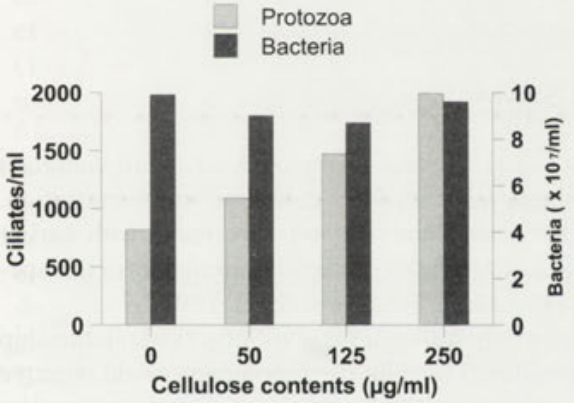

Fig. 1. The relationship between cellulose contents in the culture medium and the number of ciliates and bacteria (n = 24)

Engulfment and digestion of cellulose inside the protozoa

As many as 26.3±2.51 % of ciliates still contained cellulose particles inside the cells after the 24 h starvation period. The proportion of ciliates filled with cellulose increased to 96.0±1.01 % during the first 2 h after feeding and this increase was followed by a continuous decrease to 75.1±2.81 % 24 h after feeding. The proportion of ciliates filled with cellulose was 94.3±3.51, 92.0±2.08 and 88.1±1.73 % after 1, 6 and 12 h of incubation respectively (n = 5).

Reducing sugar assessment

Incubation of the supernatant fraction of broken protozoa with microcrystalline cellulose resulted in an increase ($p<0.01$) in the concentration of reducing sugars (Fig. 2). The concentration of these sugars, however, did not change significantly ($p>0.05$) when the supernatant fraction was incubated without cellulose. No reducing sugars were found when microcrystalline cellulose was treated with the ortho-toluidine reagent.

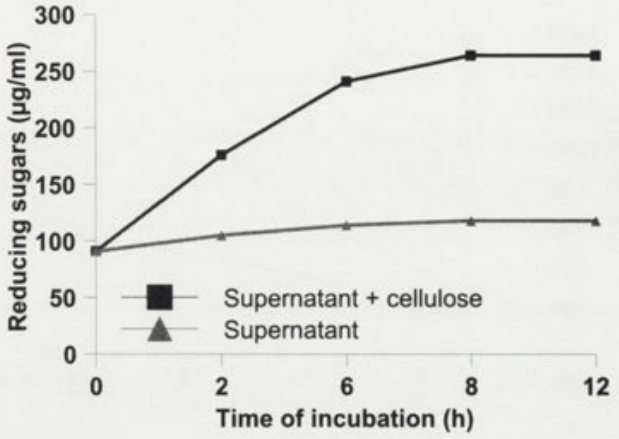

Fig. 2. The changes in concentration of the reducing sugars released from microcrystalline cellulose incubated with the supernatant fraction of broken protozoa (n = 3)

Electrophoresis

Non-denaturating polyacrylamide gel electrophoresis (PAGE) combined with CMC-ase zymogram revealed the presence of three protein bands active against carboxymethylcellulose i.e. being of a β-endoglucanase nature (Fig.3).

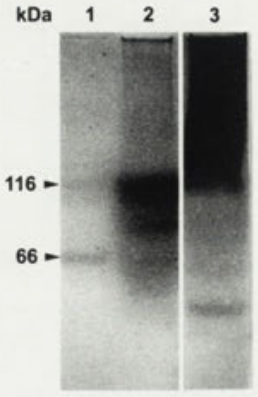

Fig. 3. PAGE of protozoal proteins combined with CMC-ase zymogram. Lane 1 - standard proteins (β-galactosidase - 116 kDa, albumin bovine - 66 kDa); lane 2 - CMC-ase activity visualized by staining with 2,3 5 triphenyltetrazolium chloride; lane 3 - protozoal proteins stained with Coomassie brilliant blue

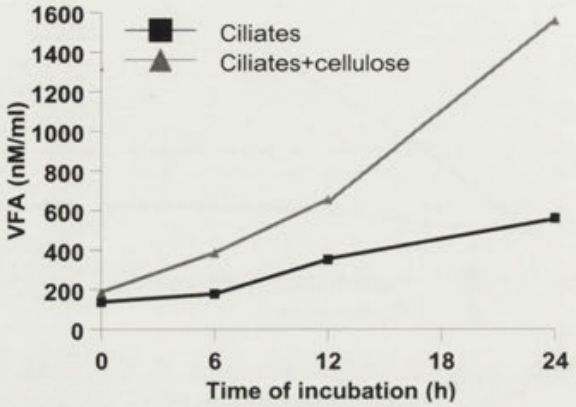

Fig. 4. Changes in the concentration of VFA during incubation of ciliates with or without microcrystalline cellulose (n = 5)

Volatile fatty acid production

Incubation of ciliates, free of external bacteria, with microcrystalline cellulose in the presence of chloramphenicol resulted in a continuous increase in VFA concentration from about 190 nM/ml at the start of the incubation to over 1550 nM/ml after 24 h ($p<0.001$). The concentration of volatile fatty acids in the control cultures (without cellulose) increased as a result of endogenous fermentation to only 560 nM/ml (Fig. 4). The differences between the concentration of VFA in experimental and control cultures noted at 6, 12 and 24 of incubation were statistically significant ($p<0.01$). The production rate of volatile fatty acids by protozoa incubated with microcrystalline cellulose was three times higher than by protozoa incubated without the polysaccharide (Fig. 5). It was calculated that 13.1±2.61 pM of VFA were produced per protozoon per hour. Acetate followed by butyrate were the main acids produced by *Eudiplodinium maggii* incubated both with cellulose and endogenously.

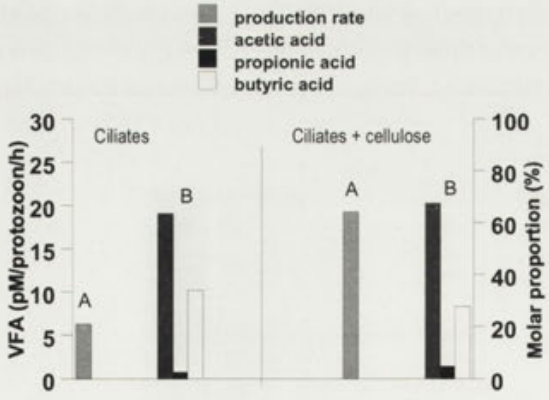

Fig. 5. The production rate of VFA (A) and molar proportion of particular acids (B) (n = 5)

Bacterial test

The ciliates from the both types of cultures mentioned above, as well as other protozoa incubated with and without chloramphenicol were examined for presence of intracellular cellulolytic bacteria. Neither the roll tube test nor incubation of broken protozoa in the liquid medium for over 3 weeks showed any presence of bacteria inside the ciliates when they were incubated with chloramphenicol for 24 h prior to disruption. Bacteria were, however, present when the antibiotic was omitted.

DISCUSSION

This study showed that growth of *Eudiplodinium maggii* was supported by cellulose supplementation. Thus the results are in good agreement with earlier findings concerning the growth requirements of this species of protozoa (Michałowski et al. 1991).

At least two explanations of the observed relationship seem possible. The cellulose supplement could improve the growth of associated bacteria which were ingested by the protozoa; the digestion of the bacteria would stimulate the development of the protozoal population. Alternatively the cellulose, as an additional source of energy, could influence the ciliates directly. This second hypothesis seems more probable as the number of bacteria was similar in all cultures of protozoa. Thus, the amount of nutrients supplied by bacteria also seems to be similar.

The ciliates readily engulfed the cellulose particles which then disappeared gradually from the cells. This was probably the results of their digestion in the endoplasm of protozoa. This suggestion is supported by the ability of the supernatant fraction of broken protozoa to release reducing sugars from cellulose. A similar ability was found earlier by Coleman (1978). However, no crystalline cellulose was used there. Thus the results presented in this paper suggest that *Eudiplodinium maggii* is able to digest this form cellulose which is more resistant to cellulolytic enzymes (Wood 1992).

Further support for this suggestion seems to be the presence of β-endoglucanase type enzymes as shown by CMC-ase zymogram. These results are in good agreement with the data presented by Bonhomme et al. (1986) in

relation to *Polyplastron multivesiculatum*. Three β-endoglucanases were found there by isoelectrofocusing and chromatofocusing methods.

Further support for the hypothesis mentioned above is the ability of *Eudiplodinium maggii* to ferment microcrystalline cellulose. The production rate of VFA from microcrystalline cellulose and proportion of particular acids found in this study are in good accordance with the data obtained by Coleman (1978) concerning the fermentation of cellulose prepared from perennial rye grass.

A very important problem is the origin of the enzymes involved in digestion of microcrystalline cellulose inside the cells of ciliates. Active β-endoglucanases were present in protozoal proteins in spite of bacteria suppression by incubation of the ciliates with chloramphenicol; similar effect of antibiotics was found by Bonhomme et al. (1986). No viable bacteria were found inside the cells of these ciliates. Moreover Williams and Ellis (1985) have found that most active subcellular fractions separated from disrupted *Polyplastron multivesiculatum* did not contain bacteria. Thus the suggestion is feasible that enzymes involved in the intracellular breakdown of microcrystalline cellulose by *Eudiplodinium maggii* were indeed of protozoal origin. This suggestion seems to be supported by the results of Benyahya et al. (1992) and Bohatier et al. (1990) who examined the cellular mechanism of the cellulosic material breakdown by *Epidinium ecaudatum* and *Polyplastron multivesiculatum*. However further confirmatory investigations by genetic methods are necessary to confirm the hypothesis that the rumen ciliate protozoon *Eudiplodinium maggii* is capable of producing cellulolytic enzymes.

REFERENCES

Anaerobe Laboratory Manual. (1973) Eds. L.V. Holdeman and W. C. E. Moore. VPI Anaerobe Laboratory, Virginia Polytechnic Institute State University. Blacksburg: Southern Printing Co.

Benyahya M., Sénaud J., Bohatier J. (1992) Colonisation et dégradation de fragments de paille de blé par les ciliés du rumen *Epidinium, Entodinium et Isotricha*: étude en microscopie électronique. *Ann. Sci. Nat. Zool. Paris 13e série*, **13:** 103-119

Bohatier J., Sénaud J., Benyahya M. (1990) In situ degradation of cellulose fibers by the entodiniomorph ciliate *Polyplastron multivesiculatum*. *Protoplasma* **154:** 122-131

Bonhomme A., Fonty G., Foglietti M. J, Robic D., Weber M. (1986) Endo-1,4-β-glucanase and β-glucosidase of the ciliate *Polyplastron multivesiculatum* free of bacteria. *Can. J. Microbiol.* **32:** 219-225

Coleman G. S. (1978) The metabolism of cellulose, glucose and starch by the rumen ciliate *Eudiplodinium maggii*. *J. Gen. Microbiol.* **107:** 359-366

Coleman G. S., Davies J. I., Cash M. A. (1972) The cultivation of the rumen ciliates *Epidinium ecaudatum caudatum* and *Polyplastron multivesiculatum in vitro*. *J. Gen. Microbiol.* **75:** 509-521

Coleman G. S., Laurie J. I, Bailey J. S., Holdgate S. A. (1976) The cultivation of cellulolytic protozoa isolated from the rumen. *J. Gen. Microbiol.* **95:** 144-150

Dogiel V. A. (1927) Monographie der Familie *Ophryoscolecidae*. *Arch. Protistkd* **59:** 1-280

Gabriel O., Wang S. F. (1969) Determination of enzymatic activity in polyacrylamide gels. *Anal. Biochem.* **27:** 545-554

Klein G. (1933) Handbuch der Pflanzenanalyse. Springer Verlag, Vien

Michałowski T. (1979) A simple system for continuous culture of rumen ciliates. *Bull. Acad. pol. Sci. Ser. Sci. Biol.* **27:** 581-583

Michałowski T. (1995) Ability of the rumen ciliate protozoon *Eudiplodinium maggii* to digestion and fermentation of microcrystalline cellulose. In: Abstracts of the Satellite Symposium "Rumen Microbiology" of IVth International Symposium of the Nutrition of Herbivores 1995. INRA Clermont-Ferrand, France 16

Michałowski T., Muszyński P., Landa I. (1991) Factors influencing the growth of rumen ciliates *Eudiplodinium maggii in vitro*. *Acta Protozool.* **30:** 115-120

Michałowski T., Szczepkowski P., Muszyński P. (1986) The nutritive factors affecting the cultivation of the rumen ciliate *Diploplastron affine in vitro*. *Acta Protozool.* **25:** 419-426

Pace J. (1955) Seed proteins. In: Modern Methods of Plant Analysis, (Eds. K. Peach and M. V. Tracey), Springer Verlag, Berlin, Göttingen, Heidelberg, 69-105

Ranft A. (1973) Gaschromatographische Bestimmung kurzkettiger flüchtiger Fettsäuren im Pansensaft. *Arch. Tierernähr.* **23:** 343-352

Ruszczyc Z. (1970) Metody Badań Zootechnicznych. PWRiL, Warszawa

Williams A. G., Ellis A. B. (1985) Subcellular distribution of glycoside hydrolase and polysaccharide depolymerase enzymes in the rumen entodiniomorphid ciliate *Polyplastron multivesiculatum*. *Curr. Microbiol.* **12:** 175-182

Wood T. M. (1992). Microbial enzymes involved in the degradation of the cellulose component of plant cell walls. In: The Rowett Research Institute Annual Report (Eds. I. Bremner and C. Cook). The Rowett Research Institute, 10-24

Received on 14th March, 1997; accepted on 3rd June, 1997

Acta Protozoologica (1997) 36: 187 - 196

ACTA
PROTOZOOLOGICA

Anionic Domains on the Cytoplasmic Surface of the Plasma Membrane of *Acanthamoeba castellanii* and their Relation to Calcium-binding Microregions

Andrzej SOBOTA[1], Kazimiera MROZIŃSKA[1] and Victor I. POPOV[2]

[1] Department of Cell Biology, Nencki Institute of Experimental Biology, Warszawa, Poland; [2] Institute of Cell Biophysics, Pushchino, Moscow Region, Russia

Summary. In this report we further characterize the plasma membrane microregions involved in formation of the calcium-dependent, electron-opaque structures. We used ruthenium red, a highly positively charged molecule to reveal clustered anionic sites on the cytoplasmic surface of the plasma membrane. To examine the presence of microregions of anionic phospholipids on this membrane polymyxin B was applied. Using conventional electron microscopy, X-ray microanalysis and freeze-etch techniques we demonstrated that in permeabilized cells, ruthenium red enters the cell interior and forms prominent globular structures located on the cytoplasmic surface of the plasma membrane. The size, location and X-ray elemental microanalysis indicated that ruthenium red-evoked structures are very similar to the submembrane calcium-structures. Polymyxin B significantly interferes with the formation of calcium-induced electron-opaque structures. Our findings indicate that negatively charged plasma membrane constituents may be organized as microdomains in response to calcium ions as well as to polycations (ruthenium red, some proteins) and finally electron-opaque structures on the cytoplasmic surface of the plasma membrane are formed.

Key words: *Acanthamoeba castellanii,* anionic domains, calcium structures, ruthenium red-binding structures.

INTRODUCTION

Wide interest has been focused on the role of calcium ions in the regulation of physiological processes occurring at the plasma membrane level, such as ion transport, endocytosis, exocytosis, membrane fusion (Augustine et al. 1987, Cheek and Barry 1993, Livett 1993, Bark and Wilson 1994, Goldin et al. 1994). These divalent cations may induce drastic changes in the structure of membranes (van Dijck et al. 1978, Haverstick and Glaser 1987, Sobota et al. 1993) as well as facilitate interactions of some submembrane proteins with the membrane (Scott et al. 1990, Bazzi and Nelsestuen 1991, Burgoyne et al. 1994, Swairjo and Seaton 1994).

The structural changes in the membrane induced by calcium ions are mainly conditioned by interactions with anionic membrane phospholipids (Tilcock and Cullis 1981, Haverstick and Glaser 1987). It is now well documented that calcium ions may cross-link phosphatidylserine anionic headgroups, providing phase separation and leading to formation of rigid domains of these lipids in bilayer membranes (for review see: Gennis 1989).

Cytochemical studies have revealed calcium-containing, electron-opaque structures "embedded" into the cytoplasmic surface of plasma membrane. The Ca-struc-

Address for correspondence: Andrzej Sobota, Departament of Cell Biology, Nencki Institute of Experimental Biology, ul.Pasteura 3, 02-093 Warszawa, Poland; Fax: (48) 22 225342; E-mail: sobota@nencki.gov.pl

tures appeared only in cells fixed and processed for electron microscopy in the presence of calcium ions (Oschman et al. 1974, Skaer et al. 1974, Sobota 1985). It was suggested that the appearance of the Ca-structures reflects the presence of special membrane constituent and submembrane proteins responsible for binding calcium ions and formation of Ca-dependent, electron-opaque aggregates (Sobota 1985). Anionic phospholipids, certain calcium-sensitive, phospholipid-binding proteins (e.g. annexins) and spectrin/F-actin aggregates are considered as compounds involved in the formation of the matrix of calcium-structures (Sobota 1989).

Calcium interacting with membrane phospholipids and proteins may be selectively replaced by some organic polycations. One of them is polymyxin B (PXB) which has a net of 6 positively charged groups and is used as a probe in studies of anionic phospholipid domains in the plasma membrane (Teuber and Miller 1977, Bearer and Friend 1982, Burt and Langer 1983, Langer 1984, Murphy and Martin 1984, Moggio and Bonilla 1985). Another suitable marker for detection of anionic groups on the plasma membrane, is ruthenium red (RR), a hexavalent polycationic dye. Ruthenium red is impermeable for intact cells and has been used mostly as a histochemical stain for acidic glycosaminoglycans located in the peripheral coat (Luft 1971). However, it was recently shown that ruthenium red inhibits the activity of the Ca^{2+}-pump by interacting with anionic phospholipids (Missiaen et al. 1990). Also, ruthenium red selectively binds to the calcium-binding sites of "EF-hand" proteins such as calsequestrin, calmodulin, troponin C, S-100 (Charuk et al. 1990).

The aim of the present report is to determine whether clusters of anionic components of the plasma membrane which are responsible for binding of calcium as well as some polycations. In order to distinguish the possible role of anionic phospholipids in the formation of the calcium structures polymyxin B was applied.

MATERIALS AND METHODS

Cultures

Acanthamoeba castellanii (Neff strain, obtained from Dr. J. Michejda, Poznań, Poland) was cultured axenically in proteose peptone/yeast extract/glucose medium as described earlier (Sobota et al. 1984). Cells (ca. 10^6 cells per ml) from 7-day-old cultures were harvested by low-speed centrifugation (1000 x g, 2 min) and the resulting pellet was washed twice with 120 mM NaCl solution containing 20 mM Hepes buffer, pH 7.4, and then treated with pronase (1-1000 mg/ml) prepared in the NaCl/Hepes buffer, for 1 h at 25°C.

Transmission electron microscopy

The pronase treated cells were washed in NaCl/Hepes solution and resuspended in fixative solution containing: ruthenium red (1 mg/ml, FLUKA, Switzerland),2.5% glutaraldehyde,100 mM NaCl,20 mM cacodylate buffer (pH 7.4). The fixation was carried out for 1 h at 20°C. Some pronase-treated cells, after washing, were resuspended in NaCl/Hepes solution supplemented with cationized ferritin (1 mg/ml, Sigma, USA) and incubated for 30 min, at room temperature, and after fast washing in NaCl/Hepes buffer were fixed (1 h, 20°C) in 2.5% glutaraldehyde/100 mM NaCl/20 mM cacodylate buffer. The samples were then rinsed in NaCl/cacodylate buffer and postfixed with or without 1% OsO_4/100 mM NaCl/50 mM cacodylate buffer for 1 h at room temperature. After dehydration in a graded series of ethanol, the samples were embedded in Epon/Araldite resin. Ultrathin sections were stained with uranyl acetate and lead citrate and observed in a JEM 100B electron microscope.

Cells not exposed to enzyme but treated with polycationic dyes or cells treated with enzyme but not incubated with the probes were applied as controls.

Electron-opaque calcium-structures were visualized as described elsewhere (Sobota et al. 1978). Briefly, the cells were fixed in 2.5% glutaraldehyde/100 mM NaCl/25 cacodylate buffer, supplemented with 5 mM $CaCl_2$, pH 7.4. All subsequent steps such as washing and fixation with osmium tetroxide were performed in the presence of 5 mM $CaCl_2$. Dehydrated samples were embedded in Epon/Araldite epoxy resin. Sections were stained with uranyl acetate and lead citrate and examined under a JEM 100B electron microscope. In some experiments before glutaraldehyde/Ca^{2+} fixation the living cells were incubated with PXB (1 - 5 mM, Sigma, USA) prepared in 100 mM NaCl/20 mM phosphate buffer, pH 7.4 (as indicated in the results).

Freeze-etching

Cells were fixed with 2% glutaraldehyde/100 mM sodium cacodylate buffer, pH 7.5 with or without 5 mM $CaCl_2$ (30 min, 20°C). In some experiments, prior to fixation, the cells were pretreated with 1 mM PXB (15 min, 20°C) prepared in 100 mM NaCl/20 mM phosphate buffer, pH 7.4, followed by glutaraldehyde fixation. The pelleted material was cryoprotected by 10 min immersion at 4°C in 10% methanol/100 mM sodium cacodylate buffer. The samples were quickly frozen within about 0.1 s by plunging them into propane (about -180°C) cooled with liquid nitrogen. The copper holders together with the samples were transferred from liquid nitrogen through the airlock into a vacuum chamber. All operations were carried out at a vacuum of 2-4 x 10^{-6} tor. Etching was performed for 40-50 min at -100°C. Platinum/carbon and carbon were used for replicas. The whole procedure was performed in a freeze-etching apparatus according to Popov et al. (1994). Replicas were floated on water, washed with 60% HNO_3 containing 4% $K_2Cr_2O_7$ during 2-4 h, and finally collected on grids. The samples were examined under a JEM 100B electron microscope.

X-ray microanalysis

For microanalysis studies two kinds of samples were prepared: (1) cells fixed with Ca/glutaraldehyde solution; (2) cells pretreated with pronase followed by ruthenium red/glutaraldehyde fixation. Epon-embedded samples, non-osmicated and non-stained, were sectioned (ca. 120 nm thick) and analyzed for elemental composition in an electron microscope JEOL 1200 EX equipped with a Link Analytical AN 10000

X-ray microanalysis system. The analysis was performed in spot mode at an excitation voltage of 80 kV; the counting time was 100 to 200 s. The diameter of the spot was 40 nm.

RESULTS

Electron-opaque structures

Acanthamoeba cells fixed with glutaraldehyde containing calcium ions displayed numerous electron-opaque structures along the cytoplasmic surface of the plasma membrane (Fig. 1A). The appearance of the structures was limited by the presence of calcium ions in fixation and washing solutions. The formed Ca-structures were ellipsoidal in shape (60-80 nm in diameter) and were distributed along the cytoplasmic surface of the plasma membrane as demonstrated earlier (Sobota 1985).

The structures, similar in shape and location, were observed in permeabilized cells exposed to ruthenium red. Pretreatment of living *Acanthamoeba* cells with pronase (1-10 mg/ml) caused permeabilization of the plasma membrane and partial damage of the cytoplasm as checked by a trypan blue test (data not shown). When the enzyme-permeabilized cells were fixed in glutaraldehyde/Ca solution, no Ca-structures were found (not shown). However, if the enzyme-treated cells were fixed with glutaraldehyde supplemented with ruthenium red (without calcium ions), electron-opaque structures were seen on the cytoplasmic surface of the membrane (Figs. 1B, C). The location and size of the ruthenium red-structures (RR-structures) were very similar to those of the structures seen in cells processed with calcium ions in the fixative (compare Figs. 1B, C with Fig. 1A).

The appearance of RR-structures was dependent on the enzyme concentration used for cell permeabilization. The RR-structures were observed after the treatment of living cells with low concentrations of pronase (1-10 mg/ml) (Figs. 1B, C). However, no RR-structures were found if the cells were pretreated with very high pronase concentration (1 mg/ml) (not shown). In cells fixed with glutaraldehyde/RR but not pretreated with enzymes, no electron-opaque structures were displayed and only a tiny coat on cell surface was decorated by the dye (Fig. 1D).

When pronase (10 mg/ml) treated cells were incubated with cationized ferritin (1 mg/ml) for 30 min followed by glutaraldehyde fixation (without calcium) some electron-opaque structures corresponding to those seen in cells prepared with calcium-containing fixative were also found at the plasma membrane (Fig. 1E).

X-ray microanalysis

X-ray microanalysis of the RR-structures revealed Si, P, Cu, Ru and vestigial amounts of Ca. The signals for phosphorus, ruthenium, and minute amounts of calcium seem to be characteristic of the RR-structures (Fig. 2A). Cytoplasmic areas adjacent to the RR-structure did not generate the P, Ru, Ca signals (Fig. 2B).

When the X-ray spectrum of Ca-structures (Fig. 2C) was compared with that generated from neighboring fields of cytoplasm, devoid of the electron-opaque material (Fig. 2D), phosphorus and calcium were detected as characteristic elements of Ca-structures. Also, several elements such as Si, Cl, Cu and minute amounts of others present in these spectra may be attributed to resin, copper grid, and residue of vapour silicon oil from the electron microscope system. Thus the analysis of the RR-structures as well as of Ca-structures indicates phosphorus to be the element involved, in combination with either calcium or ruthenium, in the formation of the corresponding structures.

Effect of polymyxin B

Formation of calcium-structures was significantly influenced by incubation of cells with PXB. Pretreatment of living cells with 1 mM PXB for 15 min at room temperature followed by glutaraldehyde/Ca fixation in the presence of the drug (1 h, 20°C) significantly disordered the formation of Ca-structures. Thin section analysis of the samples showed that submembrane calcium-structures formed under these conditions displayed numerous differences. Both number and size of the calcium-structures varied significantly, and considerable damage in the cytoplasm could be seen (Fig. 3A). The effect of PXB was much more pronounced when the cells were exposed to 5 mM PXB for 30 min followed by overnight fixation with glutaraldehyde/Ca in the presence of PXB. As a result, the Ca-structures were reduced dramatically in size and only tiny structures located close one to another were discernible at high magnifications. The structures seemed to be the part of the cytoplasmic leaflet of the membrane (Fig. 3B).

Freeze-fracture

When glutaraldehyde/Ca fixed cells were examined by freeze-etching, Ca-structures were seen as volcano-shaped knobs on the PF face of plasma membrane (Fig. 4A). On the fractured surface numerous, randomly distributed intramembrane particles (IMP) were found. The surface of the knob area was almost devoid of IMP, and only a few of them could be seen.

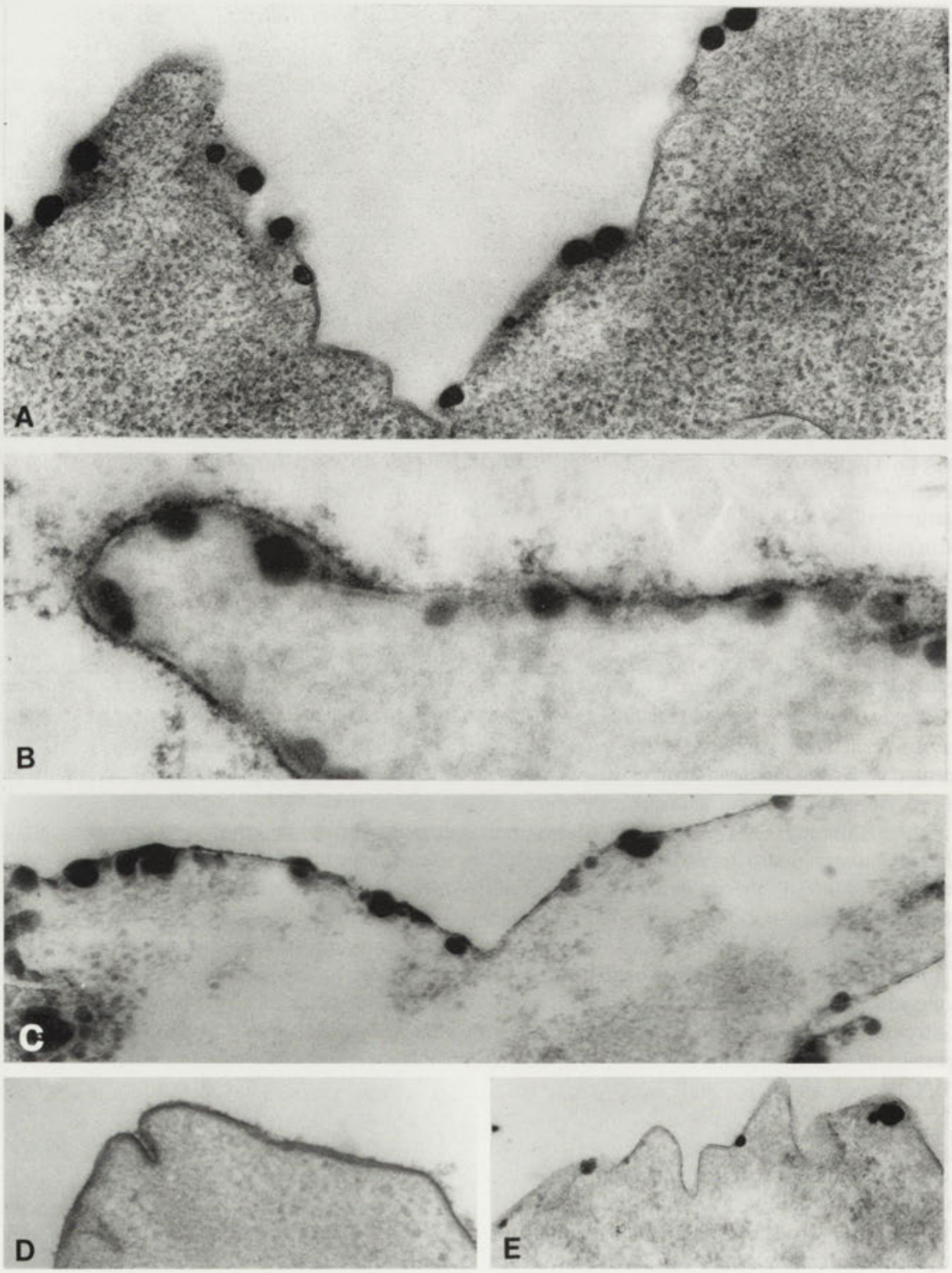

Figs. 1 A-E. Ruthenium red induces the appearance of electron-opaque structures on the cytoplasmic surface of the plasma membrane of *Acanthamoeba castellanii* which are similar to those induced by calcium. A - cells fixed with glutaraldehyde/Ca solution displayed numerous electron-opaque structures on the cytoplasmic surface of the plasma membrane, x 50000; B-C - cells pretreated with pronase followed by glutaraldehyde fixation in the presence of ruthenium red displayed RR-dependent electron-opaque structures on the cytoplasmic surface of the plasma membrane, B - pronase 1 mg/ml, x 115000; C - pronase 10 mg/ml, x 75000; D - non-pronase treated cells fixed in glutaraldehyde/ruthenium red solution. Only a tiny coat on cell surface was decorated by ruthenium red, x 60000; E - pronase-treated and cationic ferritin-exposed cells fixed in glutaraldehyde (without calcium ions) show electron-opaque structures on the cytoplasmic surface of the plasma membrane, x 48000

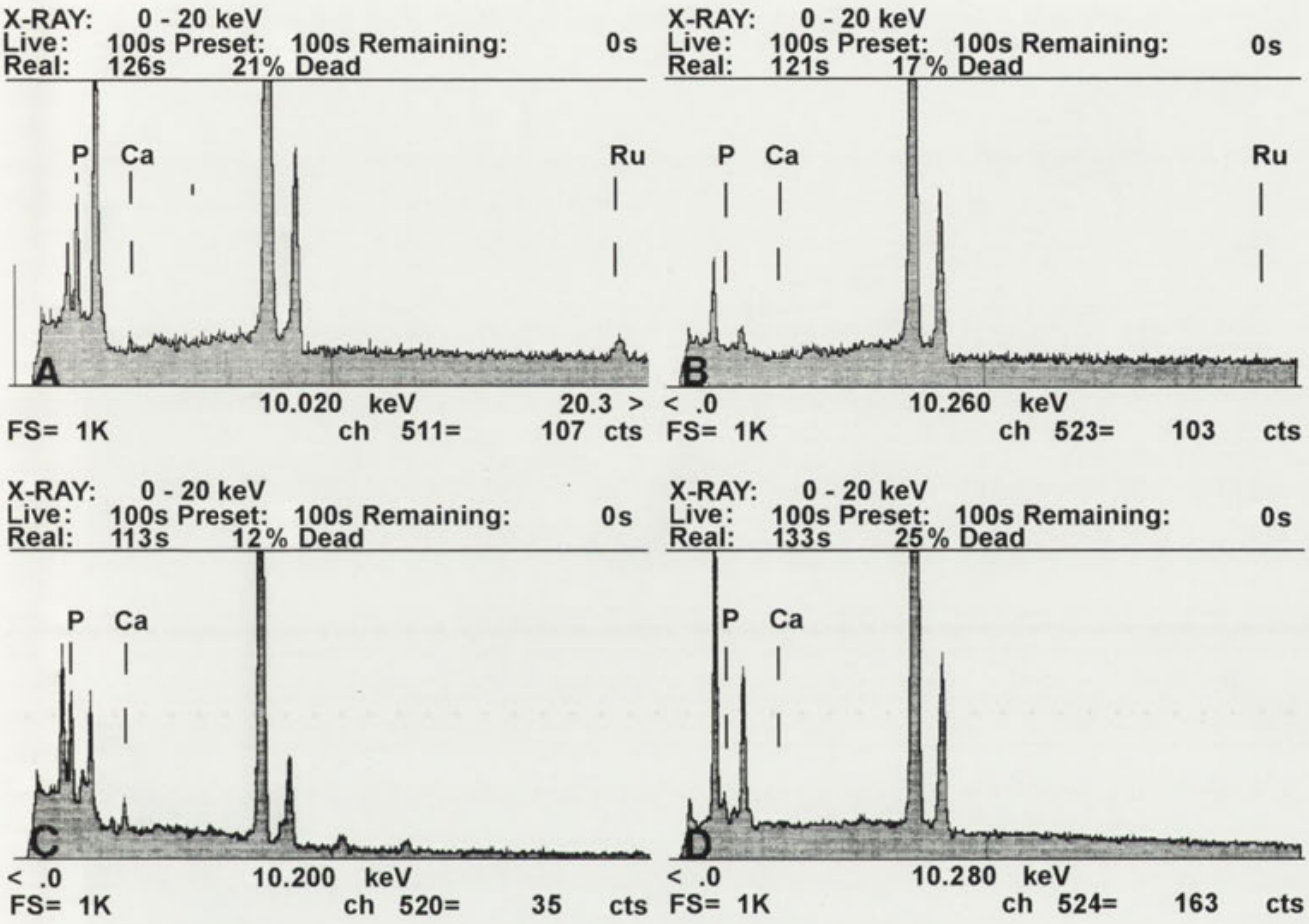

Figs. 2 A-D. X-ray energy spectra of cells exposed to either ruthenium red (A, B) or calcium ions (C, D). Spectra of electron-opaque structures evoked by RR (A) and calcium ions (C). B, D - control spectra, generated from random areas of the cytoplasm devoid of the electron-opaque structures. Phosphorus (Kα= 2.013 keV), calcium (Kα = 3.690 keV), ruthenium (Kα1 = 19.278 keV) peaks indicated. Additional peaks in all figures indicate the presence of magnesium (Kα = 1.253 keV), silicon (Kα= 1.733 keV), chlorine (Kα= 2.621 keV), copper (Kα, Kβ = 8.040 and 8.903 keV) are derived from embedding resin, supporting film and grids

Examination of freeze-etched samples exposed to 1mM PXB followed by glutaraldehyde/Ca fixation revealed prominent changes in the plasma membrane structure. The PF face of fractured membranes was covered by numerous, highly prominent knobs; some of them were fused together, forming patches (Fig.4B). The size and frequency distribution of PXB - induced knobs were different in comparison with the Ca-structures observed in samples not treated by PXB (compare Fig.4B with Fig.4A).The strong PXB on Ca-structures may indicate the importance of negatively charged phospholipids as essential consituents of the plasma membrane responsible for the generation of Ca-structures.
In controls when the cells were fixed with gluteraldehyde devoid of calcium as well as PXB, no electron-opaque, submembranous structures were observed in ultrathin sections of the samples. Also no knobs on the fracture faces of the plasma membrane were seen (Fig. 4C). The PF face was covered by numerous, randomly distributed IMP. Only a few IMP aggregates were detected in the disordered area (Fig. 4C), probably due to endocytosis as was demonstrated by Bowers (1980).

DISCUSSION

Ultrastructural studies of cells active in endocytosis, secretion and locomotion demonstrate the presence of calcium-containing, electron-opaque structures localized on the cytoplasmic surface of the plasma membrane (Sobota 1985). The structures were observed only if cell processing for electron microscopy was carried out in the presence of calcium. Magnesium had no effect on the formation of the Ca-structures. Calcium and phosphorus were the only components detected in the structures by X-ray microanalysis (Oschman et al. 1974, Skaer et al.

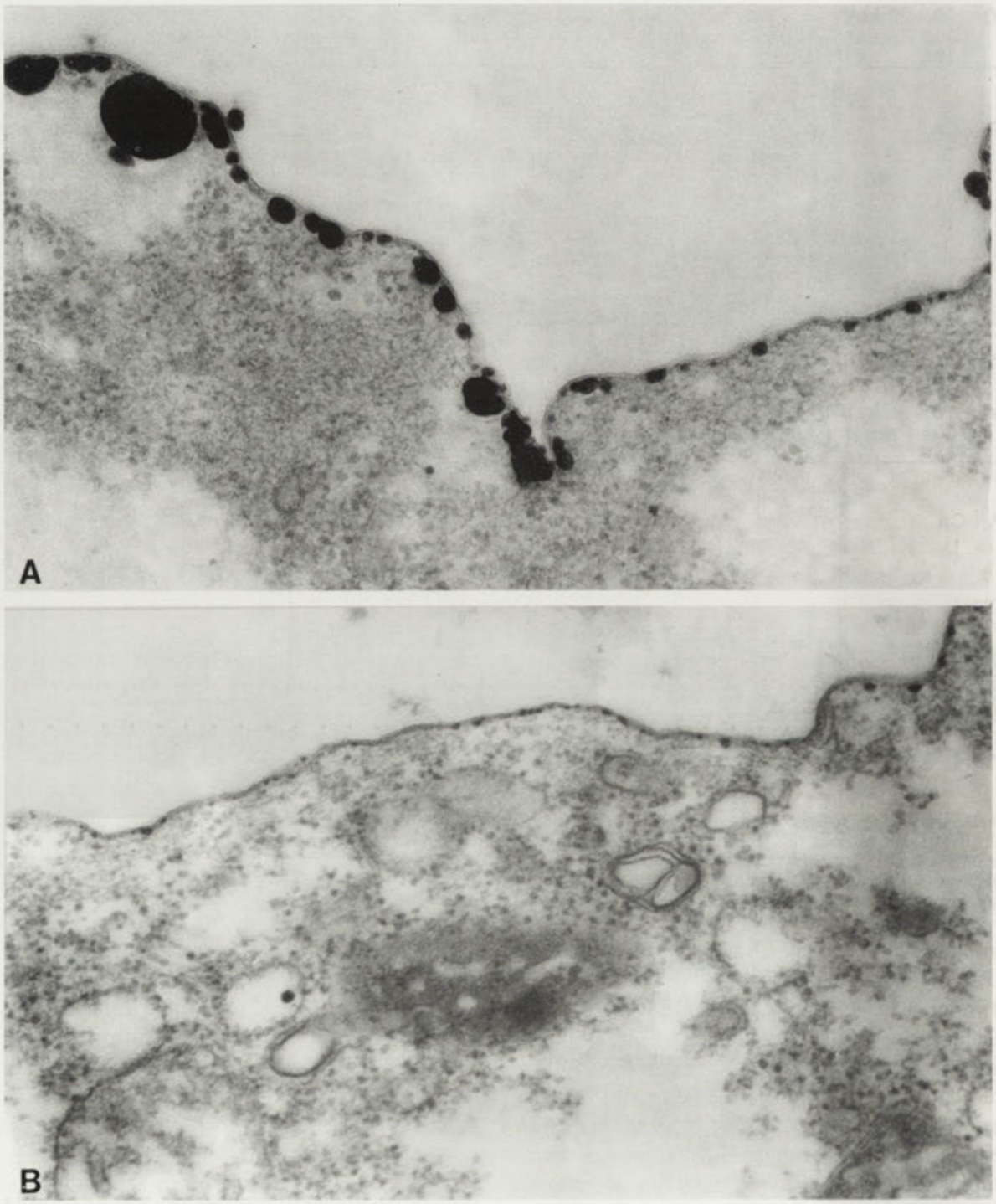

Figs. 3 A-B. Effect of polymyxin B on appearance of the calcium-structures. A - short (15 min) pretreatment of living cells with polymyxin B (1 mM) followed by 1 h glutaraldehyde/Ca fixation dramatically influenced the size and distribution of calcium-dependent structures. x 72000; B - pretreatment of living cells with 5 mM polymyxin B for 30 min at 20°C followed by overnight fixation with glutaraldehyde/Ca supplemented with polymyxin significantly reduced size of Ca-structures. Only small electron-opaque structures on the membrane can be seen, x 60000

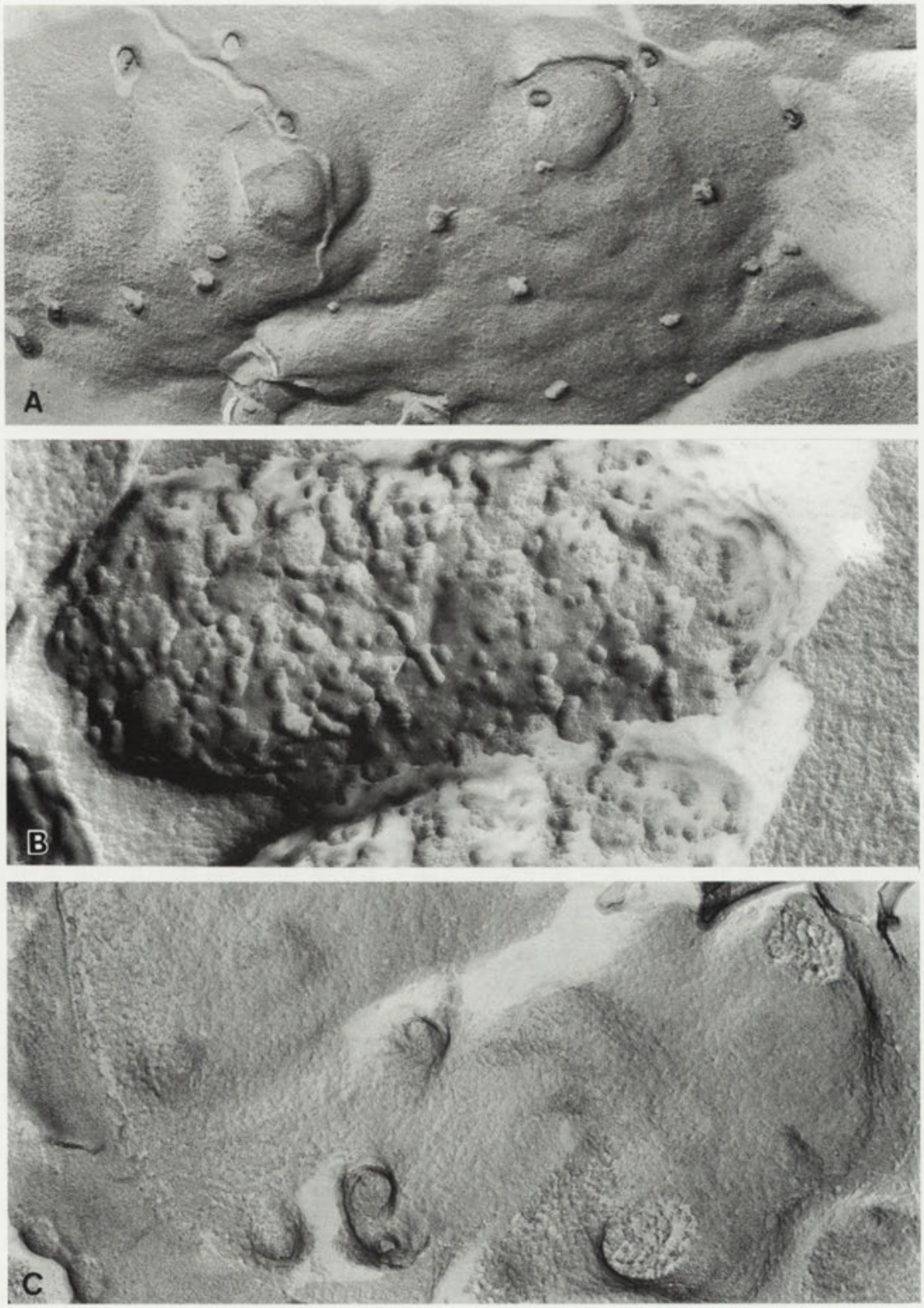

Figs. 4 A-C. Freeze-etching of *Acanthamoeba* cells. Effect of calcium ions and polymyxin B on structure of the plasma membrane. A - plasma membrane of cells fixed with glutaraldehyde/Ca. Calcium-structures were detected as knobs on PF surface of the membrane, x 46000. B - cells pretreated with 1 mM polymyxin B followed by glutaraldehyde/Ca fixation displayed significant changes in morphology of PF face of fractured plasma membrane. Numerous prominent and small knobs can be seen, x 46000. C - PF face of the plasma membrane of control cells. The cells were fixed with glutaraldehyde without calcium, x 46000

1974, Sobota et al. 1978). On the basis of such evidence it was suggested that calcium ions may be deposited on special submembrane calcium-binding microregions in the plane of the plasma membrane (Sobota 1985). The above point of view is supported by results presented in this paper.

In order to reveal cation binding domains on the cytoplasmic surface of the plasma membrane we exposed permeabilized cells to ruthenium red, a strongly positively charged dye. In intact cells ruthenium red binds to glycosaminoglycans located on the outer surface of plasma membrane. However, when the cells were pretreated with pronase the plasma membrane became permeable and ruthenium red may penetrate into the cytoplasm. Ruthenium red introduced into the cells in such a way was locally deposited as granules on cytoplasmic surface of plasma membrane (Figs. 1B, C). The size and location of these deposits were very similar to those of Ca-structures. The X-ray microanalysis showed that besides ruthenium, the main components of the RR-structures were phosphorus and minute amounts of calcium. The resemblance between RR- and Ca-structures (size, location, elemental analysis) suggests that both structures were organized in similar way. We propose that the appearance of these structures reflects the presence of calcium-binding negatively charged microregions on the plasma membrane. It has been shown that ruthenium red interferes with calcium-binding cellular constituents. Ruthenium red: (i) blocks the Ca-channel activity and Ca-pump activity (Vale and Carvalho 1973) by interacting with polyphosphoinositides (Missiaen et al. 1990); (ii) inhibits Ca^{2+} binding to calsequestrin and specifically stains the EF-hand conformation Ca^{2+}-binding proteins (Charuk et al. 1990); (iii) effectively blocks the voltage-dependent increase of Ca^{2+} in synaptosomes (Taipale et al. 1989); (iv) when microinjected into muscle fibers inhibits the rapid rise of myoplasmic Ca^{2+} evoked by the action potential (Baylor et al. 1989). The ability of ruthenium red an Ca^{2+} to interact with the same region of the plasma membrane indicates that perhaps similar anionic domains of the plasma membrane are involved in these interactions. Negatively charged components of the cytoplasmic surface of the plasma membrane are likely to participate in the RR binding, similarly as it was described for the interaction of the dye and concentrated anionic mucopolysaccharides on the cell surface. A high density of negatively charged molecules may evoke aggregation of ruthenium red as proposed by Luft (1971) and Howell (1974). According to this assumption, precipitation of ruthenium red on Ca^{2+}-binding constituents may indicate the presence of concentrated anionic domains within the plane of the cytoplasmic surface of the plasma membrane. It is possible that ruthenium red, like Ca^{2+}, induces clustering of negatively charged molecules on the cytoplasmic face of the plasma membrane. The negatively charged microdomains may bind the polycationic dye, thus making the heavily packed complex electron-opaque. Local concentration of anionic charges on the plasma membrane might be explained by the presence of, e.g. microdomains of anionic phospholipids, particularly phosphatidylserine.

According to the fluid mosaic model of biological membranes, lipids are organized in the form of a bilayer into which proteins are embedded; the lipids exhibit free lateral motion in the plane of the membrane. It has been well documented however, that these membrane constituents are non-uniformly distributed (van Deenen 1981, Edidin 1992, Glaser 1993). Studies of artificial unilamellar vesicles and erythrocyte membrane showed that the separation of lipids usually occurs when exogenous molecules, like Ca^{2+}, Ca^{2+}-binding proteins, polycations interact with the membrane acidic phospholipids. Phosphatidylserine molecules are frequently considered as phospholipids which, in the presence of calcium ions (van Dijck et al. 1978, Tanaka and Schroit 1986, Haverstick and Glaser 1987) or positively charged proteins such as cytochrome *c* or polylysine (Gad 1983, Mustonen et al. 1987) may potentially be packed together forming microdomains. Formation of the RR-structures, similar to the Ca-structures, is in good agreement with the presence of microregions of acidic phospholipids in the plane of the plasma membrane. Detection of similar amounts of phosphorus in the RR-, and the Ca-structures (Figs 2A, C) suggests that permanent membrane-submembrane constituents like phospholipids, phosphorylated proteins and other phosphate-containing compounds may be involved in binding of these cations. Anionic phospholipids may be consider as one of these Ca^{2+}-binding membrane constituents. Belitser et al. (1982) demonstrated sensitivity of the Ca-structures not only to protease but also to phospholipase A_2 treatment, implying that phospholipids are compounds of the Ca-structures.

Experiments with polymyxin B strongly support the suggestion that anionic phospholipids participate in the formation of the Ca-structures. Formation of the Ca-structures in *Acanthamoeba* cells in the presence of PXB was substantially disturbed (Fig. 3A); the structures became different in size, shape and were non-uniformly distributed on the membrane. High concentration and long exposure of the cells to the drug led to significant reduction

of calcium-dependent, electron-opaque material and only tiny electron-opaque structures were detected on the membrane (Fig. 3B). PXB, being a lipopeptide with high positive charges, interacts with anionic phospholipids and replaces phospholipide-bound calcium ions with high efficiency (Hartmann et al. 1978, Langer 1984). Thus, the effect of PXB on the appearance of the Ca-structures clearly indicates the importance of anionic phospholipid microdomains in the organization of these structures.

Worth noticing is the striking similarity between our freeze-fracture images of the Ca-structures and the freeze-etch view of the plasma membrane of cells exposed to high voltage discharge presented by Chang and Reese (1990, Figs 5, 6). The membrane of electroporated cells displayed volcano-shaped pores with common characteristics (diameter and distribution) to the Ca-structures described in this report. Chang and Reese (1990) suggested that the electropores are formed by breakdown of the local unstable regions in the plasma membrane where interactions between plasma membrane constituents and cytoskeleton take place. The similarity between the formed electropores and the Ca-, and RR-structures suggest that formation of the electropores as well as electron-opaque structures could reveal the presence of clusters of highly concentrated charged anionic membrane constituents.

Acknowledgements. We thank Prof. A. Przełęcka for stimulating discussions. We also thank Dr. B. Bowers, Dr. K. Kwiatkowska, and Dr. E. Wenegieme for critical reading of the manuscript.
The investigations were supported by the State Committee for Scientific Research to the Nencki Institute of Experimental Biology.

REFERENCES

Augustine G. J., Charlton M. P., Smith S. J. (1987) Calcium action in synaptic transmitter release. *Annu. Rev. Neurosci.* **10:** 633-693

Bark J. C., Wilson M. C. (1994) Regulated vesicular fusion in neurons; snapping together the details. *Proc. Natl. Acad. Sci. USA* **91:** 4621-4624

Baylor S. M., Hollingworth S., Marshall M. W. (1989) Effects of intracellular ruthenium red on excitation-contraction coupling in intact frog skeletal muscle fibres. *J. Physiol.* **408:** 617-635

Bazzi M. D., Nelsestuen G. L. (1991) Extensive segregation of acidic phospholipids in membranes induced by protein kinase C and related proteins. *Biochemistry* **30:** 7961-7969

Bearer E. L., Friend D. S. (1982) Modifications of anionic-lipid domains proceeding membrane fusion in guinea pig sperm. *J. Cell. Biol.* **92:** 604-615

Belitser N. V., Zaalishvili G. V., Sytnianskaja N. P. (1982) Ca^{2+}-binding sites and Ca-ATPase activity in barley root tip cells. *Protoplasma* **111:** 63-78

Bowers B. (1980) A morphological study of plasma membrane and phagosome membranes during endocytosis in *Acanthamoeba*. *J. Cell. Biol.* **84:** 246-260

Burgoyne R. D., Morgan A., Roth D. (1994) Characterization of proteins that regulate calcium-dependent exocytosis in adrenal chromaffin cells. *Ann. N.Y. Acad. Sci.* **710:** 336-346

Burt J. M., Langer G. A. (1983) Ca^{++} displacement by polymyxin B from sarcolemma isolated by 'gas dissection' from cultured neonatal rat myocardial cells. *Biochim. Biophys.Acta* **729:** 41-52

Cheek T. R., Barry V. A. (1993) Stimulus-secretion coupling in excitable cells: a central role for calcium. *J. Exp. Biol.* **184:** 183-196

Charuk J. H. M., Pirraglia C. A., Reithmeier A. F. (1990) Interaction of ruthenium red with Ca^{2+}-binding proteins. *Anal. Biochem.* **188:** 123-131

Chang D. C., Reese T. S. (1990) Changes in membrane structure induced by electroporation as revealed by rapid-freezing electron microscopy. *Biophys. J.* **58:** 1-12

Edidin M. (1992) Patches, posts and fences: proteins and plasma membrane domains. *Trends Cell Biol.* **2:** 376-380

Gad A. E. (1983) Cationic polypeptide-induced fusion of acidic phospholipids. *Biochim. Biophys. Acta* **728:** 377-382

Gennis R. B. (1989) Biomembranes. Molecular structure and function. Springer-Verlag. New York, Berlin, Heidelberg, London, Paris, Tokyo

Glaser M. (1993) Lipid domains in biological membranes. *Curr. Opin. Struct. Biol.* **3:** 475-481

Goldin S. M., Finch E. A., Reddy N. L., Hu L. Y., Subbarao K. (1994) Exocytosis, calcium oscillations, and novel glutamate release blockers as resolved by rapid superfusion. *Ann. N.Y. Acad. Sci.* **710:** 271-286.

Hartmann W., Galla H. J., Sackmann E. (1978) Polymyxin binding to charged lipid membranes an example of cooperative lipid-protein interaction. *Biochim. Biophys. Acta* **510:** 124-139

Haverstick D. M., Glaser M. (1987) Visualization of Ca^{2+}-induced phospholipid domains. *Proc. Natl. Acad. Sci. USA* **84:** 4475-4479

Howell J. N. (1974) Intracellular binding of ruthenium red in frog skeletal muscle. *J.Cell. Biol.* **62:** 242-247

Langer G. A. (1984) Calcium at the sarcolemma. *J. Mol. Cell. Cardiol.* **16:** 147-153

Livett B. G. (1993) Chromaffin cells: roles for vesicle proteins and Ca^{2+} in hormone secretion and exocytosis. *Trends Pharmacol. Sci.* **14:** 345-348

Luft J. H. (1971) Ruthenium red and violet. I. Chemistry, purification, methods of use for electron microscopy, and mechanism of action. *Anat. Rec.* **171:** 347-368

Missiaen L., De Smedt H., Droogmans G., Wuytack F., Raeymaekers L., Casteels R. (1990) Ruthenium red and compound 48/80 inhibit the smooth-muscle plasma membrane Ca^{2+} pump via interaction with associated polyphosphoinositides. *Biochim. Biophys. Acta* **1023:** 449-454

Moggio M., Bonilla E. (1985) Ultrastructural localization of anionic phospholipids in skeletal muscle plasma membrane. *Histochemistry* **83:** 519-523

Murphy C. R., Martin B. (1984) Freeze-fracture cytochemistry with polymyxin B. A study in the plasma membrane of uterine epithelial cells. *Histochemistry* **80:** 327-331

Mustonen P., Virtanen J. A., Somerharju P. J., Kinnunen P. K. J. (1987) Binding of cytochrome C to liposomes as revealed by the quenching of fluorescence from pyrene-labeled phospholipids. *Biochemistry* **26:** 2991-2997

Oschman J. L., Hall T. A., Peters P. D., Wall B. J. (1974) Association of calcium with membranes of squid axon. Ultrastructure and microprobe analysis. *J. Cell. Biol.* **55:** 58-73

Popov V. I., Nikonov A. A., Agafonova N. K., Fesenko E. E. (1994) Surface ultrastructure of olfactory receptor sense hairs in the silkmoth, *Antherae pernyi*. *J. Microsc.* **174:** 39-46

Scott D. L., White S. P., Otwinowski Z., Yuan W., Gelb M. H., Sigler P. B. (1990) Interfacial catalysis: the mechanism of phospholipase A_2. *Science* **250:** 1541-1546

Skaer R. J., Peters P. D., Emmines., J. P. (1974) The localization of calcium and phosphorus in human platelets. *J. Cell. Sci.* **15:** 679-692

Sobota A. (1985) Subplasmalemmal calcium-binding microregions in *Acanthamoeba*. *J. Cell. Sci.* **79:** 217-235

Sobota A. (1989) Calcium-affinity microregions on cytoplasmic surface of plasma membrane of *Acanthamoeba* cells. In: First Eur. Symp. on Calcium Binding Proteins in Normal and Transformed Cells, Brussels, Abstr. H8

Sobota A., Burovina I. V., Pogorelov A. G., Solus A. A. (1984) Correlation between potassium and phosphorus content and their nonuniform distribution in *Acanthamoeba castellanii*. *Histochem.* **81:** 201-204

Sobota A., Przełęcka A., Janossy A. G. S. (1978) X-ray microanalysis of calcium-dependent deposits at the plasma membrane of *Acanthamoeba castellanii*. *Cytobiologie* **17:** 464-469

Sobota A., Bandorowicz J., Jezierski A., Sikorski A. F. (1993) The effect of annexin IV and VI on the fluidity of phosphatidylserine/phosphatidylcholine bilayers studied with the use of 5-deoxylstearate spin label. *FEBS Lett.* **315:** 178-182

Swairjo M. A., Seaton B. A. (1994) Annexin structure and membrane interactions: A molecular perspective. *Annu. Rev. Biophys. Biomol. Struct.* **23:** 193-213

Taipale H. T., Kauppinen R. A., Komulainen H. (1989) Ruthenium red inhibits the voltage-dependent increase in cytosolic free calcium in cortical synaptosomes from guinea-pig. *Biochem. Pharmacol.* **38:** 1109-1113

Tanaka Y., Schroit A. J. (1986) Calcium/phosphate-induced immobilization of fluorescent phosphatidylserine in synthetic bilayer membranes: inhibition of lipid transfer between vesicles. *Biochemistry* **25:** 2141-2148

Teuber M., Miller I. R. (1977) Selective binding of polymyxin B to negatively charged lipid monolayers. *Biochim. Biophys. Acta* **467:** 280-289

Tilcock C. P. S., Cullis P. R. (1981) The polymorphic phase behavior of mixed phosphatidylserine-phosphatidylethanolamine model systems as detected by ^{31}P-NMR. *Biochim. Biophys. Acta* **641:** 189-201

Vale M. G. P., Carvalho A. P. (1973) Effects of ruthenium red on Ca^{2+} uptake and ATPase of sarcoplasmic reticulum of rabbit skeletal muscle. *Biochim. Biophys. Acta* **325:** 29-37

van Deenen L. L. M. (1981) Topology and dynamics of phospholipids in membranes. *FEBS Lett.* **123:** 3-15

van Dijck P. W. M., de Kruijff B., Verkleij A. J., van Deenen L. L. M., de Gier J. (1978) Comparative studies on the effects of pH and Ca^{2+} on bilayers of various negatively charged phospholipids and their mixtures with phosphatidylcholine. *Biochim. Biophys. Acta* **512:** 84-96

Received on 2nd December, 1996; accepted on 20th May, 1997

Acta Protozoologica (1997) 36: 197 - 219

ACTA
PROTOZOOLOGICA

Updating the Trachelocercids (Ciliophora, Karyorelictea). V. Redescription of *Kovalevaia sulcata* (Kovaleva, 1966) gen. n., comb. n. and *Trachelocerca incaudata* Kahl, 1933

Wilhelm FOISSNER

Universität Salzburg, Institut für Zoologie, Salzburg, Austria

Summary. The morphology and infraciliature of *Trachelonema sulcata* Kovaleva, 1966 and *Trachelocerca incaudata* Kahl, 1933, two trachelocercid karyorelictids from the French Atlantic coast at Roscoff, were studied in live and protargol-impregnated specimens, as well as with the scanning electron microscope. Voucher, respectively, neotype slides with protargol-impregnated specimens of each species have been deposited at the museum of natural history in Linz (LI), Austria. The somatic and oral infraciliature of *T. sulcata* and *T. incaudata* is very similar to that of other trachelocercids. However, the circumoral kinety of *T. sulcata* extends not only around the oral bulge but also along the brosse cleft, thereby assuming a unique, key-hole-like shape. This character is used to define a new genus, *Kovalevaia* gen. n., to which two species are transferred, viz. *K. sulcata* (Kovaleva, 1966) comb. n. (basionym: *Trachelonema sulcata* Kovaleva, 1966) and *K. teissieri* (Dragesco, 1960) comb. n. (basionym: *Tracheloraphis teissieri* Dragesco, 1960). *Trachelocerca incaudata* remains in the original genus because it lacks a brosse. *Trachelonema poljanskyi* Raikov, 1963 is transferred to *Tracheloraphis*: *T. poljanskyi* (Raikov, 1963) comb. n. A tabulated key to the trachelocercid genera (*Trachelocerca*, *Trachelolophos*, *Kovalevaia*, *Tracheloraphis*, *Prototrachelocerca*) is provided.

Key words: Ciliophora, infraciliature, Karyorelictea, *Kovalevaia sulcata* (Kovaleva, 1966) gen. n., comb. n., mesopsammon, *Trachelocerca incaudata*, Trachelocercidae.

INTRODUCTION

Trachelocercid karyorelictids are a highly specific component of the marine sand microbenthos (Dragesco 1960, Foissner 1997b). About 70 species have been described (Carey 1992), but detailed data on the infraciliature, i.e. the somatic and oral ciliary pattern, of representative taxa only became available recently (Foissner 1996, 1997a; Foissner and Dragesco 1996a, b). Using silver (protargol) impregnation and scanning electron microscopy, Foissner and Dragesco (1996a, b) redefined the classical genera *Trachelocerca* and *Tracheloraphis*. established the new genus *Trachelolophos*, and synonymized *Trachelonema* with *Tracheloraphis*.

Address for correspondence: Wilhelm Foissner, Universität Salzburg, Institut für Zoologie, Hellbrunnerstrasse 34, A-5020 Salzburg, Austria; FAX: (0662) 8044-5698

The present study, the last in the series, redescribes *Trachelonema sulcata* Kovaleva, 1966 and *Trachelocerca incaudata* Kahl, 1933, highlighting details of their somatic and oral infraciliature, which suggest that *T. sulcata* should be referred to a new genus, *Kovalevaia*. Very likely, *Trachelocerca*, *Tracheloraphis*, *Trachelolophos*, *Kovalevaia*, and *Prototrachelocerca* comprise most of the generic diversification of the trachelocercids, at least at the morphological level.

Only about 15 out of the 70 species assigned to the trachelocercids can be considered to be properly described (Foissner 1996, 1997a; Foissner and Dragesco 1996a, b; species redescribed in this paper). Thus, a great deal of work remains to be done. An appropriate technique is now available. We not yet know the taxonomic value of most characters used for species distinction in trachelocercids. Thus, each species must be described/redescribed in great detail, including painstaking line drawings and plentiful documentation by micrographs. "Simple" descriptions, as common in the past, should be abandoned because they only increase the prevailing disorder.

MATERIAL, METHODS AND TERMINOLOGY

Kovalevaia sulcata and *Trachelocerca incaudata* were found in September 1994 in the mesopsammon, i.e. in the upper 0-4 cm sand layer of the Atlantic coast at Roscoff (W 4°, N 48°50'), France. Samples were collected and treated as described by Fauré-Fremiet (1951). The upper 0-4 cm sand layer of shallow pools was taken with a small shovel during the tide, put into a 1 litre jar, and allowed to settle for at least 24 h. During this time many trachelocercids and other ciliates move upwards and enrich in the upper 1 cm of sand. About 20 ml sand and sea water from this layer were collected with a large-bore (5 mm) pipette and mixed with about 5 ml of a 12 % $MgCl_2$ solution to detach the ciliates. The mixture was then gently rotated in a Petri dish so that the sand collected in the centre and the detached ciliates could be picked up individually with a capillary pipette from the clear supernatant.

Cells were studied *in vivo* using a high-power oil immersion objective and bright-field or differential interference contrast (Foissner 1991). The infraciliature was revealed by protargol impregnation [Foissner 1991; protocol B (Wilbert's method)], using the fixative described by Foissner and Dragesco (1996a): 5 ml glutaraldehyde (25%), 5 ml saturated, aqueous mercuric chloride, 3 ml aqueous osmium tetroxide (2%), and 1 ml glacial acetic acid are mixed just before use. This fixative preserves all karyorelictids very well, but does not prevent contraction in contractile species. Specimens were fixed for 10-15 min and washed three times in distilled water. Specimens for scanning electron microscopy were prepared as described in Foissner (1991) using the fixative mentioned above.

Counts and measurements on silvered specimens were performed at a magnification of x 1,000. *In vivo* measurements were conducted at a magnification of x 40-1,000. Although these provide only rough estimates, it is worth giving such data as specimens usually shrink in preparations and contract during fixation. Illustrations of live specimens were based on free-hand sketches and micrographs, those of impregnated cells were made with a camera lucida. If not stated otherwise, all figures are oriented with the anterior end of the organism directed to the top of the page.

Terminology and interpretation of the trachelocercid infraciliature are according to Corliss (1979) and Foissner and Dragesco (1996a,b).

RESULTS

Morphometric data shown in Table 1 are repeated in this section only as needed for clarity. Most characters are highly variably (coefficient of variation > 20 %), as is usual in trachelocercids (Foissner and Dragesco 1996b).

Kovalevaia gen. n.

Diagnosis: Trachelocercidae Kent, 1881 with circumoral kinety not or only slightly interrupted at proximal vertex of brosse cleft and thus distinctly key-hole-shaped. Bristle kinety composed of a single row of dikinetids. One or more oblique or straight brosse kineties.

Type species: *Trachelonema sulcata* Kovaleva, 1966.

Dedication: genus dedicated to Dr. Valentina G. Kovaleva (Russian Academy of Science, St. Petersburg), who described the type species and performed many important studies on karyorelictid ciliates. Feminine gender.

Redescription of *Kovalevaia sulcata* (Kovaleva, 1966) comb. n. (Figs. 1-54, 89-99, Table 1)

Improved diagnosis (includes descriptions by Kovaleva 1966, Raikov and Kovaleva 1968, and Kovaleva and Golemansky 1979): extended cells *in vivo* about 600-1200 x 50 µm, slender and flattened ribbon-like (up to 4:1), contract slowly. Neck indistinctly, tail sharply set off from trunk; head, when fully extended, trumpet-shaped and distinctly set off from neck, bright and conspicuous because of large oral cavity lined by brown extrusomes. 9-60, usually about 30 macronuclei forming strand in middle third of body; 3-20, usually about 10 micronuclei. 10-24, usually 14-20 ciliary rows on right side of cell; left side unciliated, except for bristle kinety, glabrous stripe thus about as wide as trunk and with bright, longitudinal groove lacking large extrusomes. Brosse slit distinct, contains single brosse kinety composed of 3-7, on average 4 dikinetids. Cells dark and punctate due to two types of brown cortical

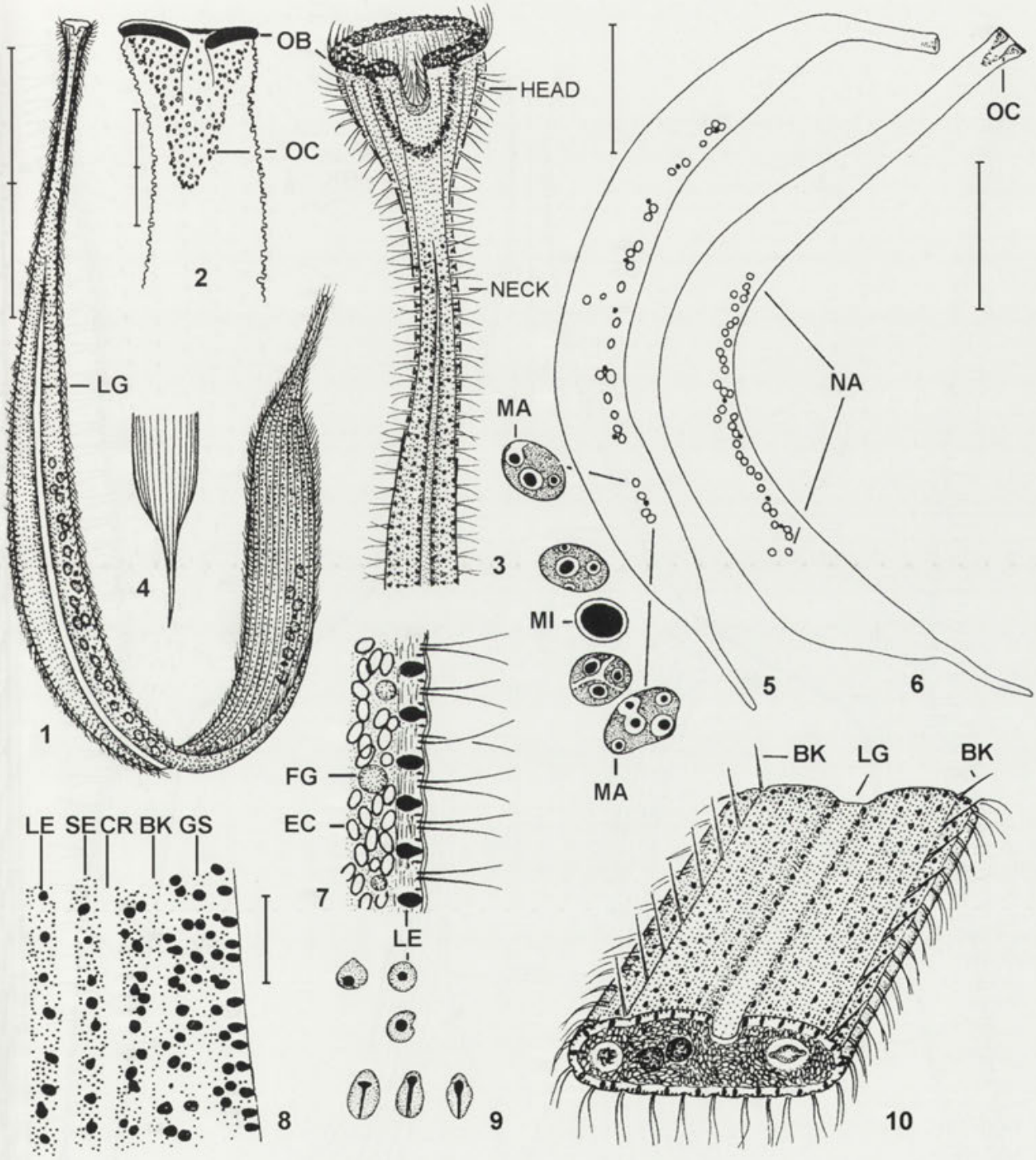

Figs. 1-10. *Kovalevaia sulcata* from life (1, 3, 4, 7, 10) and after protargol impregnation (2, 5, 6, 8, 9). 1 - typical, extended specimen. Note punctate appearance due to large, brown cortical granules (extrusomes), and bright, longitudinal groove, where the large extrusomes are lacking; 2 - enlarged detail from Fig. 6. The oral cavity and the oral bulge are lined by extrusomes; 3 - anterior body portion of fully extended specimen. Note lack of large granules (extrusomes) in cortex of head, except of oral bulge; 4 - right side view of posterior body portion. *Kovalevaia sulcata* has a distinct tail because the body is abruptly narrowed; 5, 6 - shape and nuclear apparatus of prepared specimens; 7 - optical section of cortex; 8 - surface view showing arrangement of cortical granules (extrusomes) in transition zone of right and left body side; 9 - transverse and longitudinal views of large extrusomes; 10 - transverse section of trunk; note strong flattening of cell. BK - bristle kinety, CR - ciliary row, EC - ellipsoid (crystalline ?) inclusions, FG - fat globule, GS - glabrous stripe, LE - large extrusomes (cortical granules), LG - longitudinal groove in centre of glabrous stripe, MA - macronuclei, MI - micronucleus, NA - nuclear apparatus, OB - oral bulge, OC - oral cavity, SE - small extrusomes (cortical granules). Scale bar division 100 μm (Figs. 1, 5, 6) and 10 μm (Figs. 2, 8)

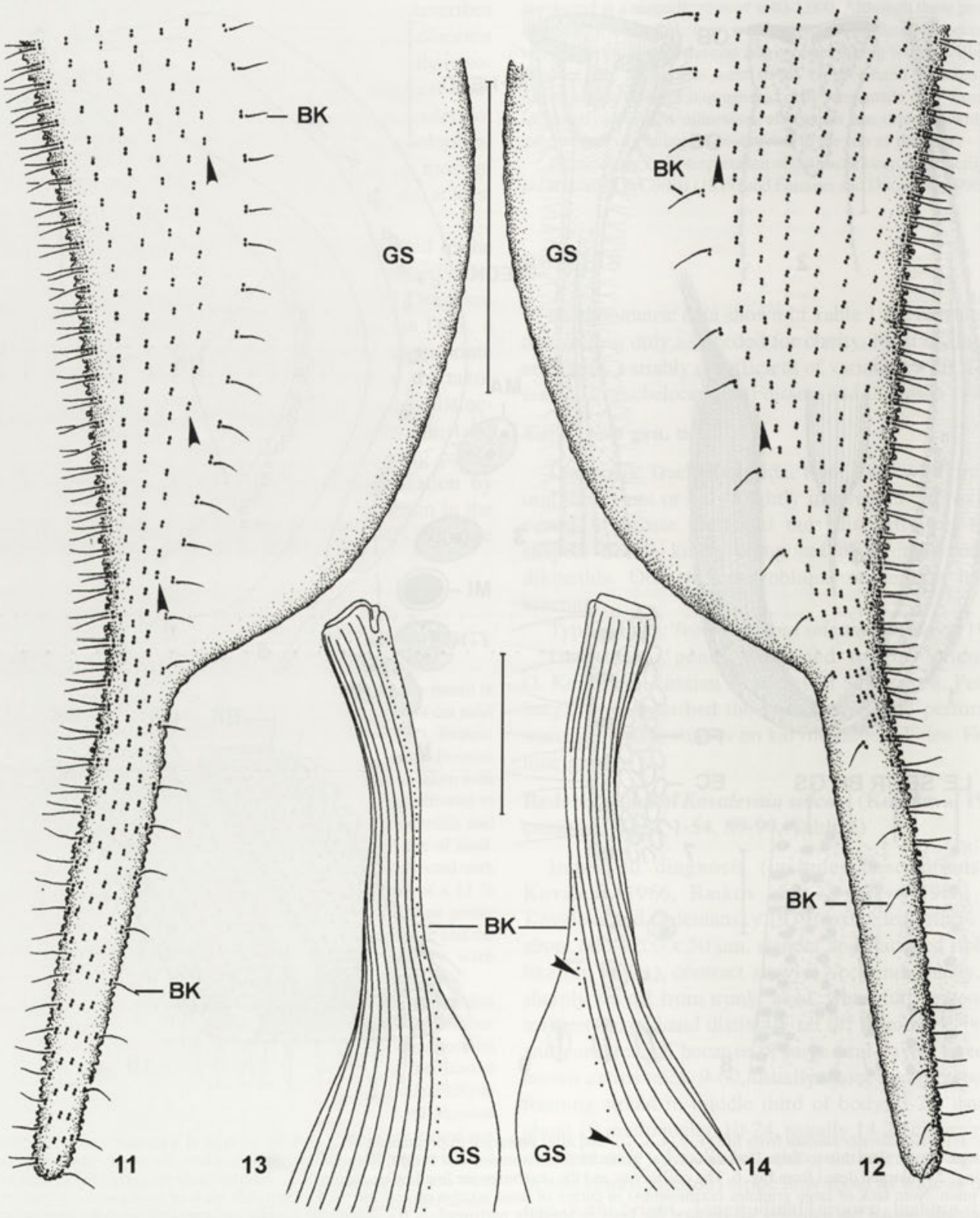

Figs. 11-14. *Kovalevaia sulcata*, somatic infraciliature after protargol impregnation. 11, 12 - lateral views of posterior body portion. Arrowheads mark shortened kineties forming posterior secant system. Note that only the anterior basal bodies are ciliated in the posterior half of the tail. The bristle kinety curves around the posterior body end; thus, the dikinetids in the right branch have the posterior basal bodies ciliated, whereas those in the left branch have the anterior basal bodies ciliated; 13, 14 - lateral views of anterior body portion. Arrowheads mark anterior secant system. BK - bristle kinety, GS - glabrous stripe. Scale bars 40 μm

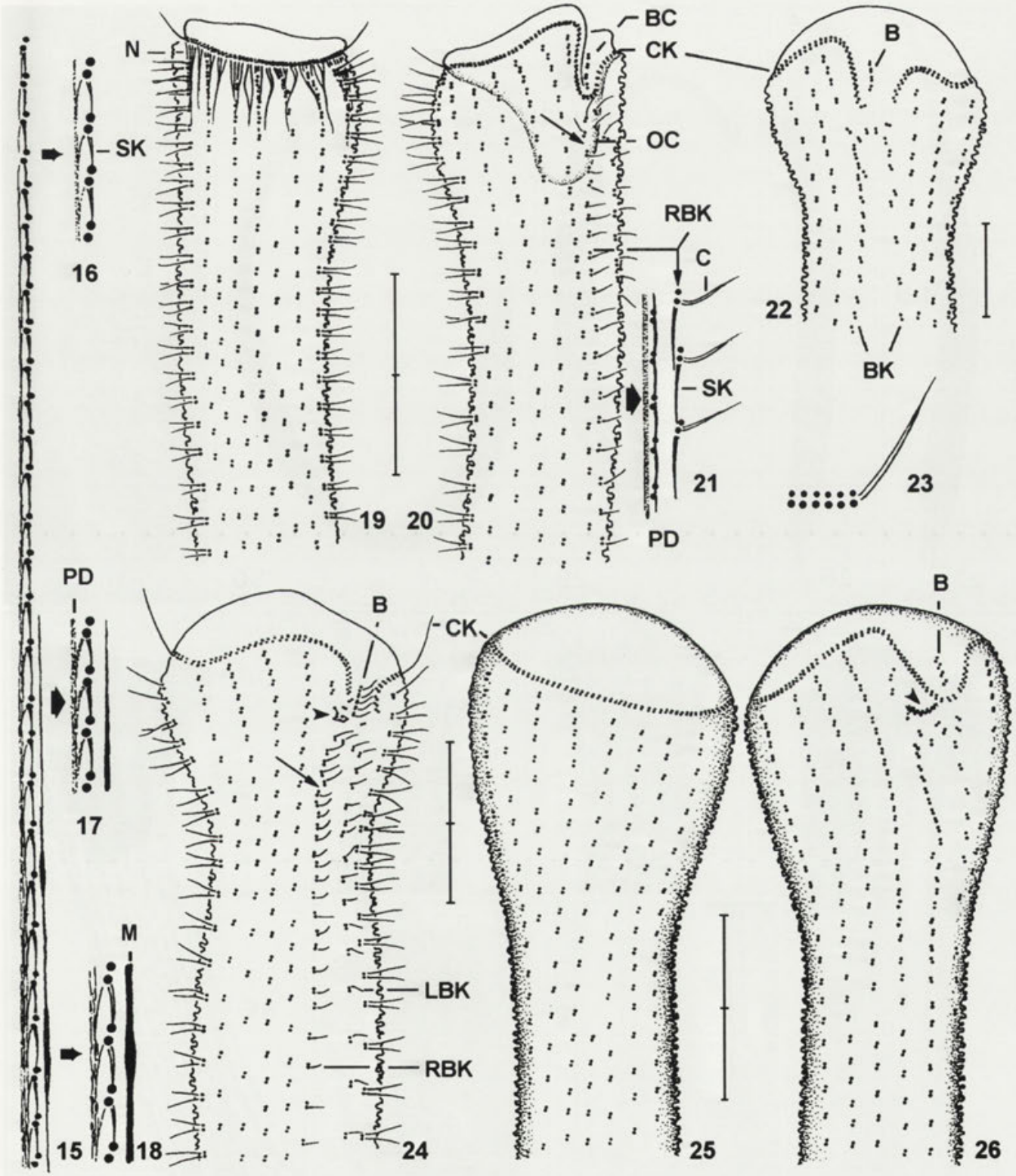

Figs. 15-26. *Kovalevaia sulcata*, fine structure of somatic and oral infraciliature in anterior body portion after protargol impregnation. 15, 16, 17, 18 - anterior portion of a somatic kinety showing fibrillar associates of dikinetids; 19, 20, 21, 24, 25, 26 - right and left side views. Arrows mark site where right end and anterior arch of bristle kinety abut and ciliation of bristle kinetids is opposed by about 180°. Arrowheads mark fuzzy structure between brosse cleft and bristle kinety; 22 - left side view of specimen whose circumoral kinety is open posteriorly; 23 - the anterior, unciliated basal bodies of the circumoral kinety are slightly smaller. B - brosse, BC - brosse cleft, BK - bristle kinety, C - cilium, CK - circumoral kinety, LBK- left branch of bristle kinety, M - myoneme, N - nematodesmata, OC - oral cavity, PD - postciliodesma, RBK- right branch of bristle kinety, SK - subkinetal microtubule ribbon. Scale bars 10 μm

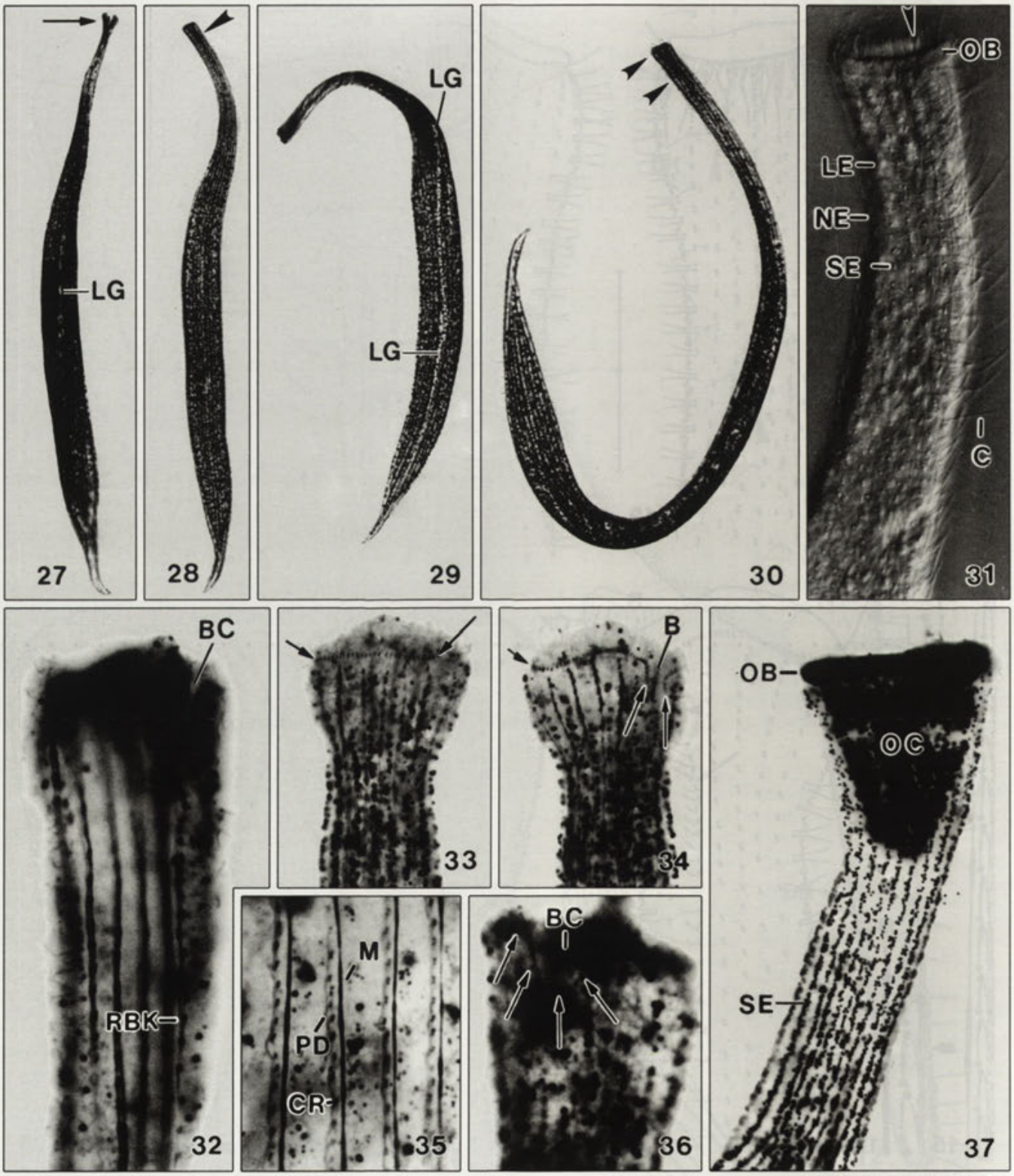

Figs. 27-37. *Kovalevaia sulcata* from life (27-31) and after protargol impregnation (32-37). For sizes, see text and Table 1. 27, 28, 29, 30, 37- extended, gliding specimens. The head (arrow) is trumpet-shaped when fully extended. Note black, punctate appearance of cell due to large, brown cortical granules (extrusomes) lacking in the longitudinal groove, which thus appears as bright line. Arrowheads mark deep oral cavity (cp. Fig. 37); 31 - anterior end showing entrance to oral cavity and cilia of circumoral kinety (arrowhead); 32, 33, 34, 35, 36 - somatic and oral infraciliature. Arrows mark circumoral kinety, which is either discontinuous (Fig. 34) or continuous (Fig. 36) at the posterior vertex of the brosse cleft. B - brosse, BC- brosse cleft, C - cilia, CR - ciliary row, LG - longitudinal groove in centre of glabrous stripe, LE - large extrusomes (cortical granules), M - myoneme, NE - neck, OB - oral bulge, OC - oral cavity, PD - postciliodesma, RBK - right branch of bristle kinety, SE- small extrusomes (cortical granules)

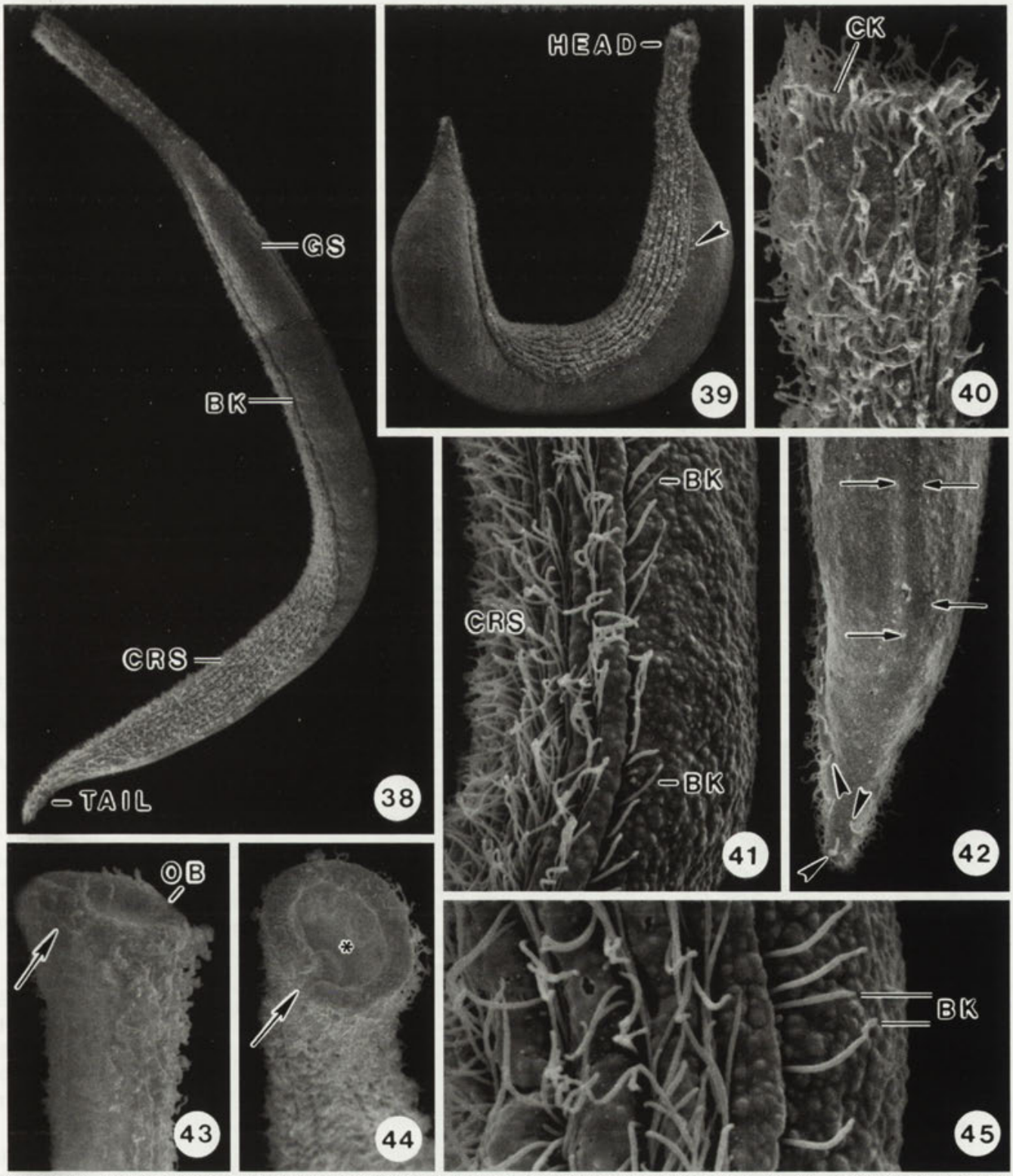

Figs. 38-45. *Kovalevaia sulcata* in the scanning electron microscope. For sizes, see text and Table 1. 38, 39 - extended and contracted specimens showing general organization, especially the glabrous stripe, which occupies the left side of the cell. Arrowhead marks bristle kinety extending in deep furrow at margin of glabrous stripe. Note that the longitudinal groove on the glabrous stripe (cp. Figs, 1, 10, 29, 42) has flattened due to the preparation procedures. 40 - head showing circumoral kinety; 41, 45 - lateral views showing bristle kinety, which consists of widely spaced cilia. The pellicle appears knobby due to the cortical granules (extrusomes); 42 - left side view of posterior end. The left side is unciliated, except for the bristle kinety (arrowheads), which curves around the cell. Arrows mark flattened longitudinal groove; 43, 44 - head in lateral and frontal view. Arrows mark brosse cleft. Asterisk denotes deep oral cavity. BK - bristle kinety, CK - circumoral kinety, CRS - ciliated right side of cell, GS - glabrous stripe, OB - oral bulge

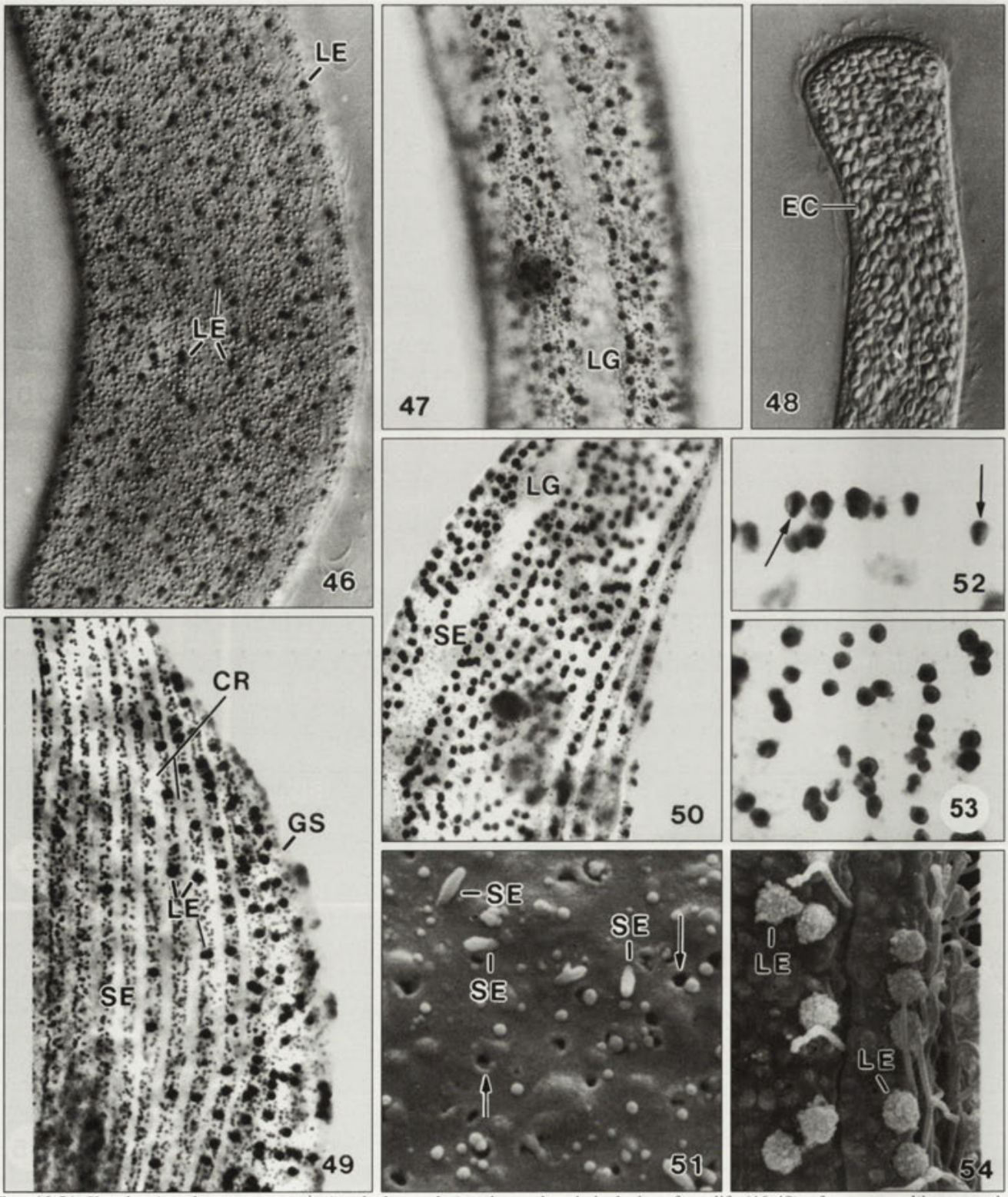

Figs. 46-54. *Kovalevaia sulcata*, extrusomes (cortical granules) and cytoplasmic inclusions from life (46-48), after protargol impregnation (49, 50,52, 53), and in the scanning electron microscope (51, 54). For sizes, see text. 46, 47, 50 - right and left side views of cortex, which contains innumerable small (about 0.4 µm) and many large (about 2 x 1 µm), brown extrusomes. The large extrusomes are lacking in the longitudinal groove extending on the glabrous stripe; 48 - anterior portion showing cytoplasm packed with ellipsoidal inclusions (about 2 x 1 µm), which were artificially spread into the head during flattening of the cell; 49 - lateral view of strongly contracted cell, showing arrangement of small and large extrusomes and tuberculate glabrous stripe; 51 - part of glabrous stripe showing globular and rod-shaped (arrowheads) extrusomes leaving cell. Arrows denote holes remaining from extruded extrusomes; 52, 53 - large extrusomes in longitudinal (arrows) and transverse view (cp. Figs. 7 - 9); 54 - extruded large extrusomes. CR - ciliary rows, EC - ellipsoidal (crystalline ?) inclusions, GS- glabrous stripe, LE - large extrusomes, LG - longitudinal groove, SE- small extrusomes

Table 1. Morphometric data from *Kovalevaia sulcata* (upper line) and *Trachelocerca incaudata* (lower line)

Character[1]	$\bar{x}$	M	SD	SE	CV	Min	Max	n
Body, length[2]	756.2	725.0	168.8	42.2	22.3	530	1100	16
	495.3	465.0	157.1	39.3	31.7	270	900	16
Body, width at head	25.0	26.0	5.0	1.3	20.2	15	32	16
	22.7	22.0	5.0	1.2	21.9	13	31	16
Body, (maximum) width at trunk[2]	64.1	64.0	7.2	1.8	11.2	55	85	16
	85.9	87.5	22.7	5.7	26.4	50	120	16
Glabrous stripe, width in mid-body[2]	about same as trunk width							
	10.1	10.0	2.8	0.7	27.3	6	15	16
Oral cavity, depth	22.4	21.0	5.1	1.3	22.6	17	35	16
	oral cavity lacking							
Anterior end to nuclear capsule	no capsule							
	260.0	245.0	86.7	21.7	33.4	125	470	16
Macronuclei, respectively,	8.1	8.0	1.4	0.3	16.8	6	10	16
nuclear capsule, length	21.3	21.0	3.9	1.0	18.4	15	30	16
Macronuclei, respectively,	7.4	7.0	1.4	0.4	19.0	5	10	16
nuclear capsule, width	19.1	19.0	2.5	0.6	12.9	15	23	16
Micronuclei, length	5.6	5.5	1.8	0.5	32.6	3	8	16
	not investigated							
Micronuclei, width	4.5	4.0	1.5	0.4	32.5	3	8	16
	not investigated							
Somatic kineties, number on head	12.9	13.0	1.6	0.4	12.6	10	15	16
	15.5	16.0	1.7	0.4	11.0	13	18	16
Somatic kineties, (maximum)	14.1	14.0	1.8	0.5	13.1	11	18	16
number on trunk	32.1	32.5	4.1	1.0	12.6	25	40	16
Circumoral dikinetids, number	not investigated							
	68.1	67.5	16.7	4.2	24.5	40	95	16
Brosse kineties, number	1.0	1.0	0.0	0.0	0.0	1	1	9
	no brosse							
Dikinetids in brosse kinety, number	4.6	4.0	1.1	0.4	24.6	3	7	9
	no brosse							
Macronuclei, number	31.5	31.5	8.0	2.3	25.3	22	50	12
	7.8	8.0	1.0	0.3	12.8	6	10	16
Micronuclei, number	9.2	8.5	4.4	1.3	47.5	5	20	12
	2.0	2.0	-	-	-	2	2	4

[1] Data based on protargol-impregnated and mounted specimens from field. Measurements in µm. Abbreviations: CV - coefficient of variation in %, M - median, Max - maximum, Min - minimum, n - number of individuals investigated, SD - standard deviation, SE - standard error of mean, $\bar{x}$ - arithmetic mean

[2] Data of very limited value because specimens contract more or less distinctly when fixed and/or become inflated due to the preparation procedures

granules (extrusomes): large extrusomes about 2 x 1 µm, in single row between each two kineties and on glabrous stripe, contain nail-shaped structure; small extrusomes about 0.4 µm across, form narrowly spaced rows in whole cortex.

Specimens investigated and voucher slides: *Kovalevaia sulcata* is very difficult to study, mainly due to the extrusomes, which impregnate heavily and conceal the infraciliature. Thus, the description of the infraciliature is based only on five mediocrely impregnated specimens; some others were of useable quality and served for completing morphometry. Voucher slides with specimens from Roscoff, prepared as described, have been deposited in the Oberösterreichische Landesmuseum in Linz (LI), Austria. Relevant specimens are marked by a black ink circle on the cover glass.

Description of Roscoff population: fully extended specimens *in vivo* about 800-1200 x 50 µm, length:width ratio 15-20:1, trunk flattened ribbon-like (3-4:1; Figs. 1, 10, 27-30, 38). Very flexible and thus usually more or less distinctly curved, occasionally even coiled like a snail-shell. Contracts slowly and not very extensively,

prepared cells thus conspicuously long (Table 1); fully contracted specimens banana-shaped, convex side with glabrous stripe distinctly protruding but only occasionally tuberculate (Figs. 39, 41, 49). Greybrown and opaque in dissecting microscope, dark and punctate under transmitted light of bright-field microscope at low magnification (≤ x 100) due to large, brown cortical granules = extrusomes (Figs. 1, 10, 27-30); left side (glabrous stripe) with narrow, longitudinal groove lacking large, brown extrusomes and thus appearing as bright line at low magnification (Figs. 1, 10, 27, 29, 47); groove usually flattened in SEM preparations (Figs. 38, 39, 42). Extended specimens slender with anterior third gradually tapering, neck thus indistinctly set off from trunk; neck very agile, looks like a groping elephant proboscis, especially when head is fully extended; posterior portion abruptly narrowed forming distinct straight or slightly curved tail (Figs. 1, 4-6, 27-30, 38). Head trumpet-shaped when fully extended (Figs. 3, 27, 43), cylindroidal when contracted (Figs. 28-30, 31), bright because hollowed by 20-40 µm deep oral cavity lined by brown extrusomes, very fragile, often quickly dissolving under cover glass (Figs. 2, 3, 28, 30, 37; Table 1). Oral bulge conspicuous because packed with brown extrusomes, interrupted at brosse cleft about half as deep as oral cavity, main part of cleft covered by head cortex, as indicated by SEM micrographs (Figs. 43, 44), cleft margin thickened by gelatinous plasm (Figs. 2, 3, 19, 20, 31, 37).

Macronuclei globular to slightly ellipsoidal, number highly variable (Table 1), individually arranged left of midline, forming long strand in middle third of cell (Figs. 1, 6); occasionally clustered to indistinct groups (Fig. 5). Micronuclei globular to slightly ellipsoidal, near and between macronuclei. No contractile vacuole.

Cortex very flexible and gelatinous, about 2 µm thick (Figs. 7, 48), tuberculate in contracted cells (Fig. 45), contains two types of conspicuous, extrusive granules, whose fine structure and genesis were investigated by Kovaleva and Raikov (1972); both extrusome types brilliant brown to darkbrown and thus well-recognizable in living cells (Figs. 46, 47), impregnate heavily with protargol (Figs. 49, 50), make cortex knobby in light and scanning electron microscope (Figs. 31, 41, 45). Large extrusomes about 2 x 1-1.5 µm, ellipsoidal to pyriform, contain nail-shaped structure after protargol impregnation (Figs. 7, 9, 52, 53), globular with slightly knobby surface when extruded (Fig. 54), arranged in single (rarely two) row between each two somatic kineties, in loose rows on glabrous stripe, except for longitudinal groove, packed in oral bulge and cortex of oral cavity, absent in head cortex (Figs. 2, 3, 8, 10, 28, 30, 46, 47, 49, 50), provide cells with dark, punctate appearance at low magnification (Figs. 27-30). Small extrusomes about 0.4 µm across, elongate to about 1 µm long rods when extruded, arranged in narrowly spaced rows in whole cortex, including head and longitudinal furrow on glabrous stripe (Figs. 3, 8, 10, 31, 37, 49-51).

Cytoplasm colourless, packed with about 2 x 1 µm sized, highly refractile (crystalline ?) granules, fat globules, and some food vacuoles containing diatoms (Figs. 7, 10, 48). Glides and winds elegantly between sand grains and organic debris.

Somatic infraciliature (Figs. 10-26, 31, 32, 35, 38-42, 45): *Kovalevaia sulcata* has only the right surface ciliated, the left is barren, i.e. occupied by the glabrous stripe, at the margins of which the bristle kinety extends. The cilia are arranged in longitudinal rows which are distinctly separate from the circumoral kinety and extend between flat cortical crests. The anterior end of the ciliary rows is occasionally slightly curved to the right and has condensed, i.e. more narrowly spaced dikinetids. Usually, the condensation is inconspicuous or even lacking in some kineties. One to three ciliary rows are gradually shortened in the neck region left of the glabrous stripe and posteriorly, where the body narrows to the tail, on both sides of the stripe (Figs. 11-14). In other words, an anterior and posterior secant system are formed at the margins of the cell where some ciliary rows abut to the bristle kinety. Thus, the head, neck and tail have slightly fewer kineties than the trunk (Table 1). The ciliary rows neighbouring the right branch of the bristle kinety are unshortened anteriorly and thus run alongside the glabrous stripe (Figs. 13, 14).

The entire infraciliature consists of ciliated dikinetids, except for 0-2 dikinetids at the anterior end of the kineties and the dikinetids in the posterior half of the tail, where only the anterior basal bodies are ciliated (Figs. 11, 12, 20, 24). The dikinetids are associated with various distinct fibres, all very likely originating from the posterior basal bodies (Figs. 15-18, 35). My observations largely agree with the transmission electron microscopic investigations by Kovaleva (1974), who, however, did not recognize the subkinetal microtubule arrays and some site-specific differences. On the other hand, the transverse microtubule ribbons and the kinetodesmal fibres did not stain in my preparations. The most conspicuous fibres are the postciliary microtubule ribbons, several of which overlap to form a

distinct bundle (postciliodesma) right of each kinety. The postciliodesmata are thinner in the head and neck region than in the trunk and tail. The subkinetal microtubule ribbons form a thin, but sharply impregnated bundle underneath or close to the left of the kineties. They are more intensively impregnated in the neck region and do not or hardly overlap so that their comma-like shape can be recognized (Figs. 15-18). No oralized somatic dikinetids were recognizable, as in *Tracheloraphis longicollis* (Foissner and Dragesco 1996b).

The contractile apparatus of *K. sulcata* consists of a myoneme close to the left of each kinety (Figs. 15-18, 35). As in the other species investigated (Foissner and Dragesco 1996b), the distinctiveness of the myonemes varies highly, depending on preparation conditions. The myonemes are flattened ribbon-like and commence as very thin bundles in the neck region (Fig. 17), gradually thickening posteriorly (Figs. 18, 35). No myonemes impregnated in the glabrous stripe and along the bristle kinety.

The glabrous stripe extends along the whole body length and width, except on the anterior neck region and head, where it gradually narrows, occupying only about one third of the head's width (Figs. 19-22, 24-26, 38, 42). The glabrous stripe is bordered by the bristle kinety which extends in a narrow groove and consists, like the ordinary ciliary rows, of individual dikinetids having about 12 µm long, rather stiff cilia (Figs. 10, 11-14, 38, 41, 45). However, the bristle kinety is easily distinguished from ordinary somatic ciliary rows because its dikinetids are more widely spaced, except in the right anterior portion (Figs. 22, 26), and more irregularly arranged and either lack or have very inconspicuous postciliary microtubule ribbons, too small to be recognized with the light microscope; the subkinetal microtubule bundles are conspicuous (Figs. 20-22, 24, 26, 32). The bristle kinety is continuous at the posterior end of the cell (Fig. 42), whereas its anterior end appears covered by a short, arched kinety ("anterior arch of bristle kinety", see Foissner and Dragesco 1996b for detailed explanation). The ciliation of the bristle dikinetids is as described in other trachelocercids (Foissner and Dragesco 1996a, b), i.e. those along the right margin of the glabrous stripe have the posterior basal bodies ciliated, whereas the dikinetids along the left stripe margin have the anterior basal bodies ciliated; at the site where the right end and the anterior arch of the bristle kinety abut, the ciliation of the bristle kinetids is opposed by about 180° (Figs. 20, 24). A fuzzy structure, possibly composed of basal bodies connected by some fibrous material, is found, in about half of the specimens, between the anterior arch of the bristle kinety and the vertex of the circumoral kinety (Figs. 24, 26).

Oral infraciliature (Figs. 3, 19, 20, 22-26, 31-34, 36, 40): the oral infraciliature of *K. sulcata* consists of a circumoral kinety and a minute brosse, difficult to recognize in living specimens. The circumoral kinety extends in the flat furrow separating the oral bulge from the head and is continuous along the brosse cleft, thus obtaining a characteristic, key-hole-like shape (Figs. 20, 26, 36). The rear portion of the kinety, which extends along the posterior vertex of the brosse cleft, was lacking in about half of the specimens (Figs. 22, 24, 34); however, this was possibly caused by insufficient impregnation and/or artificial spreading of the cleft by the preparation procedures. The circumoral kinety is composed of a single row of obliquely oriented dikinetids having only the posterior basal body ciliated (Fig. 40); the anterior, barren basal body is slightly smaller in protargol preparations (Fig. 23). Each circumoral dikinetid is associated with a comparatively short nematodesma obliquely extending into the head. The nematodesmata of neighbouring dikinetids unite to small bundles, forming a slightly cone-shaped oral basket (Fig. 19). As in the other species investigated (Foissner and Dragesco 1996b), the circumoral kinety of *K. sulcata* is very likely composed of several fragments, as indicated by small gaps, 1-2 dikinetids wide, and the bundled arrangement of the nematodesmata.

The brosse is located in a rather deep cavity, the brosse pocket, which extends underneath the anterior half of the brosse cleft. It invariably consists of a single, short kinety composed of closely spaced dikinetids having only the posterior basal body ciliated (Figs. 20, 22, 24, 26, 32, 34; Table 1).

Distribution and ecology: *Kovalevaia sulcata* was discovered by Kovaleva (1966) at the coast of the Black Sea, where this species is widespread in fine (grain size 0.25-0.30 mm), slightly polluted sand (Kovaleva and Golemansky 1979). Later, mass populations were found by Raikov and Kovaleva (1968) in fine, aerobic sands of the Posjet Gulf (Japan Sea, Pacific Basin). The present record from Roscoff (France) is the first from the Atlantic Basin. The species could be transported from Roscoff to the Salzburg laboratory, where it was one of the few trachelocercids surviving some months in the sampling jar, obviously tolerating microaerobic conditions. Furthermore, I found *K. sulcata* at the coast of Cape Town, South Africa, where it inhabited the upper, muddy sand layer of a beach (Figs. 38-45). Again, it

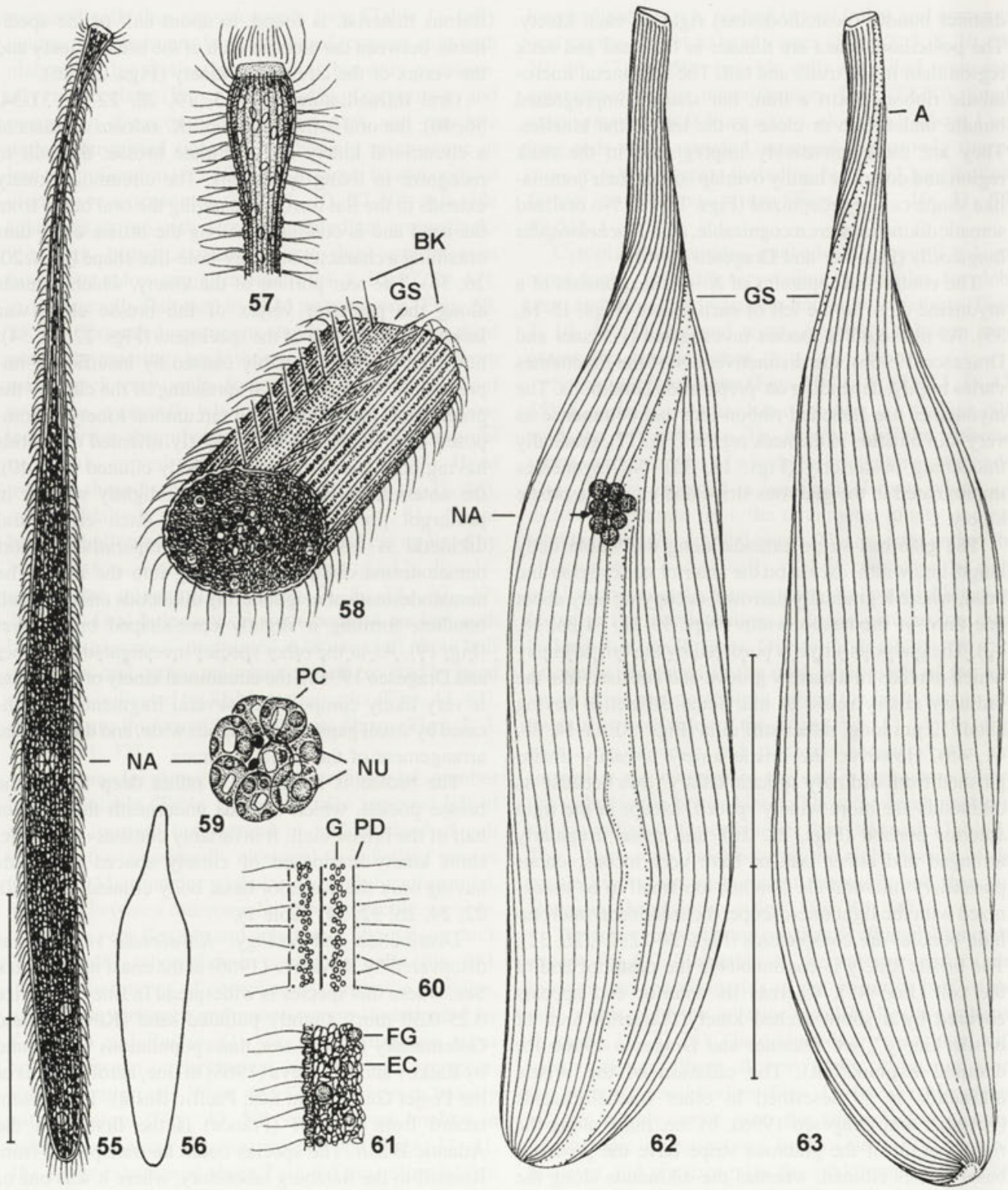

Figs. 55-63. *Trachelocerca incaudata* from life (55-61) and after protargol impregnation (62, 63). 55, 56 - typical specimen extended and contracted (drawn to scale); 57 - the head is claviform and contains minute, drumstick-shaped structures, possibly extrusomes; 58 - transverse section of trunk, which is slightly flattened in fully extended specimens; 59 - usually, 8 macronuclei and 2 micronuclei form a nuclear capsule; 60, 61 - surface view and optical section of cortex; 62, 63 - Arrangement of ciliary rows on left and right side. About half of the kineties are shortened and abut to the left branch of the bristle kinety, forming an anterior and posterior secant system. A - anterior secant system, BK - bristle kinety, EC - ellipsoidal (crystalline ?) inclusions, FG - fat globule, G - cortical granules, GS - glabrous stripe, NA - nuclear apparatus, NU - nucleoli, PC - (protein ?) crystal, PD - postciliodesma. Scale bar division 100 µm

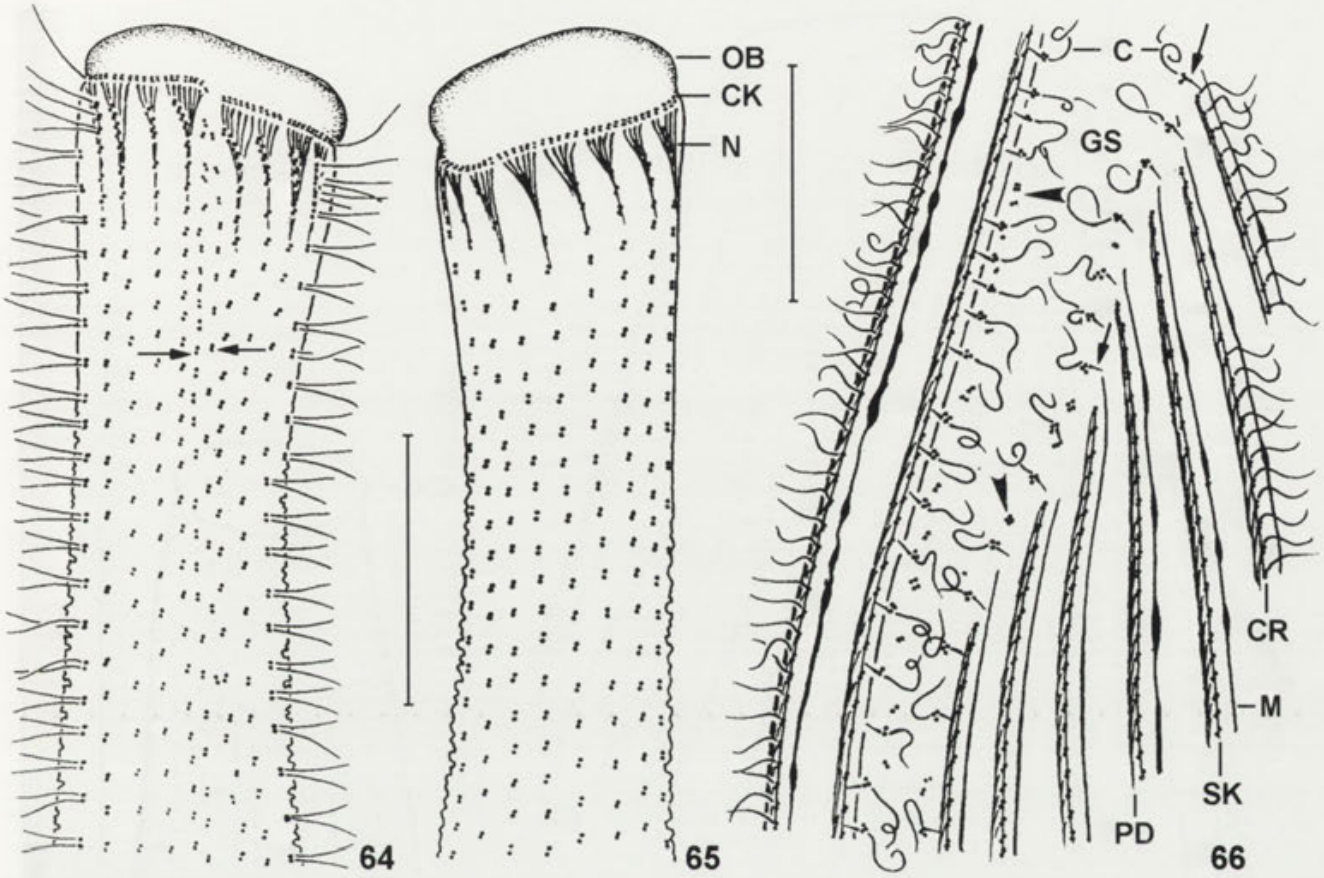

Figs. 64-66. *Trachelocerca incaudata*, oral and somatic infraciliature after protargol impregnation. 64, 65 - left and right side view of anterior body portion. Arrows mark bristle kinety bordering very narrow glabrous stripe; 66 - somatic fibrillar system in left anterior trunk region of an excellently prepared specimen (cp. Fig. 87). Arrows mark minute, laterally directed fibre originating from the ciliated basal body of the bristle dikinetids. Arrowheads denote unciliated argyrophilic granules (basal bodies ?) within and near the bristle kinety. C - cilia, CK - circumoral kinety, CR - ciliary row, M - myoneme, N - nematodesmata, OB - oral bulge, PD - postciliodesma, SK - subkinetal microtubule ribbon. Scale bars 20 µm

survived transport to the Salzburg laboratory despite anaerobic conditions in the jar. These data indicate that *K. sulcata* is a cosmopolite tolerating microaerobic and anaerobic conditions, at least for some time.

Redescription of *Trachelocerca incaudata* Kahl, 1933 (Figs. 55-88, 109-118; Table 1)

Improved diagnosis (including literature data): fully extended cells *in vivo* 400-1000 x 30-40 µm. Slender, neck rather distinctly set off from slightly flattened, fusiform trunk, head claviform and whitish or dark, posterior end rounded. 6-10, usually 8 macronuclei and 2 micronuclei forming tight cluster in centre of trunk. 25-40, usually about 32 somatic ciliary rows and 40-95, on average 68 circumoral dikinetids; glabrous stripe narrow, about one quarter of body width. Cortical granules about 1 x 0.5 µm, yellowish, form stripes between ciliary rows and narrowly spaced rows in glabrous zone.

Specimens investigated and type material: the redescription is based on 10 well-impregnated specimens; some others were of usuable quality and served for completing morphometry. No type material of *T. incaudata* has been mentioned in the literature. Thus, I have deposited three neotype slides with specimens from Roscoff, prepared as described, in the Oberösterreichische Landesmuseum in Linz (LI), Austria. Relevant specimens are marked by a black ink circle on the cover glass.

Description of Roscoff population: size of fully extended specimens *in vivo* about 800-1,000 x 30-40 µm, highly flexible and contractile, size and shape thus poorly preserved and highly variable in protargol slides (Table 1; Figs. 55, 62, 70, 81); about 1.5:1 flattened laterally (Fig. 58). Grey to blackish in dissecting and bright-field microscope due to innumerable, about 4 x 2 µm sized, refractile (crystalline ?) inclusions in trunk

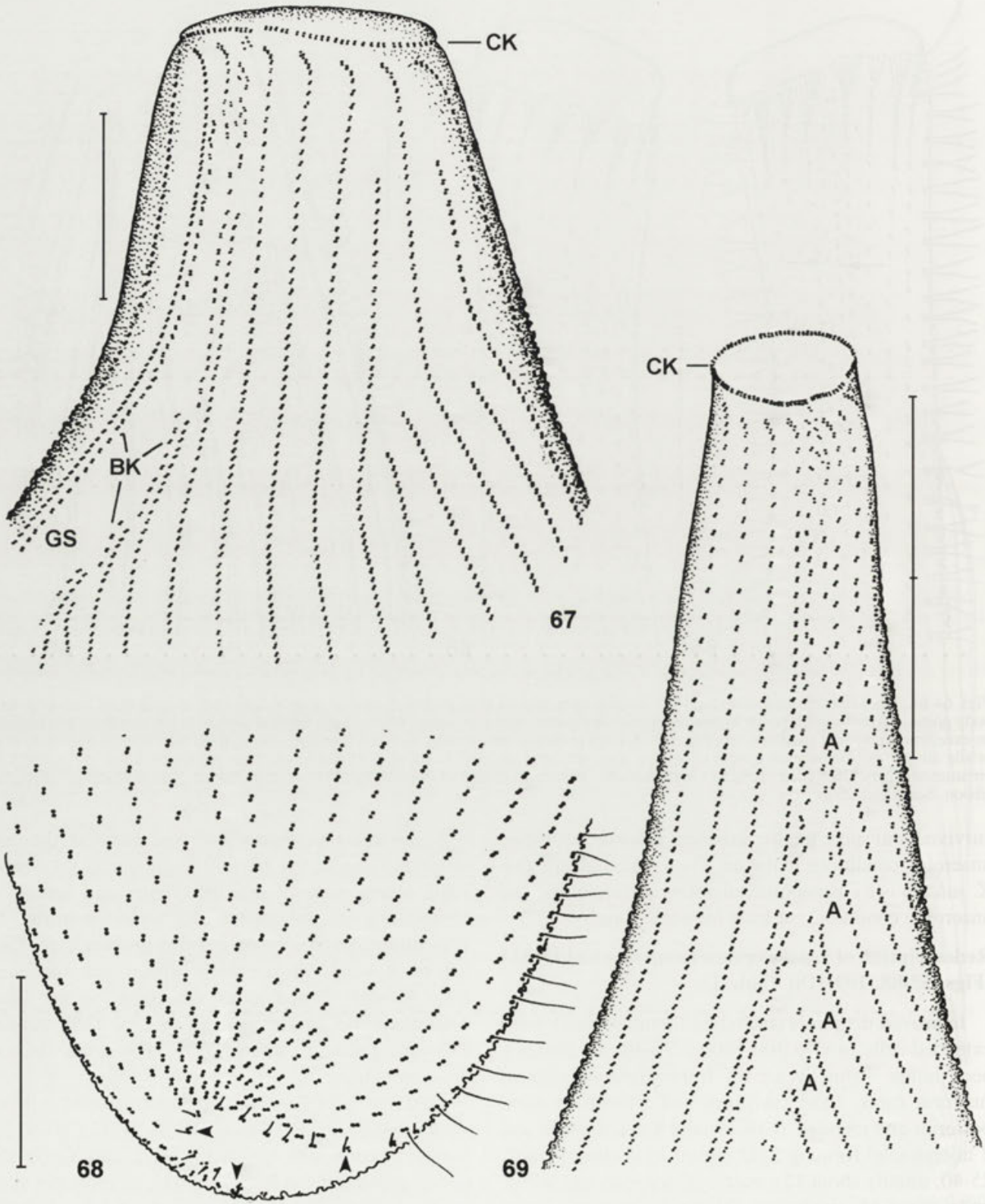

Figs. 67-69. *Trachelocerca incaudata*, somatic infraciliature after protargol impregnation. 67, 69 - left side of anterior body portion showing variability of bristle kinety; 68 - posterior end showing bristle kinety (arrowheads) extending around glabrous stripe. A - anterior secant system, BK- bristle kinety, CK - circumoral kinety, GS - glabrous stripe. Scale bar division 20 µm

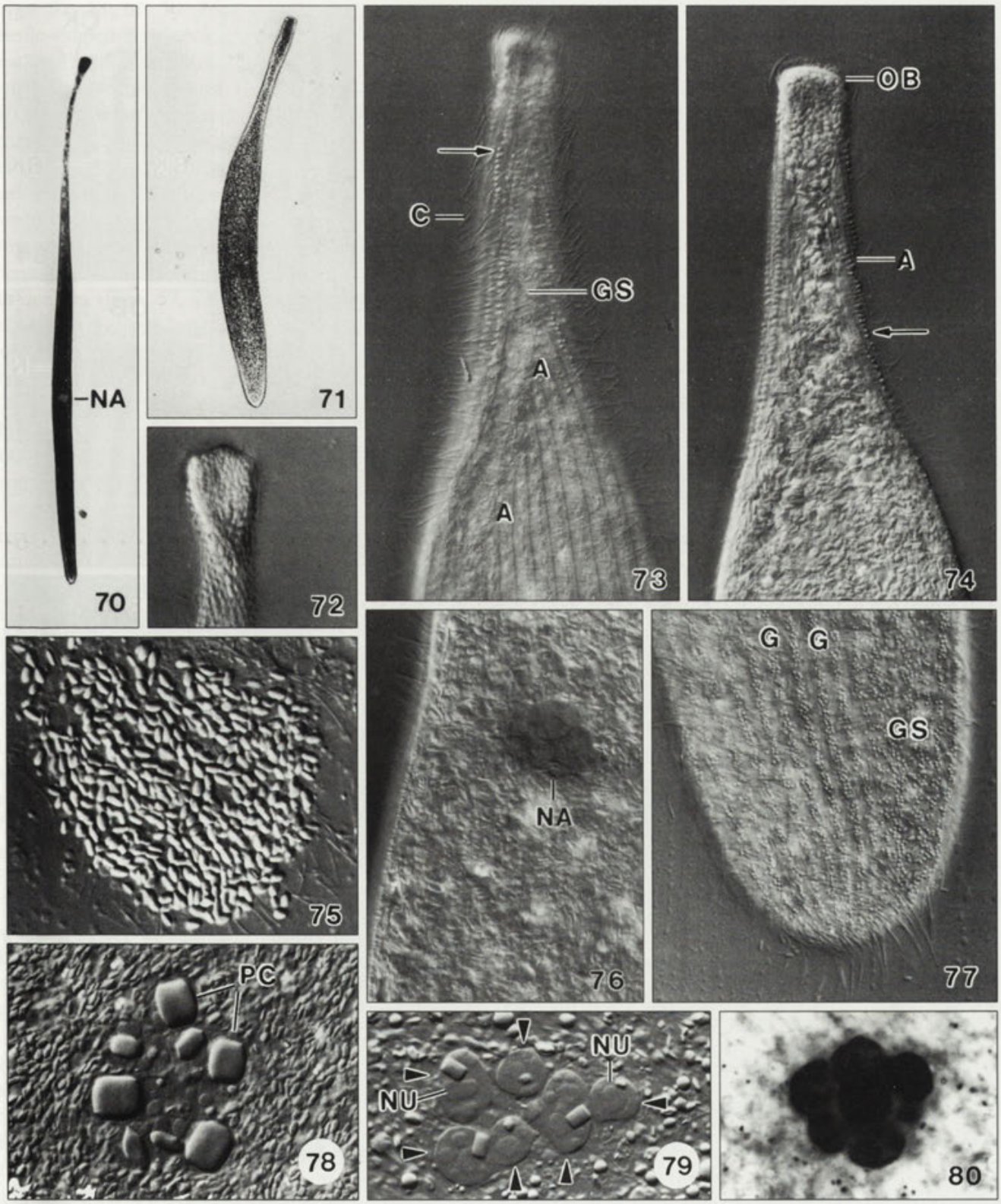

Figs. 70-80. *Trachelocerca incaudata* from life (70-79) and after protargol impregnation (80). For sizes, see text and Table 1. 70, 71 - extended and slightly contracted specimen. Note rounded posterior end; 72, 73, 74 - left anterior body portion of partially contracted specimen. Arrows mark claviform cortex blisters; 75 - ellipsoidal, highly refractile cytoplasmic inclusions making cells dark at low magnification (Fig. 70); 76, 78, 79, 80 - nuclear capsules, individual macronuclei (arrowheads) become recognizable only in squashed (79) or stained (80) capsules; 77- surface view of posterior body portion showing cortical granule stripes. A - anterior secant system, C - cilia, G - cortical granules, GS - glabrous stripe, NA - nuclear apparatus, NU - nucleoli, OB - oral bulge, PC - protein (?) crystals

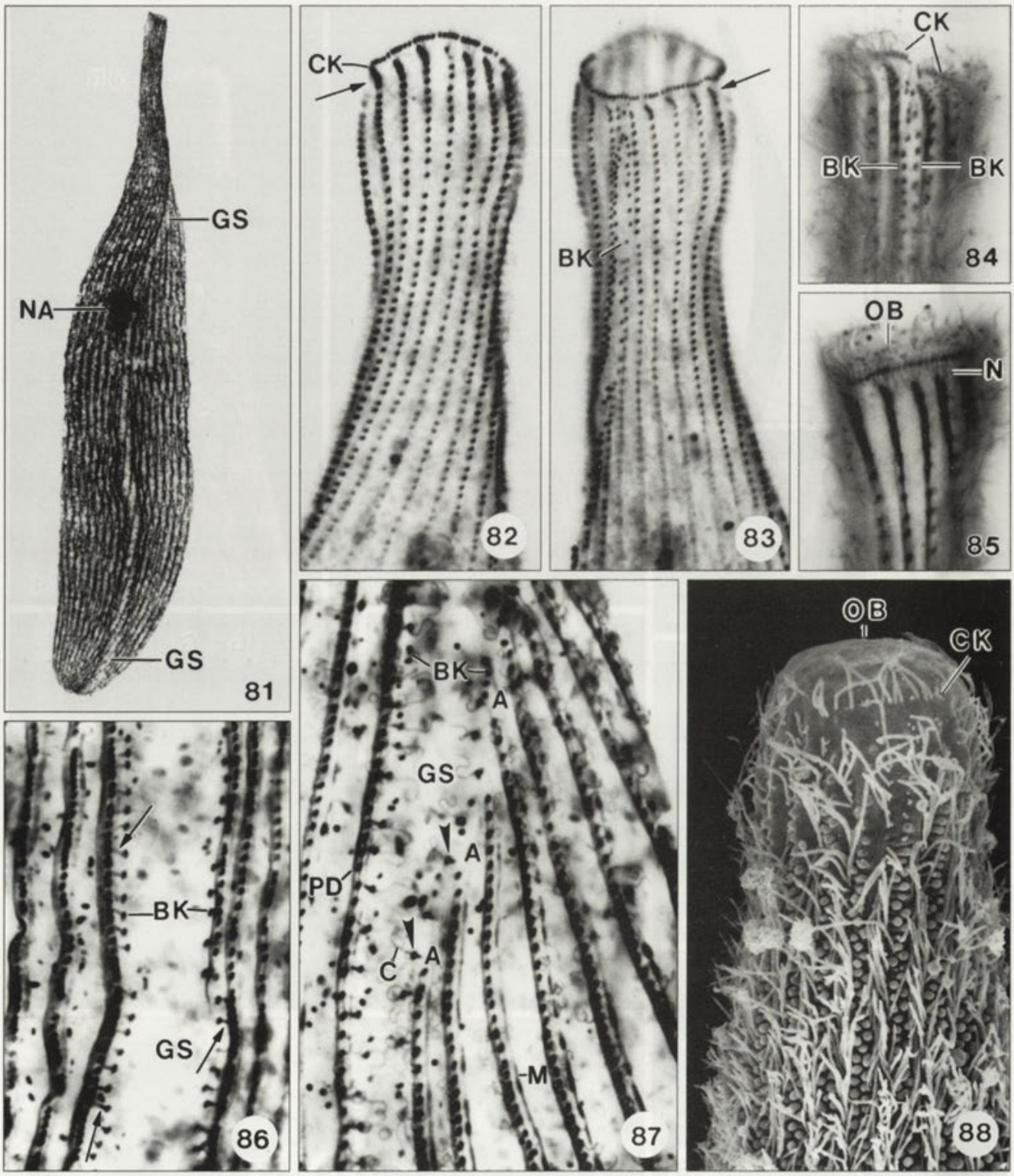

Figs. 81-88. *Trachelocerca incaudata*, somatic and oral infraciliature after protargol impregnation (81-87) and in the scanning electron microscope (88). For sizes, see text and Table 1. 81 - general left side view (cp. Fig. 62); 82, 83, 84, 85 - right and left side views of anterior body portion. Arrows mark condensed dikinetids at anterior end of kineties. 86, 87 - left side views showing details of somatic kineties and bristle kinetids at high magnification (cp. Fig. 66). Arrows mark fibre originating from ciliated basal body of bristle dikinetids, which are composed of three minute granules (arrowheads); 88 - anterior body portion of contracted specimens showing conspicuous, claviform cortical blisters. A - anterior secant system, BK- bristle kinety, C - cilia, CK - circumoral kinety, GS - glabrous stripe, M - myoneme, N - nematodesmata, NA - nuclear apparatus, OB - oral bulge, PD - postciliodesma

(Figs. 55, 58, 61, 70, 75). Fully extended specimens needle-shaped with neck rather distinctly set off from head and cylindroidal trunk; no tail, i.e. posterior region only slightly tapering and narrowly rounded (Figs. 55, 70). Head about 20 µm wide, claviform when fully extended, usually, however, cylindroidal and indistinctly set off from neck, whitish in undisturbed specimens, dark in disturbed and thus frequently contracting cells due to shifting of ellipsoidal inclusions described above from trunk to head (Figs. 57, 71, 72, 74). Oral bulge inconspicuous because indistinctly set off from head, surface flat (Figs. 57, 74, 88), centre in one specimen filled with 2-3 µm long, drumstick-shaped structures, possibly extrusomes (Fig. 57); Dragesco (1960) observed "navicular trichocysts" around the oral opening. Slightly contracted cells cylindrical or claviform (Fig. 71), fully contracted specimens fusiform and about 300 µm long *in vivo* (Fig. 56); glabrous stripe neither protruding nor distinctly tuberculate (Figs. 73, 77). Macronuclei globular, form conspicuous, about 20 µm sized capsule in centre of trunk (Figs. 55, 59, 62, 76, 80), individual nuclei recognizable only in strongly squashed capsules (Fig. 79); each nucleus contains some small and large nucleoli and, usually, one cuboid protein crystal, which often occupies more than half of the nucleus' volume and does not stain with protargol (Figs. 59, 78, 79). Micronuclei globular, in centre of macronuclear cluster. No contractile vacuole. Cortex highly flexible, about 1.5 µm thick, forms columnar tubercles between, and many small claviform blisters along ciliary rows in contracted specimens (Figs. 61, 73, 74, 88). Cortical granules about 1 x 0.5 µm in size, yellowish, arranged in broad stripes between kineties and in narrowly spaced rows in glabrous stripe (Figs. 58, 60, 61, 77). Cytoplasm packed with ellipsoid inclusions as described above, and some 3 µm sized fat globules (Figs. 58, 61, 75, 76). Movement like in other trachelocercids, i.e. elegantly gliding and winding between sand grains and organic debris.

Somatic infraciliature (Figs. 62-69, 81-88): the surface of *T. incaudata* is densely ciliated, leaving blank an only about 10 µm wide zone, the glabrous stripe, extending the whole body length in the midline of the left side (Figs. 58, 62, 81). The cilia, which are rather stiff and can be spread, are about 10 µm long and arranged in longitudinal rows which are distinctly separate from the circumoral kinety and extend between flat cortical crests. The anterior end of the ciliary rows has condensed, i.e. more narrowly spaced, dikinetids and is slightly curved to the right (Figs. 67, 69, 82, 83). About 16 ciliary rows are gradually shortened in the anterior trunk region and on the neck abutting to the left branch of the bristle kinety. Thus, the head has about half the kineties present in the centre of the trunk (Table 1). The posterior secant system consists of only about 6 shortened kineties because the body narrows only slightly, i.e. is tailless. The ciliary rows neighbouring the right branch of the bristle are unshortened anteriorly and posteriorly (Figs. 62, 66, 69, 73, 87).

The entire infraciliature consists of dikinetids which, however, have a specialized ciliation. The dikinetids are rotated 20-30° counter-clockwise to the kinety axis and associated with conspicuous, overlapping postciliary microtubule ribbons which originate from the posterior basal body of the dikinetids and form a thick, strongly impregnated postciliodesma right of each ciliary row. A thin, sharply impregnated subkinetal microtubule ribbon extends underneath each ciliary row (Figs. 66, 86, 87). Only the anterior basal body of the dikinetids is ciliated, except in the neck region, where both are ciliated.

The contractile apparatus of *T. incaudata* consists of a myoneme close to the left of each kinety (Figs. 66, 86, 87). The distinctiveness of the myonemes varies highly, depending on preparation conditions; frequently, they are partially or completely unstained. The myonemes are flattened ribbon-like and extend from the neck to the posterior end of the cell becoming slightly thicker from anterior to posterior. No myonemes were found in the glabrous stripe.

The glabrous stripe, which extends along the whole length of the body, widens gradually from the head to the trunk, where it obtains its full width corresponding to an area occupied by 2-3 kineties. The glabrous stripe is bordered by the bristle kinety, which consists, like the ordinary ciliary rows, of dikinetids having about 12 µm long, rather stiff cilia. However, the bristle kinety is easily distinguished from ordinary somatic ciliary rows because its dikinetids are more irregularly and loosely arranged and either lack or have very inconspicuous postciliary microtubule ribbons too small to be recognized with the light microscope (Figs. 58, 62, 63, 66, 73, 86, 87). Furthermore, the bristle kinetids have a unique ciliation, most parsimoniously explained by the assumption that they belong to a single kinety extending along the stripe margins (Foissner and Dragesco 1996b; Fig. 68). Both ends of the bristle kinety are very close together subapically, where some irregularly arranged

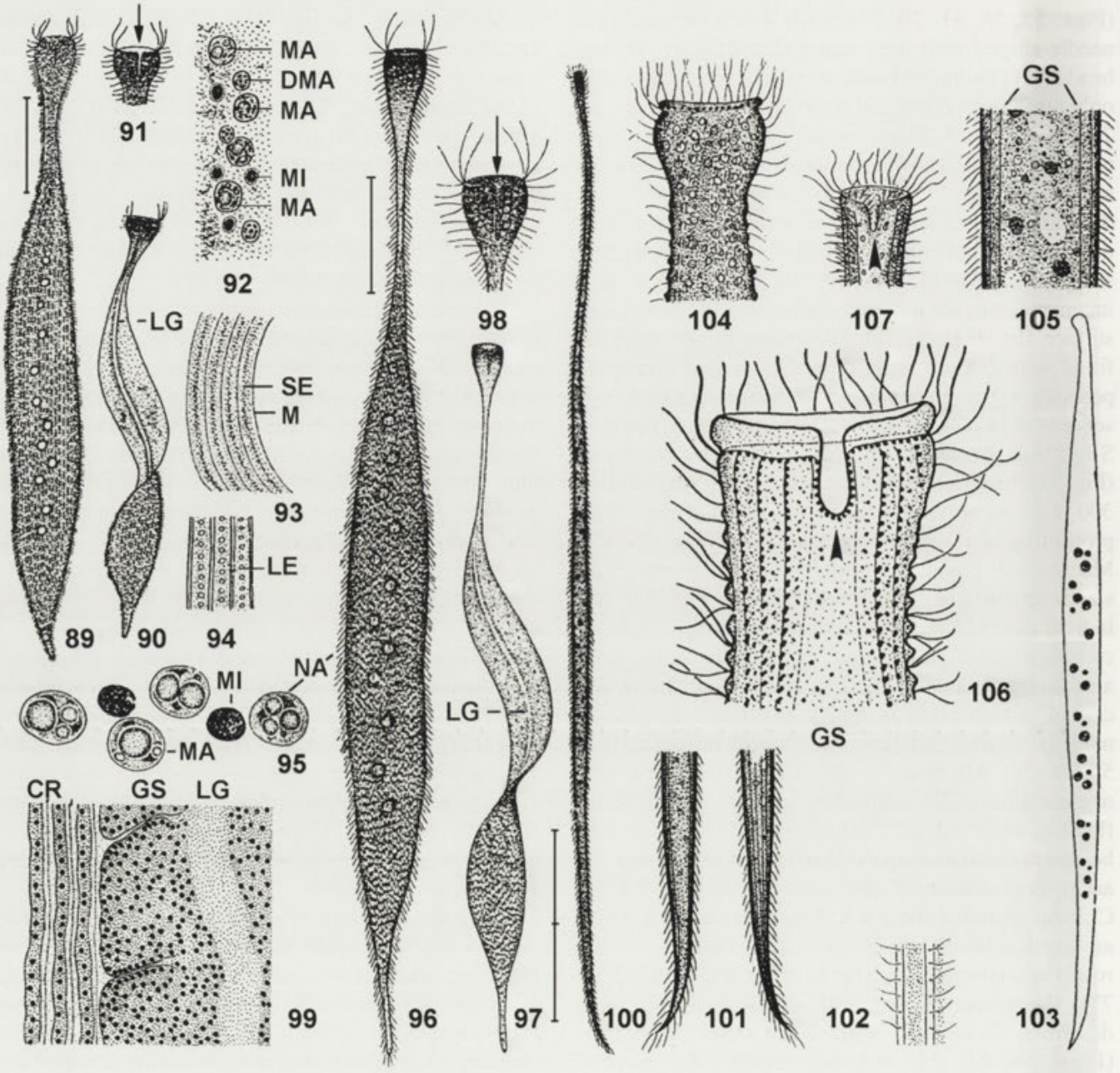

Figs. 89-107. Comparison of *Kovalevaia sulcata* (89 - 99) and *K. teissieri* (100-107). Figs. 89-99. *Kovalevaia sulcata* from life (89-91, 93, 94, 96-98), after Feulgen reaction (92, 95), and in a light green preparation (99). Russian Black Sea population (type, Figs. 89-94, from Kovaleva 1966); Bulgarian Black Sea population (Figs. 95-98, from Kovaleva and Golemansky 1979); Japan Sea population (Fig. 99, from Raikov and Kovaleva 1968). 89, 90, 96, 97 - typical gliding and swimming specimens; 91, 98 - heads, arrows mark brosse cleft; 92, 95 - nuclear apparatus; 93, 94, 99 - surface views showing cortical granulation. Figs. 100-107. *Kovalevaia teissieri* from life (100-102, 104, 105, 107), after Feulgen reaction (103), and protargol impregnation (106). Roscoff population (type, Figs. 100-105, from Dragesco 1960); Roscoff population (Fig. 106, from Dragesco 1963); Somalian population (Fig. 107, from Ricci et al. 1982). 100 - general view of typical specimen; 101 - left and right side view of posterior body portion; 102- surface view showing cortical granulation; 103 - nuclear apparatus; 104, 107 - heads; 105 - left side view of trunk region; 106 - infraciliature of anterior left side. Arrowhead marks circumoral kinety extending at margin of brosse cleft. Abbreviations: CR - ciliary row, DMA - developing macronucleus, GS - glabrous stripe, LE - large extrusomes (cortical granules), LG - longitudinal groove on glabrous stripe, M - myoneme, MA - macronuclei, MI- micronuclei, NA - nuclear apparatus, SE - small extrusomes (cortical granules). Scale bar division 100 μm

dikinetids occur (Figs. 64, 67, 69, 83, 84). The dikinetids along the right margin of the glabrous stripe have the *posterior* basal body ciliated, whereas the dikinetids along the left margin of the glabrous stripe have the *anterior* basal body ciliated. Nonciliated granules are scattered within the bristle kinety. In the best preparations, the *ciliated* dikinetids are composed of three granules forming minute triangles, and the ciliated basal body of the bristle dikinetids is associated with a short fibre directed, like the third granule, laterally towards the somatic kineties (Figs. 66, 86, 87).

Oral infraciliature (Figs. 57, 64, 65, 67, 69, 72, 74, 82-85, 88). The oral infraciliature of *T. incaudata* is very simple and consist of a single, dikinetidal circumoral kinety extending in the flat furrow separating the oral bulge from the head. The circumoral kinety is very likely composed of about 15 short fragments, as indicated by small gaps, 1-2 dikinetids wide, and the bundled arrangement of the nematodesmata. The circumoral dikinetids have only the posterior basal body ciliated and are associated with a distinct nematodesma. The nematodesmata of each dikinetidal fragment unite to small bundles extending posteriorly underneath the anterior end of the somatic kineties.

Distribution and ecology: there are numerous records of *T. incaudata* from Eurasia, but none from South America and Australia (for reviews, see Agamaliev 1967, Hartwig and Parker 1977, Hartwig 1980). However, this does not prove a restricted geographic distribution but very likely only reflects the highly limited data available from these regions. *Trachelocerca incaudata* prefers, like most trachelocercids, sand with a grain size of 0.1-0.25 mm (Agamaliev 1967, Burkovsky 1970).

DISCUSSION

Identification and synonymy of *Kovalevaia sulcata*

My observations on *K. sulcata* match the original description (Kovaleva 1966) very well and, especially so, those on a population from the Posjet Gulf (Japan Sea), later reported by Raikov and Kovaleva (1968). Thus, there is no doubt about the identification (cp. Figs. 1-10, 27-31, 46-54, 89-99). As mentioned by Raikov and Kovaleva (1968), the Posjet specimens are striking in being, with respect to the number of ciliary rows, intermediates between the type population of *K. sulcata* from the Black Sea and *Tracheloraphis poljanskyi* (Raikov, 1963) comb. n.[1] from the Japan Sea. The Posjet specimens have, similarly to those from Roscoff (Table 1), 10-16 kineties and are in this respect nearer to *T. poljanskyi* (12 kineties) than to the Black Sea form of *K. sulcata*, which has 16-24 ($\bar{x}$ 20) ciliary rows (Kovaleva 1966, Kovaleva and Golemansky 1979). Thus, I agree with Raikov and Kovaleva (1968) that the presence, respectively, absenceof a longitudinal groove on the glabrous body side should be considered as the main distinctive character between *K. sulcata* and *T. poljanskyi*. Whether or not *T. poljanskyi* belongs to the genus *Kovalevaia* needs investigation of silver-impregnated specimens (see below).

Tracheloraphis grassei (Dragesco, 1960) Foissner and Dragesco, 1996b is also rather similar to *K. sulcata* because it possesses large, brown extrusomes and a longitudinal groove on the glabrous body side. However, *T. grassei* has a unique apical prominence and a different body shape, i.e. narrows gradually to the tail. Furthermore, the small extrusomes of *T. grassei* are colourless. I thus agree with Kovaleva (1966) that *T. grassei* and *K. sulcata* are different species.

Kovalevaia as a new genus and its systematic position

The somatic infraciliature of the trachelocercids shows a great similarity, although some details, for instance, the ciliation of the dikinetids and the fine structure of the bristle kinety vary (Table 2). Thus, Foissner and Dragesco (1996b) used the shape and structure of the brosse and circumoral kinety for the generic classification of trachelocercid karyorelictids (Fig. 108, Table 2).

Kovalevaia has a "simple" circumoral kinety made up of a single row of dikinetids. Thus, it belongs to the family Trachelocercidae Kent, 1881 as defined by Foissner and Dragesco (1996b). The circumoral kinety of *K. sulcata* surrounds not only the head but also the brosse cleft, producing a unique, key-hole-shaped pattern (Figs. 20, 26, 36, 108). Admittedly, at first glance, this is a rather inconspicuous generic character. However, many *Tracheloraphis* species, although also having a brosse cleft, show a differently shaped, i.e. sigmoidal circumoral kinety (Fig. 108; Foissner and Dragesco 1996b), indicating that brosse cleft and shape of the circumoral kinety are independent from each other or, in other words, that trachelocercids with a key-hole-shaped circumoral kinety very likely represent a particular

[1] This species is transferred from *Trachelonema* to *Tracheloraphis* because *Trachelonema* is a junior, subjective synonym of *Tracheloraphis* (Foissner and Dragesco 1996b)

evolutionary branch. Thus, separation at genus level seems justified. Furthermore, some simple morphological grouping of this large assemblage (70 described and, very likely, many undescribed species; Foissner 1997b) is of practical value.

The observation on the occurrence of a key-hole-shaped circumoral kinety in trachelocercids is, in fact, not entirely new. Dragesco (1963) showed it for the first time in protargol-impregnated specimens of *Tracheloraphis teissieri* (Fig. 106), which is thus transferred to the new genus: *Kovalevaia teissieri* (Dragesco, 1960) comb. n. (basionym: *Tracheloraphis teissieri* Dragesco, 1960). *Kovalevaia teissieri* has, like *K. sulcata*, minute brown extrusomes, while large brown extrusomes and a longitudinal groove on the glabrous body side are lacking. Further differences concern the body shape, which is much more slender in *K. teissieri* than in *K. sulcata* (cp. Figs. 1, 27, 89, 96, 100), and the nuclei, which are

Table 2. Genus distinction in trachelocercid karyorelictids[1]

Character	*Trachelocerca*	*Trachelolophos*	*Kovalevaia*	*Tracheloraphis*	*Prototrachelocerca*
Brosse	absent	absent[2]	present	present	present
Ciliary tuft in oral cavity	absent	present	absent	absent	absent
Circumoral kinety, structure[3]	simple	simple	simple	simple	complex
Circumoral kinety, shape[4]	circular	circular	key-hole-shaped	sigmoidal	sigmoidal
Bristle kinety[5]	simple	simple	simple	simple or complex	mixed
Glabrous stripe	usually ≤ 1/3 of body width	≤ /3 of body width	of body width	usually ≥ 1/3 of body width	about 1/3 of body width

[1] Modified from Foissner and Dragesco (1996b)
[2] Very likely, the ciliary tuft within the oral cavity is a highly modified brosse
[3] Simple = single row of dikinetids; complex = two or more rows of dikinetids. See Foissner (1996) for details
[4] See Figure 108
[5] Simple = single row of dikinetids; complex = many minute kineties composed of 2-5 dikinetids in trunk region; mixed = basically like "simple" type, but with some minute kineties interposed, similar to "complex" type

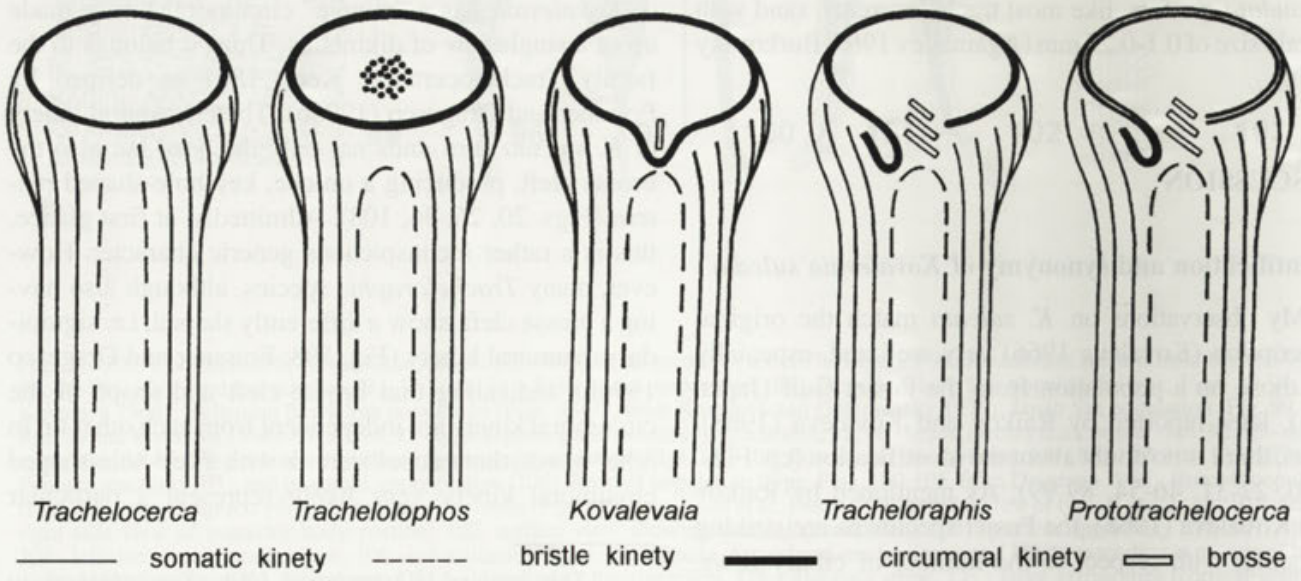

Fig. 108. Genus distinction in trachelocercid karyorelictids. For explanation, see text and Table 2

more irregularly arranged in *K. teissieri* than in *K. sulcata* (cp. Figs. 5, 6, 89, 103). The number of ciliary rows is rather similar (8-12 vs. 10-24) in both species, if the whole range reported in the literature is taken into account (Dragesco 1960, 1963; Agamaliev 1968; Ricci et al. 1982).

Kovalevaia sulcata has a very conspicuous oral cavity (Figs. 2, 3, 37, 43, 44), distinctly different from the flat oral bulge surface found in *Trachelocerca* (Fig. 88). However, *K. teissieri* apparently lacks such an oral cavity (Figs. 104, 107). Thus, the generic significance of this feature remains doubtful.

Very likely, some of the numerous *Trachelocerca* and *Tracheloraphis* species in the older literature belong to *Kovalevaia*, too, especially *Tracheloraphis grassei* (Dragesco, 1960) and *T. poljanskyi* (Raikov, 1963), as indicated by their general organization and the conspicuous brown extrusomes. However, a definite transfer should await the investigation of silver-impregnated specimens, because neither the brosse cleft nor the extrusomes and the groove on the glabrous stripe are unambiguous generic characters. Large, brown extrusomes occur, for instance, also in supposedly rather distant trachelocercids, *viz. Trachelocerca margaritata* Kahl,

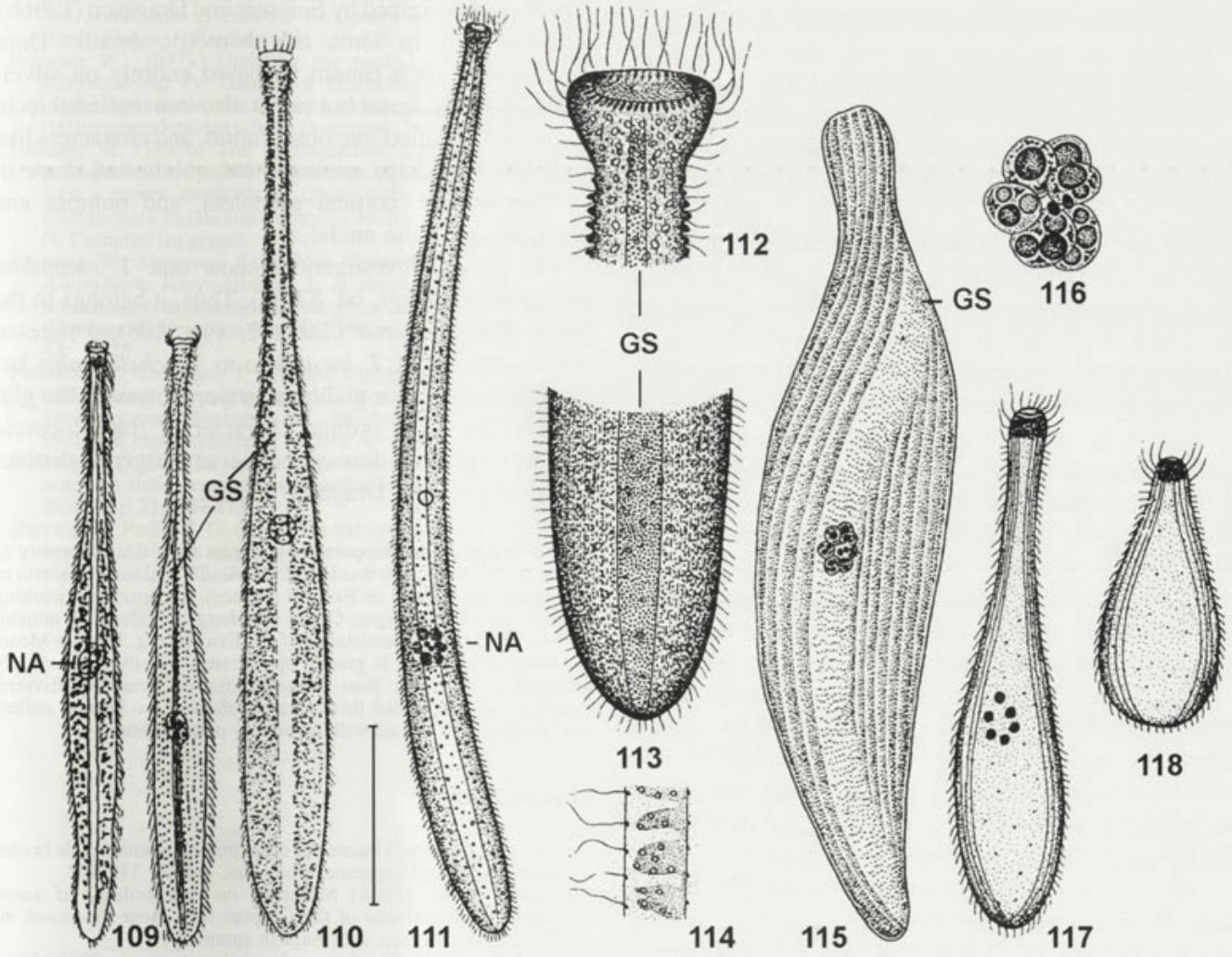

Figs. 109-118. *Trachelocerca incaudata* from life (109-114, 117, 118) and after hematoxylin staining (115, 116). 109 - left side views, length up to 500 µm (from Kahl 1933, 1935); 110 - left side view, length 500 µm (from Kiesselbach 1936); 111, 112, 113, 114 - total left side view (bar division 100 µm), head with navicular extrusomes, left side view of posterior body portion, and surface view showing cortical blisters and granules (from Dragesco 1960); 115, 116 - arrangement of ciliary rows on left side and nuclear apparatus (from Raikov and Kovaleva 1968); 117, 118 - extended and contracted specimens (very likely misidentified, as indicated by broad glabrous stripe; from Czapik and Jordan 1976). GS - glabrous stripe, NA - nuclear apparatus

1930 (see also Kahl 1935) and *T. binucleata* Dragesco, 1960. The extrusomes of *K. sulcata* have a unique structure (Figs. 9, 51-54) and origin (Kovaleva and Raikov 1972) and thus possibly represent an additional generic character. However, this can not be reliably assessed at the present state of knowledge, because the other species mentioned above have not yet been studied in this respect.

Trachelocerca incaudata

The following review shows that my observations largely agree with previous reports, i.e. that identification is beyond all doubt. However, all former data are entirely based on live observations and/or conventional histological techniques. Thus, they lack details of the infraciliature and accurate morphometrics. Furthermore, all authors obviously observed only slightly contracted specimens (cp. Figs. 55, 70, 71, 109-111).

The original description of *T. incaudata* is rather incomplete, as also mentioned by Dragesco (1960): "Extended specimens (rarely found) up to 500 µm long; shape very constant, trunk ribbon-like, slightly narrowed and rounded posteriorly; invariably only one nuclear bleb; cytoplasm darkly granulated; glabrous stripe very narrow and difficult to recognize, bordered by a row of bristles on both sides; common in marine sands at Kiel, Germany (Kahl 1933, 1935; Fig. 109). Kiesselbach (1936) found two specimens at the Adriatic coast of Italy. They had a size of 500 x 45 µm and were strongly contractile (Fig. 110). Dragesco (1960), who found *T. incaudata* at the same site as I did, i.e. at Roscoff, not only confirmed Kahl's observations but also added some important characteristics (Figs. 111-114): length 400-650 µm, very fragile; posterior end rounded; 6 macronuclei and 2 micronuclei forming tight cluster (capsule); cytoplasm packed with various inclusions; 32 meridional somatic kineties; glabrous stripe narrow, corresponding to an area occupied by about 4 kineties, contains conspicuous, highly refractile, brownish protrichocysts found also between ciliary rows; head as usual, oral opening bordered by navicular trichocysts. Raikov and Kovaleva (1968) confirmed Dragesco's observations and described a variety with 4 micronuclei and 24-30 ciliary rows. Furthermore, they extended the variation of the nominal species, which occurred concomitantly with the variety *quadrimicronucleata* in the Japan Sea, by reporting that it has 6-8 macronuclei, 2 very small (1-1.5 µm) micronuclei, and 28-32 ciliary rows (Figs. 115, 116). Czapik and Jordan (1976) studied specimens from the Baltic coast and noted a brown colour and high fragility (Figs. 117, 118). Wright (1983), who found *T. incaudata* in marine sands from the south coast of England, confirmed Dragesco (1960). His specimens were 400-800 µm long (average 600 µm) and had 6-8 macronuclei, 2 micronuclei, 28-32 ciliary rows, and a narrow glabrous stripe, corresponding to an area occupied by 2-3 kineties.

Borror (1973) suggested uniting several closely related forms to a "*Trachelocerca incaudata* complex", *viz. T. incaudata*, *T. monocaryon*, *T. gracilis*, *T. stephani*, and *T. swedmarki*. This view is consistent with my data, which show that the infraciliature of *T. incaudata* is extremely similar to that of *T. sagitta* and, especially, *T. ditis*, as redescribed by Foissner and Dragesco (1996b), differing only in some morphometric details. Thus, species separation cannot be based entirely on silver-impregnated material but needs also conventional techniques, i.e. detailed live observation, and characters like body size and shape, arrangement, colour and shape of the extrusomes (cortical granules), and number and arrangement of the nuclei.

The present investigations show that *T. incaudata* lacks a brosse (Figs. 64, 82-84). Thus, it belongs to the genus *Trachelocerca* (Table 2, Fig. 108). Dragesco (1960) transferred *T. incaudata* to *Tracheloraphis* because it possesses a glabrous stripe. However, the glabrous stripe is an ordinal character of trachelocercid karyorelictids and thus cannot serve for genus distinction (Foissner and Dragesco 1996b).

Acknowledgements. Supported by a grant from the University of Salzburg. I would like to thank Prof. Dr. André Toulmond, director of the Station Biologique de Roscoff (France), for providing working facilities, and Dr. Remigius Geiser (Salzburg) for advice on nomenclature. The technical assistance of Dr. Eva Herzog, Brigitte Moser and Mag. Eric Strobl is greatly appreciated. Finally, I am deeply indebted to Prof. Dr. Jean Dragesco (Saint-Clément-de-Rivière, France), who stimulated this research, showed me how to collect sand ciliates, and helped with laboratory organization.

REFERENCES

Agamaliev F. G. (1967) Faune des ciliés mésopsammiques de la côte ouest de la mer Caspienne. *Cah. Biol. mar.* **8:** 359-402

Agamaliev F. G. (1968) Materials on morphology of some psammophilic ciliates of the Caspian Sea. *Acta Protozool.* **6:** 225-244 (in Russian with English summary)

Borror A.C. (1973) *Tracheloraphis haloetes* sp. n. (Ciliophora, Gymnostomatida): description and a key to species of the genus *Tracheloraphis*. *J. Protozool.* **20:** 554-558

Burkovsky I. V. (1970) Ciliates of the sand littoral and sublittoral of Kandalaksha Gulf (White Sea) and the analysis on the fauna of

benthic ciliates of other seas. *Acta Protozool.* **8:** 183-201 (in Russian with English summary)
Carey P. G. (1992) Marine Interstitial Ciliates. Chapman & Hall, London, New York, Tokyo, Melbourne, Madras
Corliss J. O. (1979) The Ciliated Protozoa. Characterization, Classification and Guide to the Literature. 2nd ed. Pergamon Press, Oxford, New York, Toronto, Sydney, Paris, Frankfurt
Czapik A., Jordan A. (1976) Les ciliés psammophiles de la mer Baltique aux environs de Gdañsk. *Acta Protozool.* **15:** 423-445
Dragesco J. (1960) Ciliés mésopsammiques littoraux. Systématique, morphologie, écologie. *Trav. Stn biol. Roscoff* (N.S.) **12:** 1-356
Dragesco J. (1963) Compléments a la connaissance des ciliés mésopsammiques de Roscoff. I. Holotriches, II. Hétérotriches. *Cah. Biol. mar.* **4:** 91-119, 251-275
Fauré-Fremiet E. (1951) The marine sand-dwelling ciliates of Cape Cod. *Biol. Bull. mar. biol. Lab., Woods Hole* **100:** 59-70
Foissner W. (1991) Basic light and scanning electron microscopic methods for taxonomic studies of ciliated protozoa. *Europ. J. Protistol.* **27:** 313-330
Foissner W. (1996) Updating the trachelocercids (Ciliophora, Karyorelictea). II. *Prototrachelocerca* nov. gen. (Prototrachelocercidae nov. fam.), with a redescription of *P. fasciolata* (Sauerbrey, 1928) nov. comb. and *P. caudata* (Dragesco & Raikov, 1966) nov. comb. *Europ. J. Protistol.* **32:** 336-355
Foissner W. (1997a) Updating the trachelocercids (Ciliophora, Karyorelictea). IV. Transfer of *Trachelocerca entzi* Kahl, 1927 to the Gymnostomatea as a new genus, *Trachelotractus* gen. n. (Helicoprorodontidae). *Acta Protozool.* **36:** 63-74
Foissner W. (1997b) The karyorelictids (Protozoa: Ciliophora), a unique and enigmatic assemblage of marine, interstitial ciliates: a review emphasizing ciliary patterns and evolution. In: Evolutionary Relationships among Protozoa (Eds. A. Warren & G. Coombs) (in press).
Foissner W., Dragesco J. (1996a) Updating the trachelocercids (Ciliophora, Karyorelictea). I. A detailed description of the infraciliature of *Trachelolophos gigas* n. g., n. sp. and *T. filum* (Dragesco & Dragesco-Kernéis, 1986) n. comb. *J. Euk. Microbiol.* **43:** 12-25
Foissner W., Dragesco J. (1996b) Updating the trachelocercids (Ciliophora, Karyorelictea). III. Redefinition of the genera *Trachelocerca* Ehrenberg and *Tracheloraphis* Dragesco, and evolution in trachelocercid ciliates. *Arch. Protistenk.* **147:** 43-91
Hartwig E. (1980) The marine interstitial ciliates of Bermuda with notes on their geographical distribution and habitat (1). *Cah. Biol. mar.* **21:** 409-441
Hartwig E., Parker J. G. (1977) On the systematics and ecology of interstitial ciliates of sandy beaches in north Yorkshire. *J. mar. biol. Ass. U. K.* **57:** 735-760
Kahl A. (1930) Urtiere oder Protozoa I: Wimpertiere oder Ciliata (Infusoria) 1. Allgemeiner Teil und Prostomata. *Tierwelt Dtl.* **18:** 1-180
Kahl A. (1933) Ciliata libera et ectocommensalia. Tierwelt Nord- und Ostsee **23 (Teil II, c_3):** 29-146
Kahl A. (1935) Urtiere oder Protozoa I: Wimpertiere oder Ciliata (Infusoria) 4. Peritricha und Chonotricha. *Tierwelt Dtl.* **30:** 651-886
Kent W. S. (1880-1882) A Manual of the Infusoria: Including a Description of all Known Flagellate, Ciliate, and Tentaculiferous Protozoa British and Foreign, and an Account of the Organization and Affinities of the Sponges. Vols. I-III. D. Bogue, London (Vol. I 1880: 1-432; Vol. II 1881: 433-720, 1882: 721-913; Vol. III 1882: Plates)
Kiesselbach A. (1936) Zur Ciliatenfauna der nördlichen Adria. *Thalassia* **2:** 1-53
Kovaleva V. G. (1966) Infusoria of the mesopsammon in sand bays of the Black Sea. *Zool. Zh.* **45:** 1600-1611 (in Russian with English summary)
Kovaleva V. G. (1974) The fine structure of ciliary and cortical organoids and some structures of the ectoplasm and endoplasm of *Trachelonema sulcata* (Ciliata, Holotricha). *Tsitologiya* **16:** 217-223 (in Russian with English summary)
Kovaleva V. G., Golemansky V. G. (1979) Psammobiotic ciliates of the Bulgarian coast of the Black Sea. *Acta Protozool.* **18:** 265-284 (in Russian with English summary)
Kovaleva V. G., Raikov I. B. (1972) Saccules énigmatiques en "soucoupes" et leur relation avec les protrichocystes chez le cilié holotriche *Trachelonema sulcata* Kovaleva. *Protistologica* **8:** 413-425
Raikov I. B. (1963) Ciliates of the mesopsammon of the Ussuri gulf (Japan Sea). *Zool. Zh.* **42:** 1753-1767 (in Russian with English summary)
Raikov I. B., Kovaleva V. G. (1968) Complements to the fauna of psammobiotic ciliates of the Japan Sea (Posjet gulf). *Acta Protozool.* **6:** 309-333
Ricci N., Santangelo G., Luporini P. (1982) Researches on the coast of Somalia. Sand-dwelling ciliates. *Monitore zool. ital., Suppl. (N. S.)* **17:** 115-148
Wright J. M. (1983) Sand dwelling ciliates of South Wales. *Cah. Biol. mar.* **24:** 187-214

Received on 23rd May, 1997; accepted on 10th July, 1997

Acta Protozoologica (1997) 36: 221 - 226

ACTA
PROTOZOOLOGICA

Myxobolus squamaphilus sp. n. (Myxozoa: Myxosporea), a Common Parasite of the Scales of Bream (*Abramis brama* L.)

Kálmán MOLNÁR

Veterinary Medical Research Institute, Hungarian Academy of Sciences, Budapest, Hungary

Summary. *Myxobolus squamaphilus* sp. n. (Myxosporea: Myxozoa) is a common parasite of bream (*Abramis brama*) in Lake Balaton and the River Danube. Its lentil-shaped, relatively small plasmodia develop in the connective tissue consisting of collagen fibrils on the surface of the cartilaginous plate of scales. Mature plasmodia containing only a few hundred spores can be detected in the fish in April and May. In March primarily the developing stages while in the early summer the traces left by excreted plasmodia can be detected in the scales. In the spring months, the prevalence of infection exceeds 50% while its intensity may reach 7 per scale. By its ellipsoidal, relatively large spores this species is well distinguishable from other species known from the bream and from other cyprinids.

Key words: *Abramis brama, Myxobolus*, Myxosporea, new species, scales.

INTRODUCTION

Different *Myxobolus* species occur in diverse locations within the host organism. Numerous species parasitise the skin of fish, and several of them (*M. caudatus, M. lobatus, M. niei*) establish themselves in the external layer of the integument. Some of the latter, such as the barbel parasites *M. squamae* and *M. cutanei*, the rainbow trout parasite *M. squamalis*, and *M. squamosus* describedfrom *Hybopsis kentuckiensis* form plasmodia on the scales as a typical location (Keysselitz 1908, Kudo 1934, Iversen 1954, Alvarez-Pellitero and Gonzalez-Lanza 1985). Egusa et al. (1990) observed a *Myxobolus* infection on the scales of the mullet (*Mugil cephalus*) and, based upon the typical location of cysts, described the causative species as *M. episquamalis*. While Shulman (1966) listed 14 *Myxobolus* species as being parasitic in bream (*Abramis brama*), Landsberg and Lom (1991) recorded only 7 species which had been described originally from bream. In Hungary, *Myxobolus* infection of bream living in Lake Balaton was studied by Jaczó (1940) who, in addition to the already known *M. muelleri*, reported two additional species (*M. hungaricus* and *M. variabilis*) from the gills of bream. Data on the parasite fauna of Lake Balaton bream can be found in a paper by Molnár and Székely (1995).

The present paper describes a *Myxobolus* species occurring specifically on the scales of bream (*Abramis brama*).

Address for correspondence: Kálmán Molnár, Veterinary Medical Research Institute, Hungarian Academy of Sciences, P.O.Box 18, H-1581 Budapest, Hungary; Fax:(36-1)252-1969; E-mail: kalman@novell.vmri.hu

MATERIALS AND METHODS

During a survey of the parasite fauna of bream living in Lake Balaton, a total of 60 breams were subjected to parasitological examination in 1994 (Molnár and Székely 1995), 41 in 1995, and 61 in 1996. The

Table 1. Seasonal occurance of *M. squamaphilus* on the scales of bream in Lake Balaton and River Danube

Month	Number of infected fish						Number of uninfected fish		
	Young plasmodia			Plasmodia with spores					
	1994	1995	1996	1994	1995	1996	1994	1995	1996
February								2	
March			2						2
April	3		3	3	2	1	12		5
May	4			3	5	8	4	3	3
June							8	13	5
July				3			4		10
August							3	2	4
September							5	2	5
October								12	11
November							12		

body length of the fish was 14–38 cm. Thirty scales were removed from the dorsal part of each dissected fish, and examined under stereomicroscope for the presence of *Myxobolus* cysts. The infected scales were

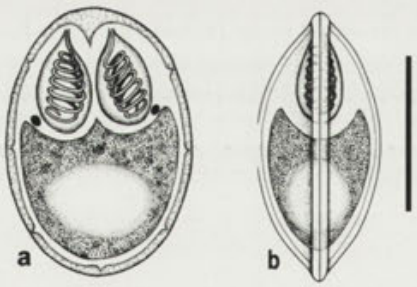

Fig. 1. Schematic drawing of the spores of *Myxobolus squamaphilus*. (a) - upper view, (b) - lateral view, bar - 10 µm

placed on a slide and examined in a light microscope at 100-fold magnification. The measurements of cysts were taken, the location of plasmodia on the scales was recorded, and the stage of maturity of plasmodia was determined. Spores were released from the spore-containing plasmodia with the help of a dissecting needle, then some of them were examined fresh while others were placed into glycerol-gelatin and processed into a permanent preparation. For histological examination, samples of infected scales were fixed in 10% buffered formalin or in Bouin's solution. To avoid epithelial injuries during scale removal and to determine the location of plasmodia more closely, large scale-covered skin pieces from the infected area were also fixed in the above solutions. The fixed samples were embedded in paraffin and cut into 4 µm thick sections which were stained with haematoxylin and eosin (H.-E.) and by the Giemsa stain. The measurements of spores were determined by comparing images of spores projected from an Olympus microscope to the screen of a video recorder with a computer-calibrated scale of measurements. The photomicrographs were taken with the help of a Jenaval photomicroscope.

RESULTS

Three *Myxobolus* species were consistently found in breams in Lake Balaton. The species *Myxobolus bramae* Reuss, 1906 was often detected in the form of small plasmodia located at the tips of the gill filaments. Less frequently a species forming large plasmodia occurred in a region close to the base of gill filaments. The spores of this latter species were identified as *M. hungaricus* Jaczó,

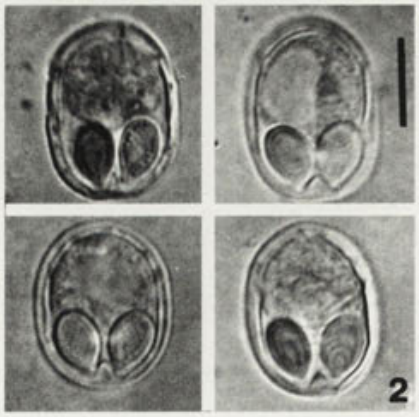

Fig. 2. Spores of *M. squamaphilus*, bar - 10 µm

1940. A hitherto unknown parasite, differing from the previously described species in cyst location and spore shape, was often found in the same fish. The plasmodia of this *Myxobolus* species were present in any location on those parts of the scales which were not covered by the neighbouring scales. In intensive infection, as many as

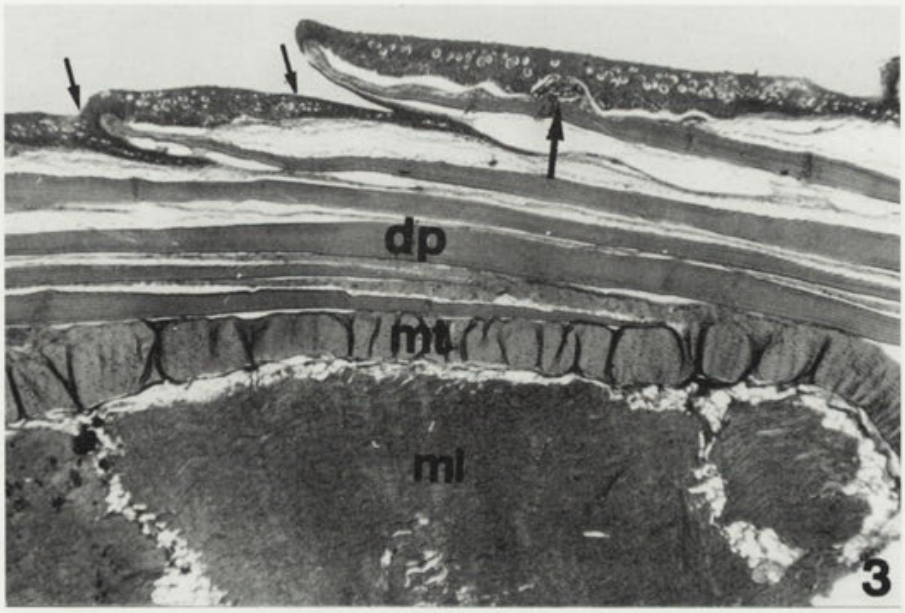

Fig. 3.Section of scales infected by *Myxobolus squamaphilus* plasmodia from bream. Cross section of the scaly skin and muscle: epidermis and its portion bent back under the scales (arrows); *Myxobolus* plasmodium (large arrow); dermis interwoven with calcified scale plates (dp); transversely running muscle bundles (mt); longitudinally running muscle bundles (ml). H.-E. (x40)

7-9 plasmodia were found on a single scale, and almost all scales proved to be infected. In less intensive infection, however, only a few scales were infected by single plasmodia.

The lentil-shaped plasmodia measuring 0.1–0.3 mm in diameter were located episquamally on the surface of the cartilaginous plate of the scales, and could be dislodged from there after epithelium removal. In majority of cases plasmodia were damaged during the removal, releasing spores or vegetative forms.

Plasmodia developing on scales were usually found on the fish since April; in one case, however, they were detected as early as March (Table 1). During the dissection of fish in April and May, *Myxobolus* plasmodia were detected on the scales of 13 out of 29 breams in 1994, 7 out of 10 breams in 1995, and 12 out of 20 breams in 1996. Subsequently the number of positive cases rapidly decreased, and only 3 out of 17 breams examined up to the end of August were found to be infected in 1994, while in the same period of 1995 no scale myxobolosis occurred at all. In fish examined in autumn, plasmodia were found only on a single occasion, in October 1996. Plasmodia examined at the beginning of April already contained mature spores; however, the majority of plasmodia still contained vegetative stages. Since the end of April, however, plasmodia were filled exclusively by mature spores (Figs. 1, 2). These relatively small plasmodia contained relatively few, 50 to 200, spores which, however, were large in size. In the summer months, small, round, transparent spots were often seen on the scales: these were of the same size as the plasmodia, and probably represented traces left behind by excreted plasmodia. The plasmodia found on a single occasion in the autumn were filled by spores containing a disintegrated sporoplasm.

Histologically, the integument of the bream was found to be similar to that of other scaly fish (Hawkes 1974, Lanzing and Wright 1976). The base of the scales is constituted by a calcified plate formed by the surrounding collagenous connective tissue. The external surface of the layer composed of collagen fibrils is bordered by a basal membrane covered by stratified epithelium. At the tip of the scales the epithelial layer turns back and covers part of the calcified collagen (cartilaginous) plate also from underneath (Fig. 3). In further parts of the plate, however, the plate-forming collagenous connective tissue is connected with the underlying plate of the scale by loose connective tissue. Beneath the overlapping scale plates, a layer of loose connective tissue binds the dermis together with the transversely or longitudinally running bundles of muscle fibres (Fig. 3). The plasmodia were always found in the corium layer composed of collagen fibrils running episquamally on the external surface of the calcified scale plate (Fig. 4). In some cases a capsule consisting of collagen fibrils had been formed around the plasmodia

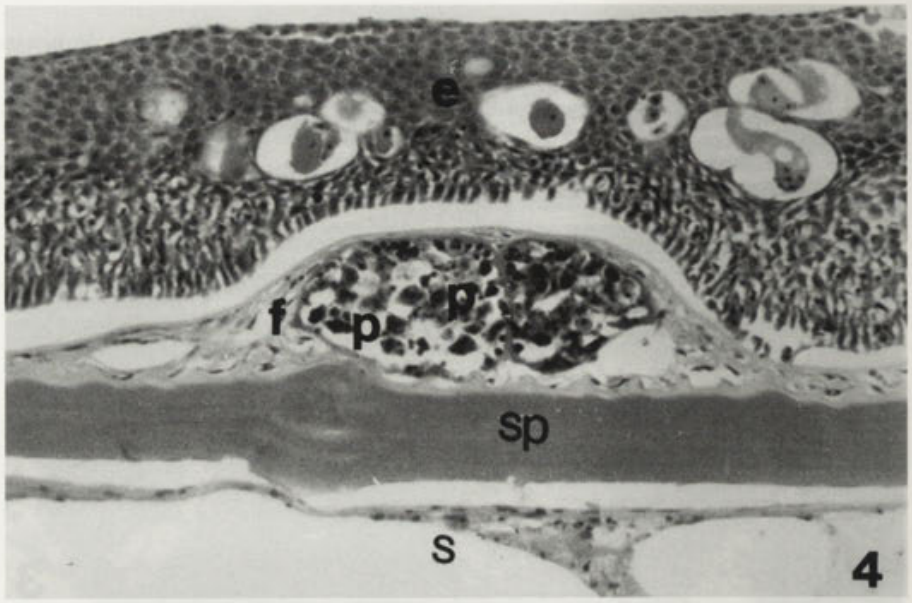

Fig. 4.Section of scales infected by *Myxobolus squamaphilus* plasmodia from bream. Location of *M. squamaphilus* plasmodium in the dermis: (e) cells of stratified epithelium with goblet cells; (f) fibrocyte layer rich in collagen fibrils in the dermis; (p) plasmodium; (sp) calcified scale plate; (s) subsquamal layer of dermis. H.-E. (x400)

(Figs. 4, 5). Scleroblast cells constituting the scale plates were not involved in the formation of the capsule. The collagenous capsule often grew very thin around plasmodia containing mature spores, and the plasmodium came into close contact with the basal membrane bordering the epidermis (Fig. 5).

Description of the newly found *Myxobolus* species:

Myxobolus squamaphilus sp. n. (Figs. 1, 2)

Type host: *Abramis brama* L.

Locality: Lake Balaton (Keszthely, Fonyód, Balatonszemes, Tihany, Csopak regions), River Danube (Surány, 30 km north of Budapest).

Site of infection: episquamal region of the connective tissue of the scales.

Type material: holotype deposited in the protozoan collection of the Zoological Department, Hungarian Natural History Museum. Coll. No. 671.

Description of the species: spores (Figs. 1, 2) relatively large, typically ellipsoidal with distinct sutural line. Spore valves symmetrical, smooth, with several sutural edge markings. Spores are 18.7 (17–19.5) µm long, 13.6 (13–14) µm wide and 11.5 (11–12) µm thick. Two polar capsules, pyriform in shape, tapering only at the discharging canals of the polar filament. They are equal in size, 6.8 (6.5–7.0) µm long and 4.2 (4–4.5) µm wide. The spore has a large triangular intercapsular appendix. Polar filaments closely coiled with 7 turns in the polar capsule, situated perpendicularly or subperpendicularly to the longitudinal axis of the capsule. A large distinct iodinophilous vacuole was found in the sporoplasm.

Differential diagnosis: different barbel species are the cyprinids best known to have parasitic *Myxobolus* species on their skin and scales. Of scale-parasitic myxosporeans, *M. squamae* living on the scales of barbel (*Barbus barbus*) is the best studied parasite. The species found on bream differs from the latter species in its markedly larger size and in the dissimilar location of plasmodia. While *M. squamaphilus* develops in the collagenous connective tissue of the scales, on the surface of the cartilaginous plate, the plasmodia of *M. squamae* are formed in deep layers of the chondrified substance. The new species described here also differs from *M. caudatus* reported from Central Asian barbel species and from *M. cutanei* detected from the scales of *Barbus barbus bocagei,* probably synonymous with the former. Namely, the latter species has a "racket-shaped" mucoid process at the caudal end of the spores. By their characteristically oval shape, the spores of *M. episquamalis* markedly differ from the mostly ellipsoidal spores of *M. squamaphilus.* Although *M. squamosus* resembles *M. squamaphilus* in spore shape, the spores of the former species have two narrow parallel ridges running parallel to the sutural ridge. In spore morphology, *M. squamaphilus* shows the highest degree of similarity with the species

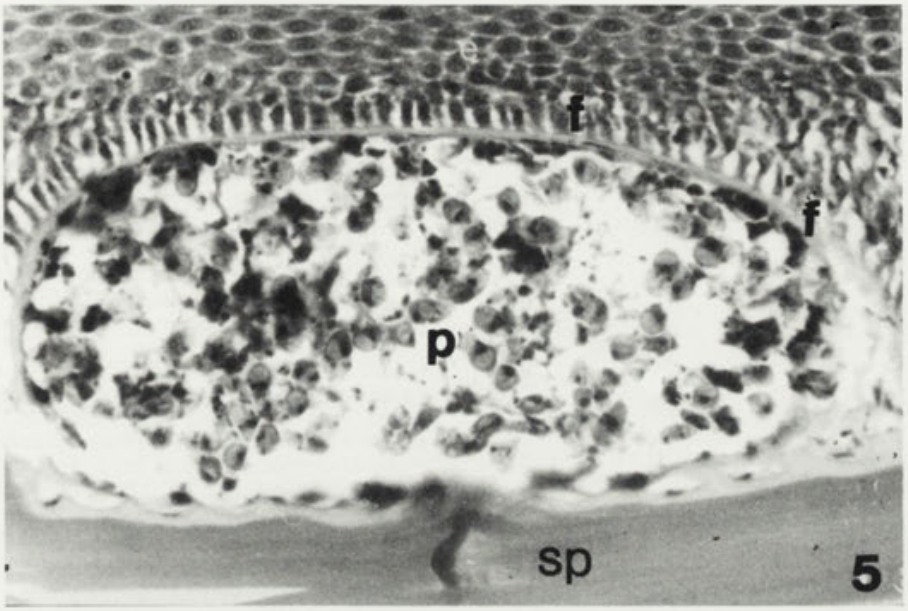

Fig. 5. Section of scales infected by *Myxobolus squamaphilus* plasmodia from bream. Episquamal plasmodium filled with spores and surrounded by a thinned-down collagenous capsule under the epithelium. (e) epithelium; (f) fibrocyte layer; (p) plasmodium; (sp) calcified scale plate. H.-E. (x800)

M. cycloides Gurley, 1894 described from bream, but is distinguishable from the latter species by its larger size, different host spectrum and location within the host.

DISCUSSION

Different *Myxobolus* species are common parasites of cyprinids and especially of the bream. Thus, it is surprising that in Lake Balaton, where more than half of the fish population is constituted by the bream, only three species have been recorded, one of which is the species described here. *Myxobolus squamaphilus* differs from *Myxobolus* species occurring in other cyprinids in both morphology and location. In addition to the morphological characteristics, knowledge of the host, organ and tissue specificity of a given parasite species is considered very important in the identification of myxosporeans (Molnár 1994). *Myxobolus squamaphilus* is a typical scale parasite whose specific location is the collagen fibril network covering the calcified plate of the scales. The parasite greatly resembles the species *M. squamae* in location; however, the plasmodia of the later species (Baska unpublished) develop in a cavity formed in the cartilaginous plate rather than episquamally, in a manner similar to that described by Iversen (1954) for the species *M. squamalis*. In its location, *M. squamaphilus* is most similar to *M. episquamalis* which, according to Egusa et al. (1990), also forms cysts apically on the surface of the ossifying plate of scales. While, however, *M. squamaphilus* forms small, uniform cysts in different areas of the calcified plate, *M. episquamalis* forms a mass consisting of cysts on the outer surface of the bony scale plate. These plasmodia are abundant in septa consisting of collagen fibrils and even blood vessels; at the same time, the plasmodia penetrate the calcified plate, causing small erosions. According to Moshu and Molnár (1997), in the European wild carp (*Cyprinus carpio carpio*) the plasmodia of the otherwise fin-parasitic *Thelohanellus nikolskii* can be found also on the scales. These plasmodia, however, always start to develop in a yet non-calcified plate area at the margin of the scale, and then develop in a cartilaginoid capsule formed by scleroblast cells. A common characteristic of all three parasites is their affinity to collagen. *Myxobolus squamaphilus* typically occurs in the spring, and spore formation is practically completed by the end of April. Most spores are released in the summer through skin injuries caused by the bursting of plasmodia. The sites of spore release are seen as tissue-less areas on the scales. In some cases, spore-containing plasmodia may occur on the scales also in other periods of the year; these, however, always contain aged spores. Signs of regenerative processes are often seen around aged and non-emptied plasmodia of numerous species. Both in *M. basilamellaris*

infection of the common carp and in *M. kotlani* infection of the eel, granulation tissue consisting of histiocytes was found to proliferate into the aged plasmodia, infiltrating and destroying the spores (Kovács-Gayer and Molnár 1983, Molnár et al. 1986). No such regenerative activity could be observed in *M. squamaphilus* infection, probably because the plasmodia enclosed in collagenous substance were inaccessible for the histiocytes.

Acknowledgements. The author wish to thank Dr Cs. Székely and Ms. Emese Papp for helping in collection of fish. Financial support to this work was provided by the National Research Fund (OTKA) project no. T014648, the US-Hungarian Joint Research fund, J. F. 326, and the Fish Management Fund of the Ministry of Agriculture.

REFERENCES

Alvarez-Pellitero M. P., Gonzalez-Lanza M. C. (1985) Studies on *Myxobolus* spp. of *Barbus barbus bocagei* from the river Esla (Leon, NW Spain). *Angew. Parasitol.* **26:** 3–12

Egusa S., Maeno Y., Sorimachi M. (1990) A new species of Myxozoa, *Myxobolus episquamalis* sp. nov. infecting the scales of the mullet, *Mugil cephalus* L. *Fish Pathol.* **25:** 87–91

Hawkes J. W. (1974) The structure of the fish skin I. General organisation. *Cell Tiss. Res.* **149:** 147–158

Iversen E. S. (1954) A new myxosporidian, *Myxosoma squamalis*, paasite of some salmonid fishes. *J. Parasitol.* **40:** 169–178

Jaczó I. (1940) Investigations on myxosporeans of fishes in Lake Balaton. I. *Magy. Biol. Kut. Int. Munkái* **12:** 277–290 (in Hungarian)

Keysselitz G. (1908) Über durch Sporozoen (Myxosporidien) hervorgerufene pathologische Veränderungen. *Verh. Ges. Deutsch. Naturforsch. und Ärztl. Vers.* **79:** 452–453

Kovács-Gayer É., Molnár K. (1983) Studies on the biology and pathology of the common carp parasite *Myxobolus basilamellaris* Lom et Molnár, 1983 (Myxozoa: Myxosporea). *Acta Vet. Hung.* **31:** 91–102

Kudo R. R. (1934) Studies on some protozoan parasites of fishes of Illinois. *Ill. Biol. Monogr.* **13:** 1–41

Landsberg J., Lom J. (1991) Taxonomy of the genera of the *Myxobolus/Myxosoma* group (Myxobolidae: Myxosporea), current listing of species and revision of synonyms. *Syst. Parasitol.* **18:** 165–186

Lanzing W. J. R., Wright R. G. (1976) The ultrastructure and calcification of the scale of *Tilapia mossambica*. *Cell Tiss. Res.* **167:** 37–47

Molnár K. (1994) Comments on the host, organ and tissue specificity of fish myxosporeans and on the types of their intrapiscine development. *Parasit. Hung.* **27:** 5–20

Molnár K., Lom J., Malik E. (1986) A skin disease of the eels caused by *Myxobolus kotlani* n. sp. *J. Appl. Ichthyol.* **2:** 42–48

Molnár K., Székely Cs. (1995) Parasitological survey of some important fish species of Lake Balaton. *Parasit. Hung.* **28:** 63–82

Moshu A., Molnár K. (1997) *Thelohanellus* (Myxozoa: Myxosporea) infection of the scales in the European wild carp, *Cyprinus carpio carpio* L. *Dis. aquat. Org.* **28:** 115-123

Shulman S. S. (1966) Myxosporidia of the Fauna of the USSR. Nauka, Moscow–Leningrad (in Russian)

Received on 3rd February, 1997; accepted on 2nd June, 1997

Acta Protozoologica (1997) 36: 227 - 233

ACTA
PROTOZOOLOGICA

Description of the Large Multinucleate Lobose Amoeba *Chaos glabrum* sp. n. (Lobosea, Amoebidae), with Notes on the Diagnosis of the Genus *Chaos*

Alexey V. SMIRNOV and Andrew V. GOODKOV

Department of Invertebrate Zoology, St. Petersburg State University and Laboratory of Invertebrate Zoology, Biological Research Institute of St. Petersburg State University, St.Petersurg, Russia

Summary. Large, free-living multinucleate lobose amoeba *Chaos glabrum* sp. n. was isolated from the freshwater lake of Valamo Archipelago (north-western Russia, the Lake Ladoga). Locomotive morphology, nuclear structure and other features of the present species were characteristic for the genus *Chaos* excepting the fine organisation of the cell coat, which consists of two layers of amorphous glycocalyx and has no discrete filaments. Mitochondrial heteromorphism was detected in this species. The justification of the diagnosis of the genus *Chaos* is proposed in this paper, and the validity of the genus *Parachaos*, which also has no filamentous glycocalyx is confirmed.

Key words: amoebae, Amoebidae, *Chaos*, Lobosea, taxonomy, ultrastructure.

INTRODUCTION

Large free-living multinucleate lobose amoebae, members of the genus *Chaos*, are among the most often noted gymnamoebae, together with members of the genus *Amoeba*. *Ch. carolinense* is a very popular laboratory object and has been studied in details (Daniels and Roth 1964, Andresen 1973, Daniels 1973, Page 1986, Gromov 1986). However, ultrastructural studies of two other known species of this genus - *Ch. nobile* (Page 1986, 1988, 1991) and, especially, of *Ch. illinoisense* (Daniels and Roth 1964, Daniels 1973) are still incomplete.

There are only two modern publications (Page 1986, Willumsen et al. 1987), which consider the systematics of the genus *Chaos*. The diagnosis of this genus, among other features, includes the multinuclearity, the presence of the honeycomb inner nuclear lamina and the filamentous glycocalyx. In this connection, *Chaos zoochlorellae* Willumsen 1982, which does not have nuclear lamina and possesses amorphous cell coat, was excluded from the genus *Chaos*, and a separate genus *Parachaos* was established for this species (Willumsen et al. 1987).

During the study of gymnamoebae from the inner lakes of Valamo Archipelago (north-western Russia), a new species of large multinucleate amoebae was found. This species doubtless belongs to the genus *Chaos*, but the ultrastructural study indicated that it does not have the typical filamentous cell coat. Recently we found that the characteristic filamentous glycocalyx is absent also in *Chaos illinoisense* (A. V. Goodkov, I. N. Skovorodkin and A. V. Smirnov, unpublished). These and other data warrant some changes in the diagnosis of the genus *Chaos*

Address for correspondence: Alexey V. Smirnov, Dept. of Invertebrate Zoology, Fac. of Biology and Soil Sci., St. Petersburg State University, Universitetskaja nab. 7/9, 199034, St. Petersburg, Russia; E-mail: SMIRNOV@SVB.RCLPH.SPB.SU

(Linnaeus, 1767) Page 1986, which are proposed in this paper.

MATERIALS AND METHODS

Samples of the upper layer of bottom sediments, containing a new species of amoebae, were collected during June-August 1993 and 1994 from Lake Leshevoe (north-western Russia, the Lake Ladoga, Valamo Island) at depths of 0,5-1 m. They were inoculated into 100 mm Petri dishes with modified Prescott-James solution (Prescott and James 1955, Yudin 1982) and 2-3 wheat grains per dish. The samples were incubated at room temperature. Amoebae were cloned and maintained in laboratory culture at the same conditions, feeding on accomplished small ciliates and flagellates.

Chaos carolinense was used in the present study as a control organism for the fixation procedures adequacy. This strain was received from Dr. F. C. Page (Institute of Terrestrial Ecology, Cambridge, England) in 1984 and since this time has been maintained in the culture collection of the Laboratory of Cytology of Unicellular Organisms, Institute of Cytology, RAS.

Light-microscopic investigations were carried out using phase -contrast and Nomarski contrast optics. Nuclei were examined in preparations fixed with Bouin's solution and stained with iron haematoxylin as described by Page (1988).

For electron-microscopic investigations the following fixation procedures were tried. (Procedure 1): 4% glutaraldehyde (40 min.), washed 3 times; 2% osmium tetroxide. (Procedure 2): 0.5% osmium tetroxide (5 min.), 4% glutaraldehyde (30 min.), washed 3 times; 1% osmium tetroxide (60 min.). (Procedure 3): 0.5% osmium tetroxide (15 min.), 1% osmium tetroxide (60 min.). All fixatives were made with 0.2 M phosphate buffer (pH 7.4), and the same buffer was used for washing specimens. After dehydration in a grade series of ethanol, amoebae were embedded in Epon-Araldite. Sections were stained with saturated solution of uranyl acetate in 50% ethanol and Reynolds' lead citrate and examined in a "Tesla BS-500" and "Hitachi H-300" electron microscopes.

RESULTS

Light-microscopic observations

The most typical form of amoebae in continuous locomotion was elongated (Fig. 2), "orthotactic" form (termed by Grebęcki and Grebęcka 1978); small lateral lobopodia sometimes were developed (Fig. 3), but they never became dominant ones. The body had distinct longitudinal peripheral wrinkles and most lateral parts of the body usually were somewhat flattened. The frontal hyaline cap was always present, but often it was very narrow, crescent-shaped. Average length of the orthotactic form was 816 μm (420-980 μm); average breadth - 60 μm (42-98 μm). Average Length/Breadth ratio (L/B) was 11.

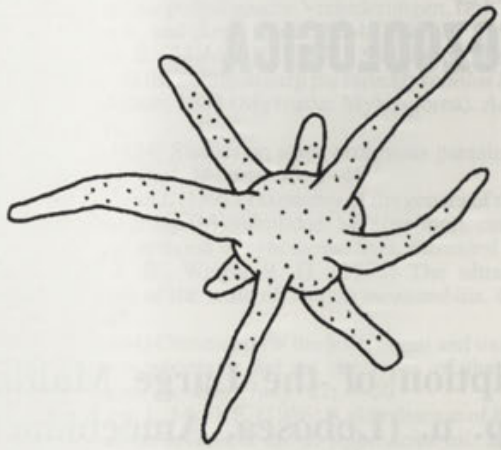

Fig. 1. Floating form of *Ch. glabrum*

When not rapid advance amoebae had well developed polytactic form (Fig. 6), with a few anteriorly directed pseudopodia. One of these pseudopodia was distinctly dominated at every moment during the locomotion and the overall outline of specimens remained rather elongated (Figs. 4, 5). Bulbous or compact morulate uroid frequently presented in active locomotion (Figs. 2-5). Average length of the polytactic amoebae usually was about 500 μm.

Floating forms were rarely seen in the cultures of this species. They were of radial type, with the compact central mass of the granuloplasm and 4-9 thick pseudopodia with rounded ends (Fig. 1). Pseudopodia of the floating form were never seen to be branched, their maximal length was 3-4 times more than the diameter of the central cytoplasmic mass.

The amoebae contained 6-30 (average 10) discoid, biconvex granular nuclei about 20 μm in diameter (Figs. 7, 8). The single contractile vacuole was usually situated posteriorly in moving amoebae. The cytoplasm was full of bipiramidal, spindle-shaped and cubical crystals, plate-like crystals, refractive spheres and small opaque granules.

The present species is a polyphag. In mixed cultures it feeds on bacteria, small protozoa and cysts of different protists. Clonal culture was successfully maintained on the ciliate *Colpidium striatum*. Cysts were never seen in cultures.

Electron - microscopic study

The nucleus was of granular type and nucleolar pieces were mostly arranged in a peripheral layer (Fig.9). Fibrous inner nuclear lamina had honeycomb-like organisation

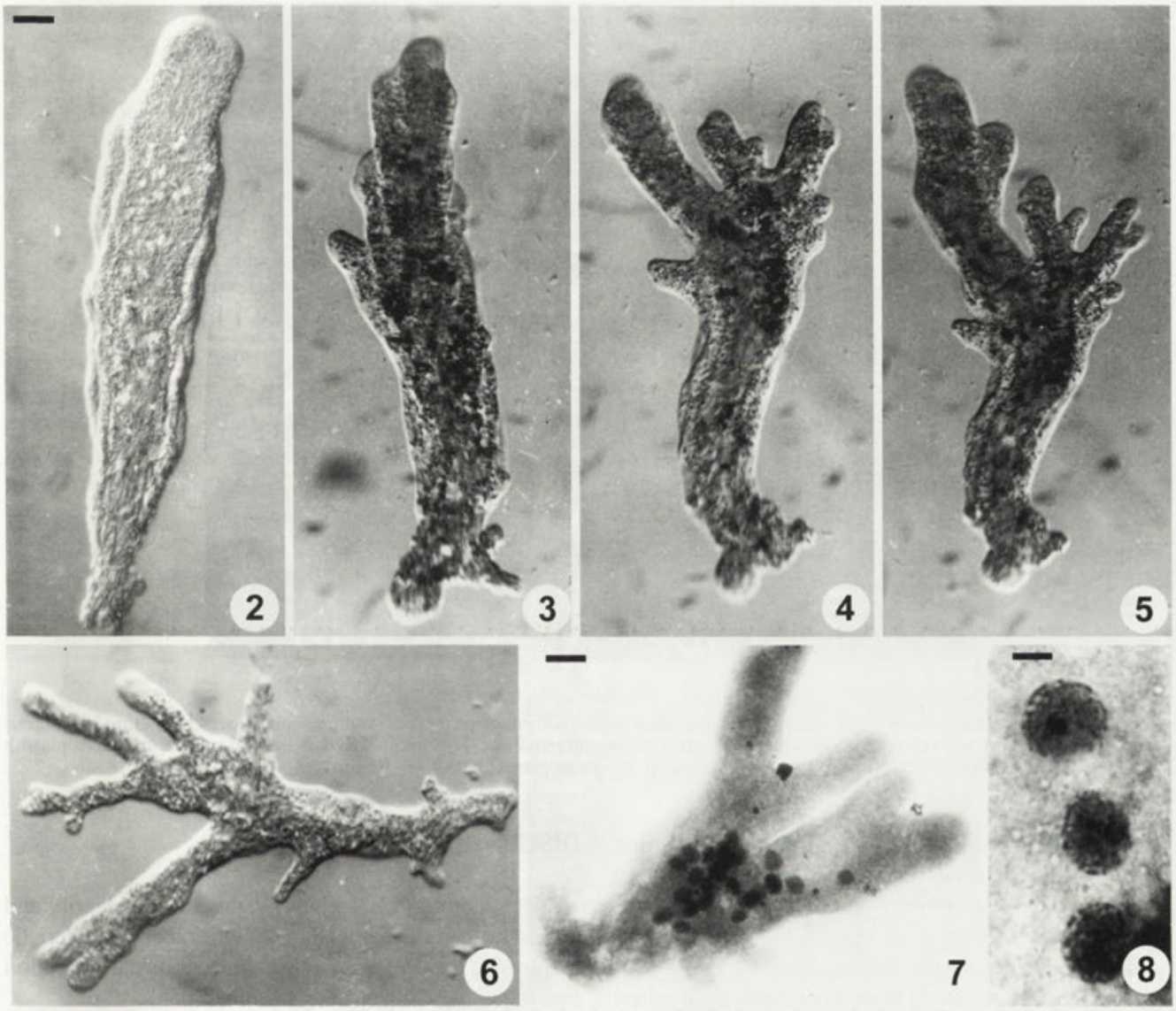

Figs. 2-6. Locomotive forms of *Chaos glabrum*, bar - 50 µm. Figs. 7,8. Stained preparations of *Ch. glabrum*. 7 - the general view of the stained amoeba, bar - 50 µm; 8 - nuclei, bar - 10 µm

(Figs.10,11); its thickness was about 110 nm and the inner diameter of the cellules was about 120 nm. Nuclear pores were situated at the bottom of every cellula. Characteristic helices of RNP and their stellate clusters were often seen in the nucleoplasm (Figs. 11,12).

Numerous dictyosomes (Fig. 13) consisted of 8-10 flattened cisternae; these organelles were very similar to those of *A. proteus*, *A. borokensis* and *Ch. carolinense* (Page and Kalinina 1984, Page 1986). Contractile vacuole complexes with the spongiom and associated mitochondria (Fig. 14) had the same organisation as in most amoebidans.

Mitochondria of this species had tubular branching cristae. When the cells were fixed using the procedure (1), two morphologically different types of mitochondria were clearly visible (Figs. 15,16). Mitochondria of the first type had electron-dense matrix and comparatively large cristae. In sections their cristae looked like tubes or "channels" with numerous anastomoses in dark surrounding. Elongate profile in sections was fairly common for these mitochondria. Mitochondria of the second morphological type possessed considerably less electron-dense matrix and comparatively narrower cristae with few anastomoses. As a rule these mitochondria had rounded profiles.

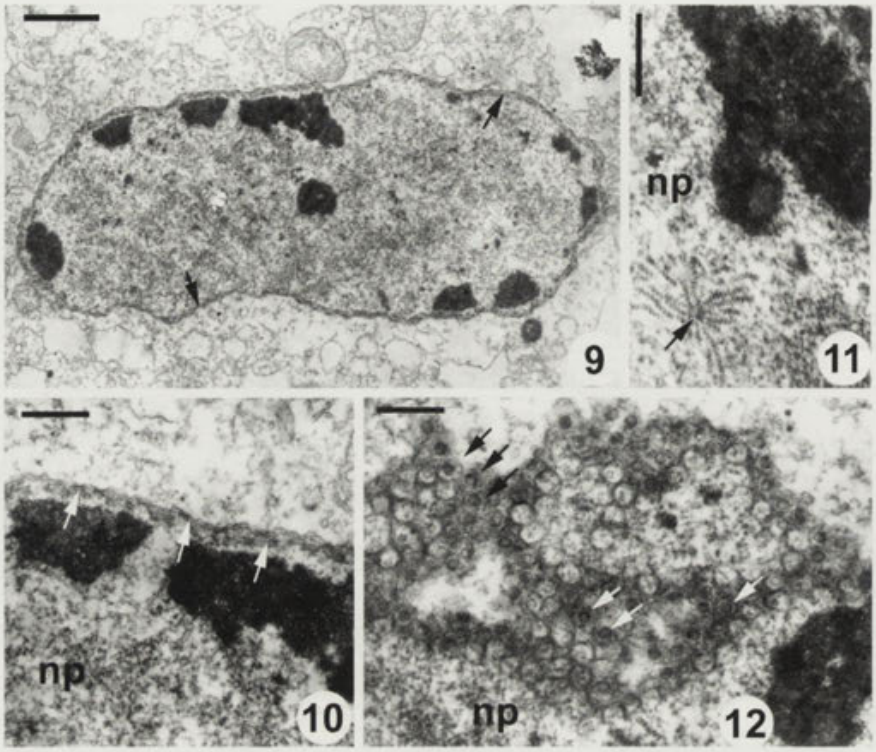

Figs. 9-12. Nuclei of *Ch. glabrum*. 9- section of entire nucleus showing nuclear envelope (arrows) and nucleolar pieces, bar - 2μm; 10 - fibrous inner nuclear lamina (arrows) with distinct periodicity indicating honeycomb structure; 11 - cluster of RNP helices (arrowed)(np - nucleoplasm); 12 - cellules of honeycomb-like lamina and nucleopores (arrows) (np - nucleoplasm), bars 9-11 - 0,5μm

The fixation procedures (2) and (3) eliminated distinct morphological differences of mitochondria and all of them appeared to have electron-transparent matrix.

All studied specimens contained considerable number of rod-like bacteria, which lay freely in the cytoplasm (Fig. 17), they differed well from those bacteria ingested into phagosomes (Fig. 18). The division of rod-like bacteria in the cytoplasm of this species was reported previously (Smirnov et al. 1995, as *Chaos* sp.).

The cell coat of this species appeared as thick amorphous glycocalyx which was subdivided into two layers: compact, electron-dense basal layer and loose, more electron-transparent upper one (Fig. 19). Total thickness of the cell coat was 50-60 nm. Sometimes elongate patches of amorphous filamentous material were seen over the surface of the glycocalyx, but no evidence of filamentous layer was found in five different fixations, made with all three procedures listed above.

Simultaneously, we investigated *Ch. carolinense*, whose surface organisation is well known (see: Pappas 1959, Page 1986), as a control for fixation procedure (1) adequacy. The results demonstrated that the filamentous surface layer in this species was well preserved (Fig. 20).

DISCUSSION

The locomotive morphology, the multinuclearity and the nuclear structure, together with the other characteristic features of the present species, warrant its classification into the genus *Chaos* (family Amoebidae).

Modern diagnosis of the genus *Chaos* includes the following character: "cell coat of discrete, crinkled or wavy filaments" (Page 1986) or "cell surface coat of distinct, separate filaments radiating from plasma membrane" (Willumsen et al. 1987). Moreover, this feature is still considered to be characteristic of the family Amoebidae (Page 1986), in spite of the fact that *Amoeba leningradensis* has the cell coat "consisting of only an amorphous layer outside the plasma membrane and no discrete filaments radiating outward from the membrane" (Page and Kalinina 1984). This forced F. C. Page to include a special remark in the diagnosis of the genus *Amoeba*: "Cell coat of discrete, crinkled filaments except in one species" (Page 1986). Moreover, in the same paper he noted, that *Deuteramoeba* (*Amoeba*) *algonquienensis*, another typical amoebidian species, does not have distinct, separate filaments radiating from the plasma membrane.

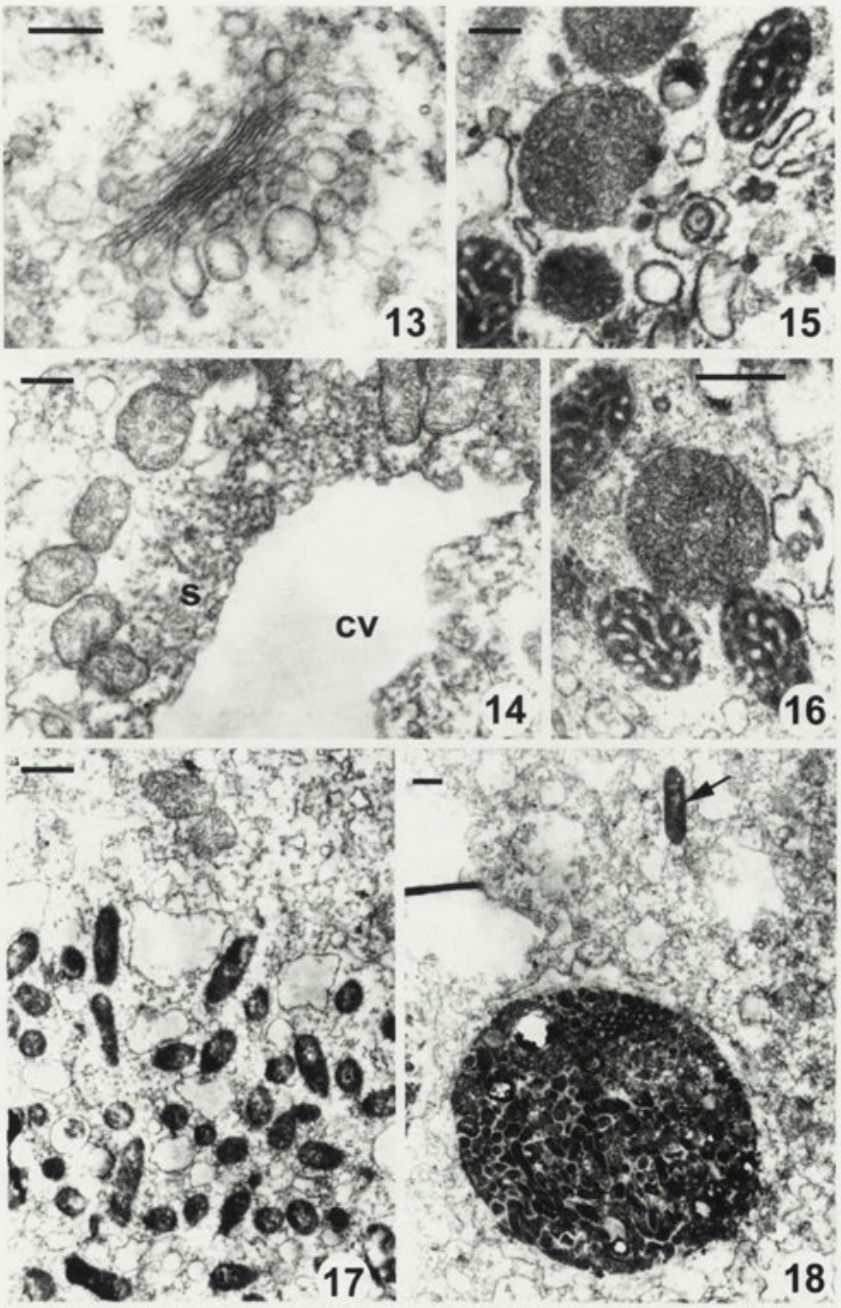

Figs. 13-18. Cytoplasmic organelles and inclusions. 13 - dictyosome, bar - 0,2μm; 14 - contractile vacuole (CV) with spongiom (S); 15,16 - two morphologically different types of mitochondria, bars - 0,5μm; 17 - endocytobiotic bacteria; 18 - phagosome with bacterial material and endocytobiont in the cytoplasm (arrowhead), bars 17, 18- 1μm

Results of the present study indicated that "characteristic filamentous cell coat" is absent in this strain of *Chaos*. Recently we found that glycocalyx of *Chaos illinoisense* also does not have discrete filamentous structure (A. V. Goodkov, I. N. Skovorodkin and A. V. Smirnov, unpublished). Thus, the present diagnosis of the genus *Chaos* needs justification (the re-diagnosis see below).

The proposed justifications do not require total systematic revision of the genus *Chaos*. It is only necessary to consider the validity of the genus *Parachaos*, which was separated from the genus *Chaos* based, among others, on the fact that *P. zoochlorella* (the type species of the genus) has amorphous glycocalyx without distinct, separated filaments radiating from the plasma membrane (Willumsen

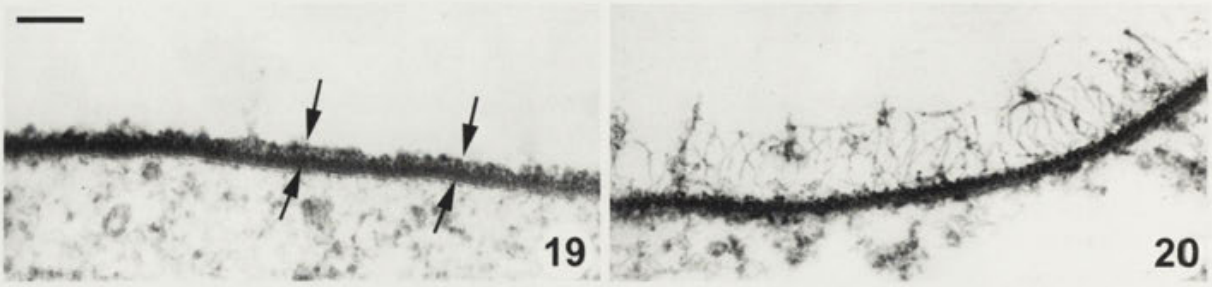

Figs.19,20. Cell surfaces. 19 - *Ch. glabrum* (two amorphous layers are aroused);. 20- *Ch. carolinense,* bar - 0,15 μm

et al. 1987). It is very similar to the cell coat of the present species. However, *P. zoochlorella* does not has filamentous inner nuclear lamina - the characteristic structure of all known members of the genus *Chaos*. It differs from the members of the genus *Chaos* also in its locomotive form, which is (according to a few published photographs) smooth, without lateral wrinkles (Willumsen 1982). It is much more similar in locomotion to *Trichamoeba sinuosa* or *Hydramoeba hydroxena* than to *Chaos* spp. Thus, the genus *Parachaos* Willumsen, Siemensma et Suhr-Jessen, 1987 is still considered to be valid taxon.

Among three valid members of the genus *Chaos* - *Ch. carolinense, Ch. illinoisense* and *Ch. nobile*, the present strain is most similar to the last one, although it has essential differences. Orthotactic locomotive form does not seem characteristic for *C. nobile* - it is noted in none of the works, in which this species is mentioned. Floating form with rebranching pseudopodia characteristic for *Ch. nobile* (Page, 1988) has never been observed in the present strain, which has usual radial floating form with straight or slightly curved non-branching pseudopodia. The surface coat of *Ch. nobile* possesses distinct crinkled filaments (filaments extending commonly up to 200 nm above the plasma membrane) (Page 1986), but only amorphous glycocalyx was observed in the present strain. The above differences warrant a description of a new species - *Ch. glabrum* sp. n. (the diagnosis see below).

Detailed consideration of the fact that two morphologically different types of mitochondria are present in the cytoplasm of *Ch. glabrum* - the phenomena which we termed as "mitochondrial heteromorphism" " (A. V. Goodkov et al. in prepare) - is not a purpose of the present paper, but it is necessary to note that mitochondria of such well-known species as *Amoeba proteus* normally are of two morphological types - so called "dark" and "light" (Flickinger 1974, Ord 1976, Smith and Ord 1979), as in *Ch. glabrum*. It is known that under the fixation procedures differing from the procedure (1) in this paper, the mitochondrial matrix could be lost, thus eliminating the morphological differences of mitochondria (Flickinger 1974). This fact was supported in the present paper. There are all reasons for suggestion that the mitochondrial heteromorphism is much more widely distributed in the family Amoebidae, than it was supposed until recently

Diagnoses

Genus *Chaos* (Linnaeus 1758) Page 1986, emend.

Commonly polypodial, with pseudopodia produced from one main stem whose diameter is grater than that of the pseudopodia; may acquire the monopodial-like (orthotactic) form in active locomotion. Multinucleate, nuclei of granular type; filamentous inner nuclear lamina, often organised as a honeycomb-like layer.

Type species: *Chaos chaos* (Linnaeus 1758), unidentifiable.

Known species*: Chaos carolinense, Chaos nobile, Chaos illinoisense, Chaos glabrum.*

Chaos glabrum sp. n.

Regularly orthotactic (monopodial-like with distinct lateral wrinkles) with bulbous uroid in active locomotion. Length of polypodial form about 500 μm; when orthotactic length 420-980 μm (average 816 μm), breadth 42-98 μm (average 60 μm). Number of the nuclei is 6-30 per cell (average 10). Nuclei biconvex, about 20 μm in diameter. Glycocalyx amorphous, up to 50-60 nm, of two distinct layers. Possesses mitochondrial heteromorphism.

Known habitat: Fresh water, north-western Russia.

Type slides are deposited with the museum of preparations of the Laboratory of Invertebrate Zoology, Biological Research Institute, St. Petersburg State

University: Holotype, 1994: 704; Paratypes 705, 706. Bottom sediments of Lake Leshevoe (Valamo Island, Lake Ladoga), from depths of 0,5-1 m, 1994.

Differential diagnosis: In respect to the nuclear size and number, *Chaos glabrum* differs well from all known members of the genus *Chaos,* excluding *Ch. nobile* (both other species - *Ch. carolinense* and *Ch. illinoisense* have several hundred nuclei per cell). From *Ch. nobile* it differs well with stable orthotactic locomotive form, bulbous uroid and with the organisation of the floating form. At the ultrastructural level, *Ch. glabrum* has a different structure of the cell coat than *Ch. nobile.*

Acknowledgements. The work was supported with the grant from RBRF No 96-04-50858 provided to A. V. Goodkov and with the grant a459-b from International Science Foundation provided to A. V. Smirnov. Collection of the material was carried out at the field station of Valamo Expedition of St. Petersburg Society of Naturalists; it was supported with the grant from the St. Petersburg Society of Naturalists

REFERENCES

Andresen N. (1973). General morphology. In: The Biology of Amoeba (Ed. K. W. Jeon), Academic Press, New York, London 99-123

Daniels E. W. (1973) Ultrastructure. In: The Biology of Amoeba. Acad. Press, N. Y., London, 125 -169

Daniels E. W., Roth L. E. (1964) Electron microscopy of mitosis in a radiosensitive giant amoeba. *J. Cell Biol.* **20:** 75-84

Flickinger C. J. (1974) The fine structure of four "species" of *Amoeba*. *J. Protozool.* **21:** 59-68

Grebęcki A., Grebęcka L. (1978) Morphodynamic types of *Amoeba proteus*: a terminological proposal. *Protistologica* **14:** 349-358

Gromov D. B. (1986) Ultrastructure of nuclei of the multinucleate amoeba *Chaos carolinense* (Wilson). *Tsitologiya* **28:** 446-447 (in Russian, English summary)

Ord M. J. (1976) The interaction of nuclear and cytoplasmic damage after treatment with toxic chemicals. *J. Theor. Biol.* **62:** 369-387

Page F. C. (1986) The genera and possible relationships of the family Amoebidae, with special attention to comparative ultrastructure. *Protistologica* **22:** 301-316

Page F. C. (1988) A new key to freshwater and soil Gymnamoebae. Freshwater Biological Assoc., Ambleside

Page F. C. (1991) Nackte Rhizopoda. Protozoenfauna, b.2. Gust. Fisher, Stuttgart, New York

Page F. C., Kalinina L. V. (1984) *Amoeba leningradensis* n. sp. (Amoebidae): a taxonomical study incorporating morphological and physiological aspects. *Arch. Protistenk.* **128:** 37-53

Pappas G. D. (1959) Electron microscope studies on amoebae. *Ann. N. Y. Acad. Sci.* **78:** 448-473

Prescott D. M., James T. W. (1955) Culturing of *Amoeba proteus* on *Tetrahymena*. *Exp. Cell. Res.* **8:** 256-258

Smirnov A. V., Ossipov D. V., Rautian M. S. (1995) Endocytobionts in representatives of two amoebian orders, Euamoebida and Leptomyxida (Lobosea, Gymnamoebia). *Tsitologiya* **37:** 403-414 (in Russian, English summary)

Smith R. A., Ord M. J. (1979) Morphological alterations in the mitochondria of *Amoeba proteus* induced by uncoupling agents. *J. Cell Sci.* **37:** 217-229

Willumsen N. B. S. (1982) *Chaos zoochlorellae* nov. sp. (Gymnamoebia, Amoebidae) from Danish freshwater pond. *J. Nat. Hist.* **16:** 803-813

Willumsen N. B. S., Siemensma P., Suhr-Jenssen P. A. (1987) Multinucleate amoeba, *Parachaos zoochlorellae* (Willumsen, 1982) comb. nov., and proposed division of the genus *Chaos* to the genera *Chaos* and *Parachaos* (Gymnamoebia, Amoebidae). *Arch. Protistenk.* **134:** 303-314

Yudin A. L. (1982) Nucleocytoplasmic relationships and cell heredity in amoebae. Nauka, Leningrad (in Russian)

Received on 10 th September, 1996; accepted on 14th April, 1997

Acta Protozoologica (1997) 36: 235

ACTA
PROTOZOOLOGICA

Book Review

Bestimmung und Ökologie der Mikrosaprobien nach DIN 38 410. By Helmut Berger, Wilhelm Foissner and Fritz Kohmann. Gustav Fischer Verlag, Stuttgart, Jena, Lübeck, Ulm, 1997. 291 pp., with 940 photographs and line drawings on 86 plates plus 10 tables; soft cover

The idea to use the composition of freshwater biota as indicators of organic pollution goes back to the turn of the century, and protozoa (in particular ciliates) and certain conspicuous bacteria were included from the beginning as a component of a "saprobiological index"(Saprobiensysteme). A wast amount of literature on this subject has since then appeared. This formalised system is based on the presence and pseudo-quantification of different species; to this day it seems to play a role for the classification of running waters according to the degree of pollution. The underlying principle is, of course, that different species have different habitat preferences, some being sulphide tolerant, obligate anaerobes while others thrive only in oligotrophic and oxygen rich waters (to take the extremes).

The purpose of this book is to provide a practical aid to make confident species identifications for the monitoring of river pollution. To this end the book includes a general introduction to the "Saprobiensysteme", with comprehensive tables listing individual species and their "saprobic valence" and a chapter on techniques for collecting, studying and identifying the species. A last Chapter 5 is a glossary of morpholgical terms. Chapter 4, then, represents the main part of the book: identification keys and detailed description of 7 species of rhizopods, 21 species of flagellates, and 48 species of ciliates, in addition to 9 species of easily recognisable bacteria (in this book somewhat old fashioned referred to as "schizomyzetes") and to 2 fungal species.

As could be expected from this team of protozoologists, the species descriptions are superb both in terms of the text and in terms of the (esthetically pleasing) plates which include precise drawings and (in the case of protozoa) photographs of living cells and often of silver impregnated individuals as well as SEM photographs. Descriptions include notes on the possibility of confounding the species with other, similar ones, and brief notes on the ecology. The authors have succeeded in the stated purpose of the book; I do not think that a better guide to the identification of protists for practical workers without professional background in protozoology could have been written.

This being said, I am left with an unanswered question. Not having any particular expertise or knowledge on water pollution, it has always puzzled me why so much sophistication (having to identify almost 100 species of protozoa) is necessary for monitoring the outlet and eventual fate of sewage in a river: are simple chemical methods for quantifying dissolved organic matter, oxygen, ammonia, etc. (and the characteristic odour of sulphide) not sufficient? But then again - some of the pictures of protozoa in this book document that even organic pollution presents some beauty, and so here is perhaps one rational for the "Saprobiensysteme".

Tom Fenchel, University of Copenhagen, Denmark

INSTRUCTIONS FOR AUTHORS

ACTA PROTOZOOLOGICA publishes original papers embodying the results of experimental or theoretical research in all fields of protistology with the exception of faunistic notices of local character and purely clinical reports. Short (rapid) communications are acceptable but also long review articles. The papers should be as concise as possible, be written in English. Submission of a manuscript to ACTA PROTOZOOLOGICA implies that it has not been submitted for publication elsewhere and that it contains unpublished, new information. There are no page charges except colour illustration. Names and addresses of suggested reviewers will be appreciated. In case of any question please do not hesitate to contact Editor. Authors should submit papers to:

Miss Małgorzata Woronowicz
Managing Editor of ACTA PROTOZOOLOGICA
Nencki Institute of Experimental Biology,
ul. Pasteura 3
02-093 Warszawa, Poland
Fax: 48- 22 225342

Organization of Manuscripts

Submissions

Please enclose three copies of the text, one set of original of line drawings (without lettering!) and three sets of copies with lettering, four sets of photographs (one without lettering). In case of photographs arranged in the form of plate, please submit one set of original photographs unmounted and without lettering, and three sets of plates with lettering.

The ACTA PROTOZOOLOGICA prefers to use the author's word-processor disks (3.5"and 5.25" format IBM or IBM compatible, and MacIntosh 6 or 7 system on 3.5" 1.44 MB disk only) of the manuscripts instead of rekeying articles. If available, please send a copy of the disk with your manuscript. Preferable programs are Word or Wordperfect for Windows and DOS Wordperfect 5.l. Disks will be returned with galley proof of accepted article at the same time. Please observe the following instructions:

1. Label the disk with your name: the word processor/computer used, e.g. IBM; the printer used, e.g. Laserwriter; the name of the program, e.g. Word for Windows or Wordperfect 5.l.
2. Send the manuscript as a single file; do not split it into smaller files.
3. Give the file a name which is no longer than 8 characters.
4. If necessary, use only italic, bold, underline, subscript and superscript. Multiple font, style or ruler changes, or graphics inserted the text, reduce the usefulness of the disc.
5. Do not right-justify and use of hyphen at the end of line.
6. Avoid the use of footnotes.
7. Distinguish the numerals 0 and 1 from the letters O and l.

Text (three copies)

The text must be typewritten, doublespaced, with numbered pages. The manuscript should be organized into Summary, Key words, Abbreviations used, Introduction, Materials and Methods, Results, Discussion, Acknowledgments, References, Tables and Figure Legends. The Title Page should include the full title of the article, first name(s) in full and surname(s) of author(s), the address(es) where the work was carried out, page heading of up to 40 characters. The present address for correspondence, Fax, and E-mail should also be given.

Each table must be on a separate page. Figure legends must be in a single series at the end of the manuscript. References must be listed alphabetically, abbreviated according to the World List of Scientific Periodicals, 4th ed. (1963). Nomenclature of genera and species names must agree with the International Code of Zoological Nomenclature, third edition, London (1985) or International Code of Botanical Nomenclature, adopted by XIV International Botanical Congress, Berlin, 1987. SI units are preferred.

Examples for bibliographic arrangement of references:

Journals:

Häder D-P., Reinecke E. (1991) Phototactic and polarotactic responses of the photosynthetic flagellate, *Euglena gracilis*. *Acta Protozool.* **30:** 13-18

Books:

Wichterman R. (1986) The Biology of Paramecium. 2 ed. Plenum Press, New York

Article's from books:

Allen R. D. (1988) Cytology. In: Paramecium, (Ed. H.-D. Görtz). Springer-Verlag, Berlin, Heidelberg, 4-40

Zeuthen E., Rasmussen L. (1972) Synchronized cell division in protozoa. In: Research in Protozoology, (Ed. T. T. Chen). Pergamon Press, Oxford, **4:** 9-145

Illustrations

All line drawings and photographs should be labeled, with the first author's name written on the back. The figures should be numbered in the text as arabic numerals (e.g. Fig. 1). Illustrations must fit within either one column (86 x 231 mm) or the full width and length of the page (177 x 231 mm). Figures and legends should fit on the same page. Lettering will be inserted by the printers and should be indicated on a tracing-paper overlay or a duplicate copy.

Line drawings (three copies + one copy without lettering)

Line drawings should preferably be drawn about twice in size, suitable for reproduction in the form of well-defined line drawings and should have a white background. Avoid fine stippling or shading. Computer printouts of laser printer quality may be accepted, however *.TIF, *.PCX, *.BMP graphic formats on disk are preferred.

Photographs (three copies + one copy without lettering)

Photographs at final size should be sharp, with a glossy finish, bromide prints. Photographs grouped as plates (in size not exceeding 177 x 231 mm **including legend**) must be trimmed at right angles accurately mounted and with edges touching and mounted on firm board. The engraver will then cut a fine line of separation between figures. Magnification should be indicated. Colour illustration on transparent positive media (slides 60 x 45mm, 60 x 60mm or transparency) are preferred.

Proof sheets and offprints

Authors will receive one set of page proofs for correction and are asked to return these to the Editor within 48-hours. Fifty reprints will be furnished free of charge. Orders for additional reprints have to be submitted with the proofs.

Indexed in Chemical Abstracts Service, Current Contents (Agriculture, Biology and Environmental Sciences), LIBREX-AGEN, Protozoological Abstracts. POLISH SCIENTIFIC JOURNALS CONTENTS - AGRIC.& BIOL. SCI. data base is available in INTERNET under URL (UNIFORM RESOURCE LOCATOR) address: http://saturn.ci.uw.edu.pl /psjc/ or http://ciuw.warman.org.pl /alf/psjc/ any WWW browser; in graphical operating systems: MS Windows, Mac OS, X Windows - mosaic and Netscape programs and OS/2 - Web Explorer program; in text operating systems: DOS, UNIX, VM - Lynx and www programs.

ACTA
PROTOZOOLOGICA

REVIEW ARTICLE

ORIGINAL ARTICLES

1997 AUGUST
VOLUME 36 NUMBER 3